Design of novel functionalized nucleosides and their applications(Dissertation_全文)

AUTHOR(S):

Tanaka, Kazuo

CITATION:

Tanaka, Kazuo. Design of novel functionalized nucleosides and their applications. 京都大学, 2004, 博士(工学)

ISSUE DATE:

2004-03-23

URL:

https://doi.org/10.14989/doctor.k10833

Design of Novel Functionalized Nucleosides and Their Applications

Kazuo Tanaka

2004

Kyoto University

Preface

The study presented in this thesis was carried out under the direction of Professor Isao Saito at the Department of Synthetic Chemistry and Biological Chemistry of Kyoto University during April 1999 to March 2004. The study is concerned with application of modified nucleosides to biotechnology and nanotechnology.

The author wishes to express his sincere gratitude to Professor Isao Saito for his kind guidance, valuable suggestions, and encouragement throughout this work. The author is deeply grateful to Assistant Professor Akimitsu Okamoto for his helpful advice, discussions and encouragement. The author is also indebted to Associate Professors Kazuhiko Nakatani, Kenzo Fujimoto, Assistant Professors Hisafumi Ikeda, Shinsuke Sando and Kazuhito Tanabe for their helpful suggestions.

The author thanks Professor Shigeyoshi Sakaki for the measurements of fluorescence decay. The author thanks Dr. Mitsuru Iida and Dr. Teruhisa Kato of Ohtsuka Pharmaceutical co. ltd. for generous gift of PCR products of the BRCA1 gene. The auhor is grateful to Mr. Haruo Fujita, Mr. Tadao Kobatake and Ms. Hiromi Ushitora for the measurements of NMR spectra and mass spectra. The author is thankful to Professor Jun-ichi Yoshida for the measurements of cyclic voltammetry. The author is thankful to Professors Susumu Kitagawa, Kazunari Akiyoshi and Tadashi Mizutani for the measurements of circular dichroism. The author is thankful to Assistant Professor Hideo Ohkita for the measurements of transient absorption. The author thanks Messrs. Toshiji Taiji, Tetsuo Fukuta, and Ken-ichiro Nishiza for collaboration. The author is grateful to Dr. Takashi Nakamura, Dr. Shigeo Matsuda, Dr. Chikara Dohno, Dr. Shinya Hagihara, Dr. Heike Heckroth, Dr. Yoshio Saito and Dr. Akio Kobori for their helpful suggestions. The author is also grateful to Messrs. Kohzo Yoshida, Kaoru Adachi, Takashi Yoshida, Naoki Ogawa, Yutaka Ikeda, Hideaki Yoshino, Masayuki Hayashi, Hiroyuki Kumasawa, Kazuki Tainaka, Keiichiro

Kanatani, Atsushi Ogawa, Souta Horie, Akio Nakazawa, Takuo Okuda, Takeshi Inasaki, Yohei Miyauchi, Hitoshi Suda, Takashi Murase, Motoya Nishida, Tomohisa Ichiba, Yuji Ochi, Yuki Goto, Taku Kamei, Kenji Omoto, Gousuke Hayashi, Miss. Tomo Unzai, and other members of Professor Saito's research group for their helpful suggestions and hearty encouragement.

The author thanks Japan Society for the Promotion of Science for financial support (Fellowship for Japanese Junior Scientists).

The author expresses his deep appreciation to his parents, Mr. Toshiyuki Tanaka and Mrs. Sakiko Tanaka, for their constant assistance and encouragement.

Last but not least, the author heartily thanks to his wife, Eun-Hwa, for her helpful supports and heartwarming encouragement.

Kazuo Tanaka

January, 2004

Contents

General Introduction ····· 1

Chapter 1 Rational Design of DNA Wire Possessing an Extremely High Hole Transport Ability ····· 17

Chapter 2 Protocol for the Construction of Logic Gates Using DNA ·· 41

Chapter 3 Enzymatic Synthesis of DNA Nanowire ····· 55

Chapter 4 Unique Hole-Trapping Property of a Novel Degenerate Base, 2-Amino-7-Deazaadenine ····· 73

Chapter 5 A Novel Nucleobase That Releases Reporter Tags upon DNA Oxidation ····· 87

Chapter 6 Design of Base-Discriminating Fluorescent Nucleoside and Its Application to T/C SNP Typing ····· 109

Chapter 7 Cytosine Detection by a Fluorescein-Labeled DNA Probe Containing Base-Discriminating Fluorescent Nucleoside ····· 123

Chapter 8 A New SNPs Typing Method Using Base-Discriminating Fluorescent Nucleosides ·····143

Chapter 9 2-Amino-7-Deazaadenine Forms Stable Base Pairs with Cytosine and Thymine ····· 157

Chapter 10 Public-Key System Using DNA as a One-Way Function for Key Distribution • 171

List of Publications • 187

General Introduction

The remarkable recognition properties of DNA are appropriate for the molecularly designed and controlled nanostructure.[1] Furthermore, self-assemblies of DNA are suitable for further development of encompassing site-specific fabrication and the functionalization.[2] Synthetic oligonucleotide analogs[3,4] have greatly aided functionalization of DNA. Efficient solid-phase and enzyme-assisted synthetic methods as well as the availability of modified base analogs have expanded to the utility of oligonucleotides.

Applications of Modified Nucleobases

Universal Bases

Natural nucleobases display exquisite selectivity in recognizing complementary bases. A universal base can be defined as an analog that can substitute for any of the four natural bases in oligonucleotides without significantly impairing the duplex stability. In general, universal base analogs use aromatic ring stacking, instead of specific hydrogen bonds, to stabilize a duplex. However, universal recognition by imidazole-4-carboxamide nucleoside has been attributed to specific hydrogen-bonding contacts.[5] The efficiency of oligonucleotide primers containing multiple substitutions of 5-nitroindole[6,7] and 3-nitropyrrole[8,9] has been studied and compared in DNA sequencing and in polymerase chain reactions. These analogs can be used at primer sites corresponding to degenerate base positions and specifically where the sequence data is incomplete. The use of 2-amino-6-methoxyadenosine[10] in oligonucleotide templates results in a nucleotide misincorporation during PCR amplefication, and it has been suggested that this property can be further used to generate mutant gene libraries.

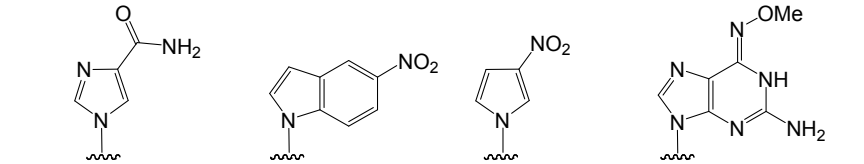

Figure 1. Universal bases. They can be defined as an analog that can substitute for any of the four natural bases in oligonucleotides without impairing the duplex stability.

Fluorescent Nucleosides

Many fluorescent nucleosides have been used as site-specific probes for studying structures and dynamics of nucleic acids.[11] Nucleoside possessing various fluorophores have been explored, including fluorescent nucleoside analogues and fluorophore-linked base conjugates, as exemplified by 2-aminopurine (2AP),[12] 1,N-ethenoadenine,[13] ethynyl-extended pyrimidines and deazapurines,[14] and nucleoside analogues[15] replaced by flat aromatic fluorophores.[16] 2AP has been used extensively to detect changes in oligonucleotide conformation.[17] It can substitute for adenosine in base pairing with thymidine without distorting the double helix. The absorption and excitation maximum for 2AP is at 330 nm and has an emission at 380 nm. The quantum yield of 2AP fluorescence, when substituted in oligonucleotides, depends on the degree of base stacking.[18] Therefore, any change in its fluorescence is a sensitive indicator of structural perturbations in the modified oligonucleotide and provides an insight into the dynamics of such processes. Temperature-dependent conformational changes in oligonucleotides[19] and the dynamics of mismatched base pairs in oligodeoxynucleotides have been followed in the monitoring of change in fluorescence intensity of 2AP.[20]

Fluorescent reporter groups have also been attached to the 5-position of deoxyuridine via various linkers to follow oligonucleotide-protein interactions.[21] These nucleosides can easily be incorporated into oligonucleotide by enzymatic means.[22]

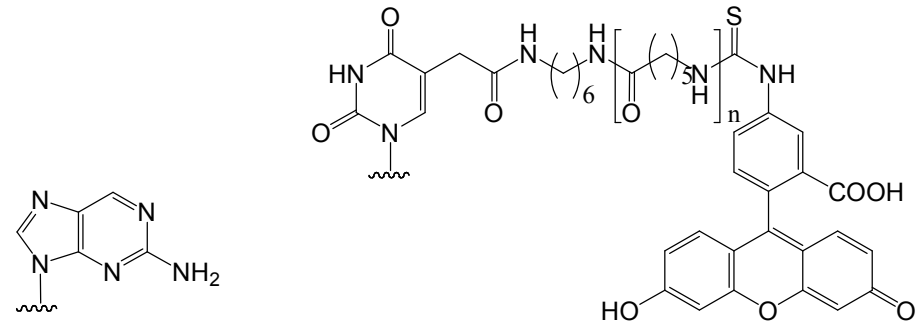

Figure 3. Fluorescent modified bases. Various functional molecules have been attached to 5-position of deoxyuridine.

Electron-Donating Bases

In 1993, Barton and Turro et al.[23] constructed DNA assembly containing donor and acceptor metallointercalators to each end of the duplex and produced experimental evidence suggesting that DNA serves as a molecular wire or "π-way". After that, various kinds of electron donor were synthesized and incorporated into oligodeoxynucleotides (ODNs) to examine hole transport reaction through DNA.[24] More recently, electrochemical active molecules were synthesized for development of DNA-based electrochemical biosensor.[25]

In recent studies,[26] the mechanism of long-range hole transfer through DNA has been proposed to involve the guanine (G)-hopping process that consists of a series of short-range hole transfer between G radical cation (G^+) and G. The basis of the hopping mechanism is that G^+ cannot oxidize adenine (A) due to the higher ionization potential (IP) of A compared with that of G, but can oxidize another G. It is actually predicted by electron transfer theory that lowering the IP of a bridge increases the electronic coupling for the superexchange interaction between donor and acceptor; both the IP[27] and the base stacking[28,29] of the bridge sequence were important for improvement of hole transport efficiency. Artificial nucleobases that have the low IP can be used as effective hole carriers[30] or

hole traps.[31] An efficient hole-trapping nucleobase which causes site-specific strand cleavage would be used as a very effective tool for modulating long-range hole transport through DNA. An effective hole carrier could be appropriate for consisting of a DNA wire.

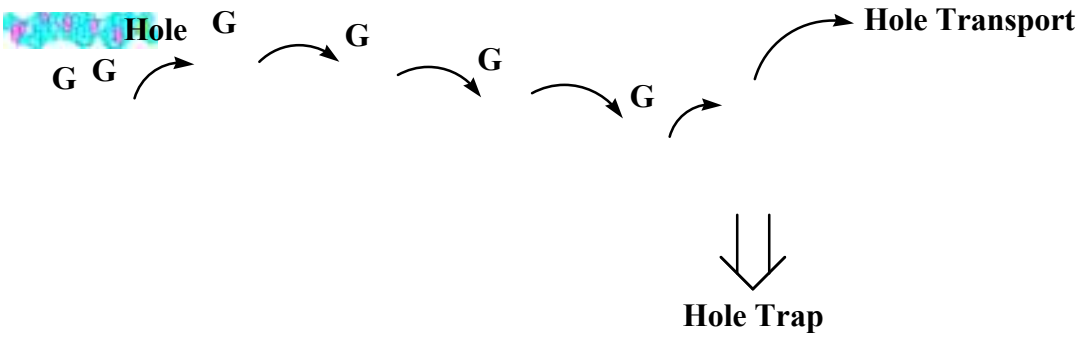

Figure 4. Long-range hole transport reaction in DNA. Electron-donating bases are expected to be an efficient hole trap or a good hole carrier.

Electron-donating nucleobases are expected to possess high chemical reactivity. Therefore, for DNA modifications, various chemical reactions would be applicable under mild conditions. For example, the Diels–Alder reaction is a very attractive approach for bioconjugation due to the remarkable acceleration of the reaction in aqueous systems.[32,33] Only a few examples of nucleic acid modifications utilizing the Diels–Alder reaction have been reported.[34-37] However, most of these methods required long reaction times and/or a specific sequence that may catalyze the reaction. Furthermore, currently available Diels–Alder bioconjugation methods are restricted to only strand ends. A modified nucleobase 7-vinyl-7-deazaguanine has low IP because of its extended π-conjugated system, and this base can produce adducts with maleimides through Diels–Alder cycloaddition under very mild conditions.[38] By this method, post-synthetic modification to oligonucleotides with diverse functionality

(carboxylic acid, pyrene, benzophenone, succinimidyl ester, nitroxide and biotin) was accomplished.

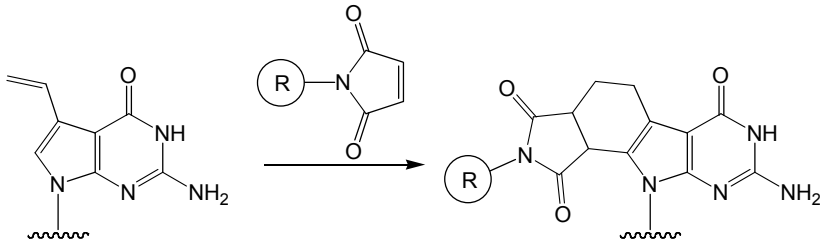

Figure 5. Diels-Alder cycloaddition of 7-vinyl-7-deazaguanine. This reaction proceeded under very mild conditons.[38]

DNA as a Sophisticated Material for Nanotechnology

DNA Computer

Molecular biology is used to suggest a new way of solving a NP-complete problem. The idea is to use strands of DNA to encode the problem and to manipulate them using techniques commonly available in any molecular biology laboratory, to simulate operations that select the solution of the problem, if it exists. In 1994, Adleman demonstrated the first small-scale molecular computation.[39] From this ground-breaking experiment sprang the rapidly evolving field of DNA computation, or biomolecular computing which uses biotechnological techniques to do computation. Routine recombinant DNA techniques for detection, amplification, and editing of DNA can be used for massively parallel molecular computation, because they simultaneously operate on each strand of DNA in a test tube. The advances in molecular biology technology allow recombinant DNA operations to be routine in all the molecular biology laboratories, while these techniques were once considered very sophisticated. Combination of these methods according to the algorithm solved chess problems,[40] SAT problems,[41] and graph coloring problems[42] as well as the Hamiltonian path problem. The parallelism allows DNA computers to solve lager hard problems such as NP-complete

problems in linearly increasing time, in contrast to the exponentially increasing time required by a Turing machine.

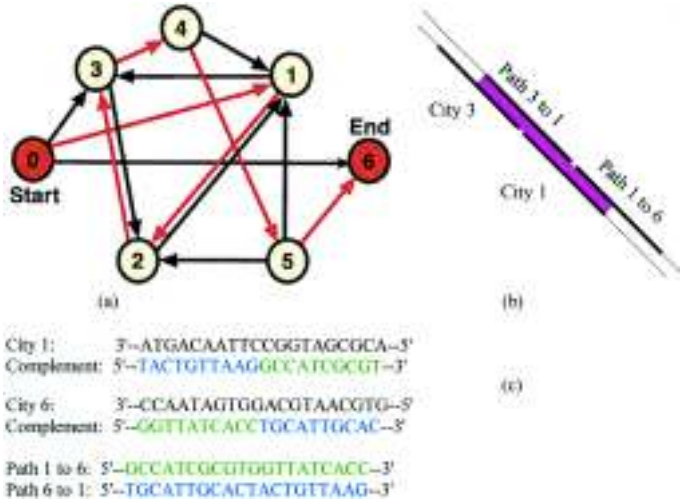

Figure 5. Traveling salesman problem of Leonard Adleman.[40] The object is to find the path by which each city is visited exactly once. (a) Each circle represents a different city and each arrow represents a path with a specific direction; the paths shown are the only ones allowed. There are a several possible routes, but only one that represents the correct path. (b) Adleman represented each city (0–6) with a small sequence of DNA. Each path between the cities is represented with partial complementary sequences of two different cities, such as the path between city 3 and 1 as seen in (b). When the DNA strands interact, they hybridize to form "bridges" between the city strands and create possible routes for the traveling salesman. The correct solution to the problem is: 0 to 3 to 6 to 1 to 2 to 5 to 4. (c) The encoding of the cities and paths is specific and the encoding of the path from city 1 to city 6 is not the same as that of path from city 6 to city 1. The base sequences for the cities were chosen at random; the sequences for the paths were chosen to be complementary to the cities they connect.

DNA Memory

DNA provides a compact means of data storage and a degree of parallelism far beyond that of conventional silicon-based computers. In principle, more than 10^{21} bits of information are packed into each gram of

dehydrated DNA. Recently, Risca *et al.* constructed the method to hind information in DNA.[43] A DNA-encoded massage is first camouflaged within the enormous complexity of human genomic DNA and then further concealed by confining this sample to a microdot. A prototypical 'secret message' DNA strand contains an encoded message flanked by PCR primer sequences. Encryption is not of primary importance in steganography, so we can use a simple substitution cipher to encode characters in DNA sequences. Because the human genome contains about 3×10^9 nucleotide pairs, fragmented and denatured human DNA provides a very complex background for concealing secret-message DNA. For example, a secret message 100 nucleotides long added to treated human DNA at one copy per haploid genome would be hidden in a roughly three-million-fold excess of physically similar DNA strands. Confining such a sample to a microdot might then allow even the medium containing the message to be concealed from an adversary. However, the intended recipient, knowing both the secret-message DNA PCR primer sequences and the encryption key, could readily amplify the DNA and then read and decode the message. Even if an adversary somehow detected such a microdot, it would still prove extremely difficult to read the message without knowing the specific primer sequences.

Molecular Computer

Molecular computation is a term that includes a number of distinct bottom-up approaches toward the design of molecular scale electronics, chemical, and biological computers. By analogy to conventional microprocessors which use elementary logic gates to form electronic circuits capable of performing Boolean logic, design of addressable molecular logic gates has been a major goal in the field of molecular computation. One approach is to use organic and/or inorganic materials in the fabrication of patterned nanoscale electronic logic gates and circuits. An alternative approach has employed molecular or supramolecular systems to create logic gates that respond to chemical and photonic signals. The

advantage afforded by electronic systems in the assembly of circuits lies in its speed and the common input/output signal used, the electron, which permits gates to easily be connected (wired) together. By analogy, if a supramolecular system can be developed using a single class of input/output molecules, then chemical circuits should also be within reach. Ghadiri *et al.* reported progress toward this goal by using the recognition properties of DNA to create photonic logic gates capable of AND, NAND, and INHIBIT logic operation.[44] They coupled two molecular recognition events in series to cause a change in the photonic output of the gate in solution. Sen *et al.* also reported DNA-based molecular switch as a biosensor.[45]

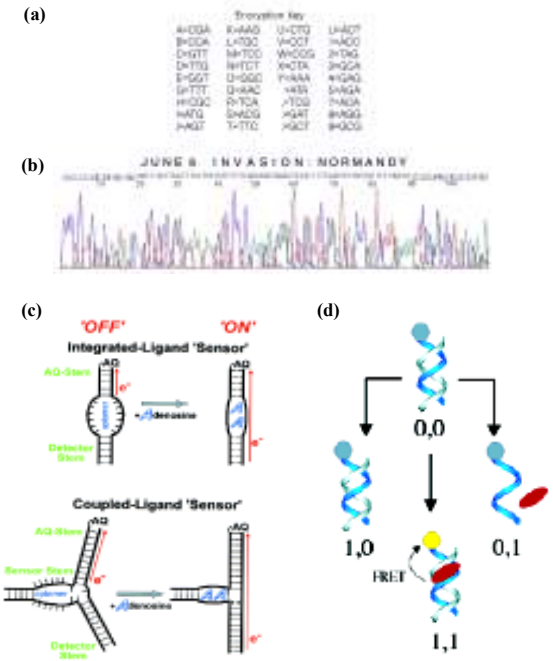

Figure 7. Genomic steganography[43] and DNA logic gates.[44,45] (a) Key used to encode a message in DNA. (b) The result of sequencing using the encryption key to decode the message. The secret message encoded into DNA was decoded with the key described in (a). (c) In the absence of ligand (adenosine), both ODNs adopt open, unstructured conformations, which only allow charge transfer (indicated by arrows) from the AQ stems. (d) The schematic representation of the molecular basis of the logic operations. Output signals were obtained from relative fluorescence emission.

Survey of This Thesis.

This thesis consists of ten chapters on the design of functional modified nucleobases and the application to nanotechnology and biotechnology.

Chapter 1 concerns a protocol for the design of a DNA wire that can effectively mediate hole transport that is not adversely affected by oxidation during hole transport through DNA duplex. A stable and effective DNA wire was synthesized by incorporating a designer nucleobase which has a lower oxidation potential and wider stacking area but is not decomposed during hole transport.

Chapter 2 concerns the modulation of the hole transport efficiency of DNA by complementary bases and the development of a protocol for the preparation of molecular logic gates by using the hole transport properties of designed DNA duplexes. All types of logic gates can be easily prepared according to the protocol. As an example, one of the combinational logic gate, full adder, was prepared according to the protocol.

Chapter 3 concerns the enzymatic synthesis and connection of DNA nanowires. Primer extension with modified nucleoside triphosphate was examined. Ligation reaction with modified ODNs was accomplished. Long-range hole transfer reaction was proceeded through synthesized and connected ODNs.

Chapter 4 concerns the first hole-trapping degenerate base that can control long-range hole migration through an ODN by its unique hole-trapping capacity. The hole-trapping efficiency of the degenerate base is superior to that of the GGG step and similar to that of 7-deazaguanine.

Chapter 5 concerns the development of a novel nucleoside that efficiently releases various function units by oxidation. The use of ODN containing the fluorescence-labeled base facilitates the detection of long–range hole

transport through duplex DNAs without time–consuming analysis steps.

Chapter 6 concerns the development BDF probes containing methoxybenzodeazaadenine (^{MD}A) and methoxybenzodeazainosine (^{MD}I), which give strong fluorescence only when the base on the complementary strand is cytosine and thymine, respectively. A combination of ^{MD}A- and ^{MD}I-containing BDF probes facilitated the T/C SNP typing of a heterozygous sample.

Chapter 7 concerns a novel method for detecting a base at the specific position in DNA sequences using the fluorescence emission of a commonly used fluorophore. A new base–discriminating fluorescent nucleobase which shows a C–selective fluorescence emission was synthesized, and the efficiency of fluorescence resonance energy transfer (FRET) efficiency to fluorescein was measured.

Chapter 8 concerns the development of the novel method for discriminating the genotype in biological samples using BDF probes. BDF probes can detect SNPs in BRCA1 gene without using expensive reagents and time-consuming steps. The BDF probes can be used as a very effective tool for the detection of single base alterations, such as SNPs and point mutations.

Chapter 9 concerns the incorporation of 2-Amino-7-deazaadenine into oligodeoxynucleotides and their base-pairing properties with natural nucleobases were investigated. 7-deazaadenine formed a stable base pair not only with thymine but also with cytosine without any duplex destabilization. While 2-Amino-7-deazaadenine was an effective degenerate base, only dTTP was incorporated opposite to 2-Amino-7-deazaadenine in a single-nucleotide insertion reaction.

Chapter 10 concerns the novel method for key distribution using DNA

based on public-key system. Concealment with dummies and extraction of the key-encoded sequence by PCR amplification can be a one-way functional operation. The key-encoded sequence cannot be read out when an incorrect primer was used in PCR amplification. If enemies are trying to detect the primer sequences or wiretap the concealing key-encoded sequence, they would be required exponential time and labor, that is, security is protected by mathematical and experimental barriers.

References

1. Seeman, N. C. *Biochemistry* **2003**, *42*, 7259-7269.
2. Okamoto, A.; Tainaka, K.; Saito, I. *Tetrahedron Lett.* **2002**, *43*, 4581-4583.
3. Bloomfield, V. A.; Crothers, D. M.; Tinoco, I., Jr. *NUCLIC ACIDS structures, properties, and functions*; University Science Books: California, 2000. Seela, F.; Tran-Thi, Q. H.; Franzen D. *Biochemistry* **1982**, *21*, 4338-4343.
4. Verma, S.; Eckstein, F. *Annu. Rev. Biochem.* **1998**, *67*, 99-134.
5. Sala, M.; Pezo, V.; Pochet, S.; Wain-Hobson, S. *Nucleic Acids Res.* **1996**, *24*, 3302-3306.
6. Loades, D.; Brown, D. M. *Nucleic Acids Res.* **1994**, *22*, 4039-4043.
7. Loades, D.; Brown, D. M.; Linde, S.; Hill, F. *Nucleic Acids Res.* **1995**, *23*, 2361-2366.
8. Nichols, R.; Andrew, P. C.; Zhang, P.; Bergstrom, D. E. *Nature* **1994**, *369*, 492-493.
9. Bergstrom, D. E.; Zhang, P.; Toma, P. H.; Andrew, P. C.; Nichols, R. *J. Am. Chem. Soc.* **1995**, *117*, 1201-1209.
10. Hill, F.; Loakes, D.; Brown, D. M. *Nucleosides Nucleotides* **1997**, *16*, 1507-1511.
11. (a) Wojczewski, C.; Stolze, K.; Engels, J. W. *Synlett* **1999**, 1667-1678. (b) Hawkins, M. E. *Cell Biochem. Biophys.* **2001**, *34*, 257-281.
12. (a) Ward, D. C.; Reich, E.; Stryer, L. *J. Biol. Chem.* **1969**, *244*, 1228-1237. (b) Menger, M.; Tuschl, T.; Eckstein, F.; Porschke, D. *Biochemistry* **1996**, *35*, 14710-14716. (c) Lacourciere, K. A.; Stivers, J. T.; Marino, J. P. *Biochemistry* **2000**, *39*, 5630-5641.
13. (a) Secrist, J. A., III; Barrio, J. R.; Leonard, N. J. *Science* **1972**, *175*, 646-647. (b) Holmen, A.; Albinsson, B.; Norden, B. *J. Phys. Chem.* **1994**, *98*, 13460-13469.
14. (a) Seela, F.; Zulauf, M.; Sauer, M.; Deimel, M. *Helv. Chim. Acta* **2000**, *83*, 910-927. (b) Hurley, D. J.; Seaman, S. E.; Mazura, J. C.; Tor,

Y. *Org. Lett.* **2002**, *4*, 2305-2308.
15. Miller, D. P. *Curr. Opin. Struct. Biol.* **1996**, *6*, 322-326.
16. (a) Strassler, C.; Davis, N. E.; Kool, E. T. *Helv. Chim. Acta* **1999**, *82*, 2160-2171. (b) Kool, E. T. Acc. *Chem. Res.* **2002**, *35*, 936-943.
17. Ward, D. C.; Reich, E.; Stryer, L. *J. Biol. Chem.* **1969**, *244*, 1228-1237.
18. Xu, D.; Evans, K. O.; Nordlund, T. M. *Biochemistry* **1994**, *33*, 9592-9599.
19. Guest, C. R.; Hochstrasser, R. A.; Sowers, L. C.; Miller, D. P. *Biochemistry* **1991**, *30*, 3271-3279.
20. Hustedt, E. J.; Kirchner, J. J.; Spalstenstein, A.; Hopkins, P. B.; Robinson, B. H. *Biochemistry* **1995**, *34*, 4369-4375.
21. (a) Allen, D. J.; Benkovic, S. J. *Biochemistry* **1989**, *28*, 9586-9563. (b) Purohit, V.; Grindley, N. D. F.; Joyce, C. M. *Biochemistry* **2003**, *42*, 10200-10211.
22. Obayashi, T.; Masud, M. M.; Ozaki, A. N.; Ozaki, H.; Kuwahara, M.; Sawai, H. *Bioorg. Med. Chem. Lett.* **2002**, *12*, 1167-1170.
23. Murphy, C. J.; Arkin, M. R.; Jenkins, Y.; Ghatlia, N. D.; Bossmann, S. H.; Turro, N. J.; Barton, J. K. *Science* **1993**, *262*, 1025-1029.
24. (a) Ly, D.; Sanii, L.; Schuster, G. B. *J. Am. Chem. Soc.* **1999**, *121*, 9400-9410. (b) Nakatani, K.; Dohno, C.; Saito, I. *J. Am. Chem. Soc.* **1999**, *121*, 10854-10855. (c) Lewis, F. D.; Kalgutkar, R. S.; Wu, Y.; Liu, X.; Liu, J.; Hayes, R. T.; Wasielewski, M. R. *J. Am. Chem. Soc.* **2000**, *122*, 12346-12351. (d) Giese, B.; Amaudrut, J.; Köhler, A. –K.; Spormann, M.; Wessely, S. *Nature* **2001**, *412*, 318-320.
25. Yu, C. J.; Wang, H.; Wan, Y.; Yowanto, H.; Kim, J. C.; Donilon, L. H.; Tao, C.; Strong, M.; Chong, Y. *J. Org. Chem.* **2001**, *66*, 2937-2942.
26. Nakatani, K.; Dohno, C.; Saito, I. *Tetrahedron Lett.* **2000**, *41*, 10041-10045.
27. (a) Saito, I.; Nakamura, T.; Nakatani, K.; Yoshida, Y.; Yamaguchi, K.; Sugiyama, H. *J. Am. Chem. Soc.* **1998**, *120*, 12686-12687. (b) Saito, I.; Takayama, M.; Sugiyama, H.; Nakatani, K.; Tsuchida, A.; Yamamoto,

M. J. *J. Am. Chem. Soc.* **1995**, *117*, 6406-6407.
28. (a) Lewis, F. D.; Liu, X.; Miller, S. E.; Wasielewski, M. R. *J. Am. Chem. Soc.* **1999**, *121*, 9746-9747. (b) Lewis, F. D.; Wu, T.; Zhang, Y.; Letsinger, R. L.; Greenfield, S. R.; Wasielewski, M. R. *Science* **1997**, *277*, 673-676.
29. Nakatani, K.; Dohno, C.; Saito, I. *J. Org. Chem.* **1999**, *64*, 6306-6311.
30. Nakatani, K.; Dohno, C.; Saito, I. *J. Am. Chem. Soc.* **2002**, *124*, 6802-6803.
31. Ikeda, H.; Saito, I. *J. Am. Chem. Soc.* **1999**, *121*, 10836–10837.
32. Lewis, F. D.; Liu, X.; Liu, J.; Miller, S. E.; Hayes, R. T.; Wasielewski, M. R. *Nature* **2000**, *406*, 51-53.
33. Sartor, V.; Henderson, P. T.; Schuster, G. B. *J. Am. Chem. Soc.* **1999**, *121*, 11027-11033.
34. Hall, D. B.; Barton, J. K. *J. Am. Chem. Soc.* **1997**, *119*, 5045-5046.
35. Kelley, S. O.; Holmlin, R. E.; Stemp, E. D. A.; Barton, J. K. *J. Am. Chem. Soc.* **1997**, *119*, 9861-9870.
36. Sugiyama, H.; Saito, I. *J. Am. Chem. Soc.* **1996**, *118*, 7063-7068.
37. Ramzaeva, N.; Seela, F. *Helv. Chim. Acta* **1995**, *78*, 1083-1090.
38. Okamoto, A.; Taiji, T.; Tainaka, K.; Saito, I. *Bioorg. Med. Chem. Lett.* **2002**, *12*, 1895-1896.
39. Adleman, L. *Science* **1994**, *266*, 1021-1025.
40. Faulhammer, D.; Cukras, A. R.; Lipton, R. J.; Landweber, L. F. *Proc. Natl. Acad. Sci. U.S.A.* **2000**, *97*, 1385-1389.
41. Liu, Q.; Wang, L.; Frutos, A. G.; Condon, A. E.; Corn, R. M.; Smith, L. M. *Nature* **2000**, *403*, 175-179.
42. Liu, Y.; Xu, J.; Pan, L.; Wang, S. *J. Chem. Inf. Comput. Sci.* **2002**, *42*, 524-528.
43. Clelland, C. T.; Risca, V.; Bancroft, C. *Nature* **1999**, *399*, 533-534.
44. Saghatelian, A.; Völcker, N. H.; Guckian, K. M.; Lin, V. S. –Y.; Ghadiri, M. R. *J. Am. Chem. Soc.* **2003**, *125*, 347-348.
45. Fahlman, R. P.; Sen, D. *J. Am. Chem. Soc.* **2003**, *125*, 4310-4316.

CHAPTER 1

Rational Design of DNA Wire Possessing an Extremely High Hole Transport Ability

Abstract: DNA is a promising conductive biopolymer. However, there are problems that need to be solved to realize real DNA wires. These include the low efficiency of hole transport and the serious oxidative damage that can occur during hole transport. We have demonstrated a protocol for the design of a DNA wire that can effectively mediate hole transport that is not adversely affected by oxidation during hole transport through the DNA duplex. We have synthesized a stable and effective DNA wire by incorporating a designer nucleobase, benzodeazaadenine derivatives, which have lower oxidation potentials and wider stacking areas but are not decomposed during hole transport.

Introduction

In recent years, DNA has attracted much attention as a conductive biopolymer.[1] Recent efforts to elucidate the mechanism of long-range hole transport in DNA has encouraged us in the view that DNA can be a good mediator for hole transport by the selection of an appropriate sequence.[2] However, when natural DNA is used as a molecular wire, serious unavoidable oxidative degradation of G bases occurs. In addition, the hole transport in natural DNA is strongly influenced by the sequence and the transport distance.[2,3] Of great importance in the realization of a real DNA wire is the molecular design of an artificial nucleobase that can effectively mediate hole transport and, at the same time, is not oxidatively decomposed. We now report on a protocol for designing an artificial nucleobase that can act as an effective mediator for long-range hole transport without subsequent decomposition. By incorporating a designer nucleobase into DNA, we have accomplished an extremely effective hole transport between two GGG sites that are 76 Å apart without any detectable nucleobase decomposition.

Results and Discussion

We have designed an artificial nucleobase benzodeazaadenine (^{BD}A). This nucleobase would suppress the oxidative damage caused by the addition of water and/or oxygen to the resulting radical cation (hole), which occurs in G runs,[4] and is expected to increase the hole transport efficiency because of the enhanced π-stacking arising from the expanded aromatic system. The synthesis of ^{BD}A nucleoside (**2**) was readily achieved in two steps from 4-chloro-1*H*-pyrimido[4,5-*b*]indole[5] as shown in Scheme 1, and **2** was incorporated via phosphoramidite **5** into DNA using a DNA synthesizer.

Scheme 1[a]

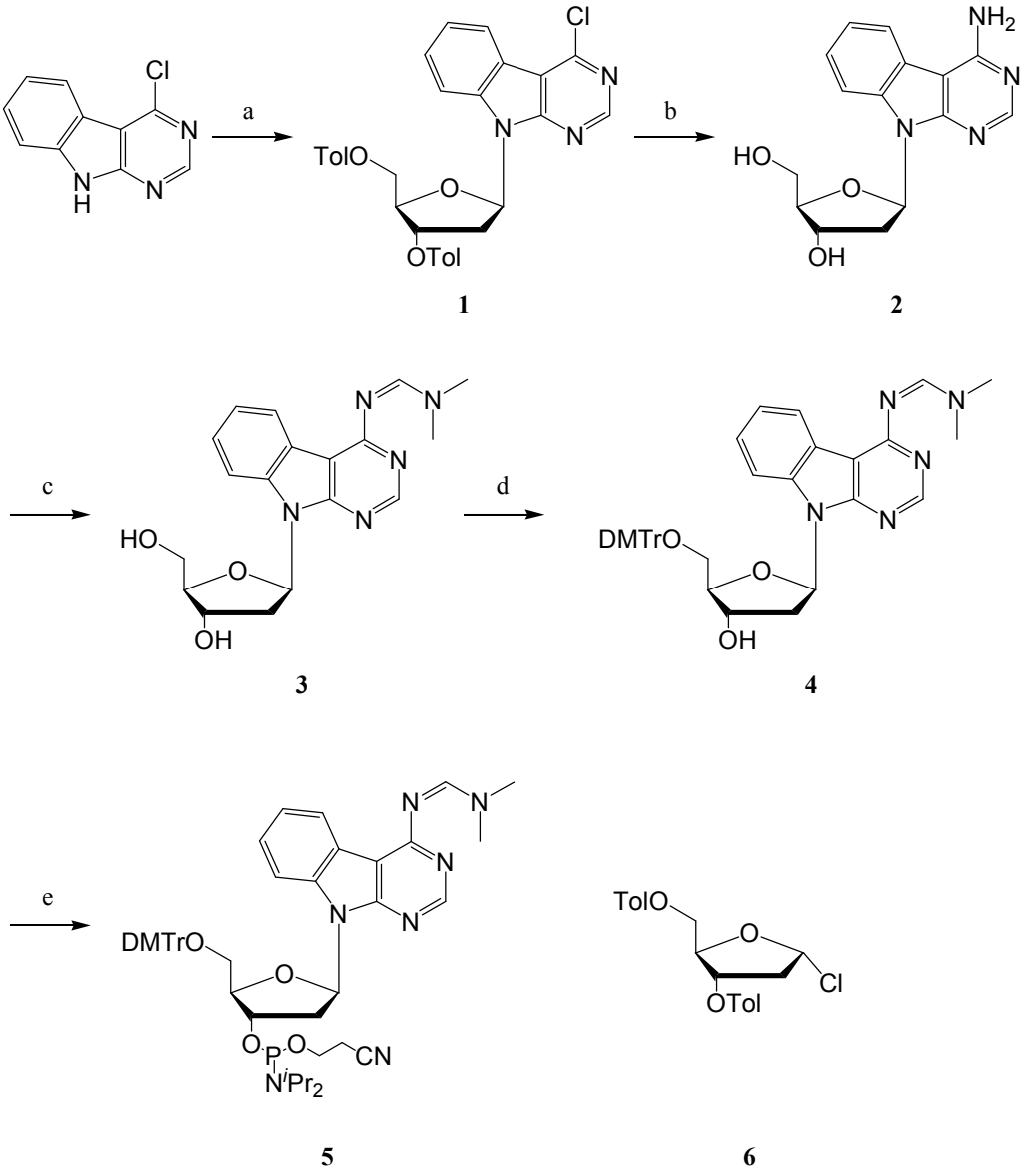

[a]*Reagents:* (a) Sodium hydride, acetonitrile, room temperature, 91%; (b) methanolic ammonia, 150 ˚C, 72%; (c) DMF-dimethylacetal, DMF, 55 ˚C, 87%; (d) 4,4'-dimethoxytrityl chloride, pyridine, room temperature, 72%; (e) 2-cyanoethyl tetraisopropylphosphorodiamidite, tetrazole, acetonitrile, room temperaure, quant.

Initially, we examined the long-range hole transport through ^{BD}A-containing DNA to evaluate the hole transport efficiency and the degree of oxidative degradation of ^{BD}A. The method for determining the hole transport efficiency of the ^{BD}A-containing sequence is shown in Figure 1a. A hole was injected into duplex DNA by an electron-transfer reaction between cyanobenzophenone-substituted uridine (U*)[6] and an adjacent G by photoirradiation at 312 nm. Two GGG steps, which are known as an effective hole trap,[3,7] were incorporated into both sides of the sequence I/II separated by a T spacer. The hole transport efficiency of the sequence I/II was defined by the ratio of oxidative damage at the proximal (G_a) and distal GGG (G_b), as quantified by PAGE. The hole transport efficiency of $^{BD}A_5$ (denoting five consecutive ^{BD}A units) as compared with those of related sequences is shown in Figure 1b. In the reaction of $^{BD}A_5$, a reasonable hole transport value (G_b/G_a = 0.36) was observed, with no oxidative cleavage of $^{BD}A_5$ even after a hot piperidine treatment. After photoirradiation, HPLC analysis of the enzyme-digested DNA showed no degradation of ^{BD}A (in contrast to G runs, where a 5% consumption of G was observed) (Figure 2 and Table 1). In the G runs (i.e., G_5), the hole transport efficiency was relatively low (G_b/G_a = 0.10), and the DNA was strongly damaged at the G_5 site. In the reaction of a sequence where the central ^{BD}A unit of the $^{BD}A_5$ run was replaced by A separating the ^{BD}A units, and for a sequence where an

ATA 3-base bulge[8] was inserted, the G_b/G_a damaging ratios decreased to 0.28 and 0.20, respectively. This showed that the hole transport efficiency decreases by breaking the stacking between the ^{BD}A units. These results imply that a stack of ^{BD}A runs can provide a high hole transport efficiency. It is also noteworthy that the length of the spacer separating the sequence I/II and the GGG hole trap also affected the G_b/G_a damaging ratio.[2f] When the spacer length, *m*, was changed from 2 to 1, the G_b/G_a damaging ratio greatly increased to 0.78 ± 0.06, suggesting that $^{BD}A_5$ is inherently a very effective hole transport mediator.

(a)

hole trap G_a hole trap G_b

5'-^{32}P-AGT *GGG* $(T)_m$- **I** -$(T)_m$ *GGG* -3'

3'— U*CA CCC $(A)_m$- **II** -$(A)_m$ CCC-5'

hole generation

For example (**I**/**II** = $^{BD}A_5/T_5$, spacer m = 2)

5'-^{32}P-ATTTATAGTGTGGGTT^{BD}A^{BD}A^{BD}A^{BD}A^{BD}ATTGGGTTATTAT-3'

3'-TAAATA**U***CACACCCAAT T T T TAACCCAATAATA-5'

U* = 5-[3-(4-cyanobenzyl)phenylethynyl]-2'-deoxyuridine

(b)

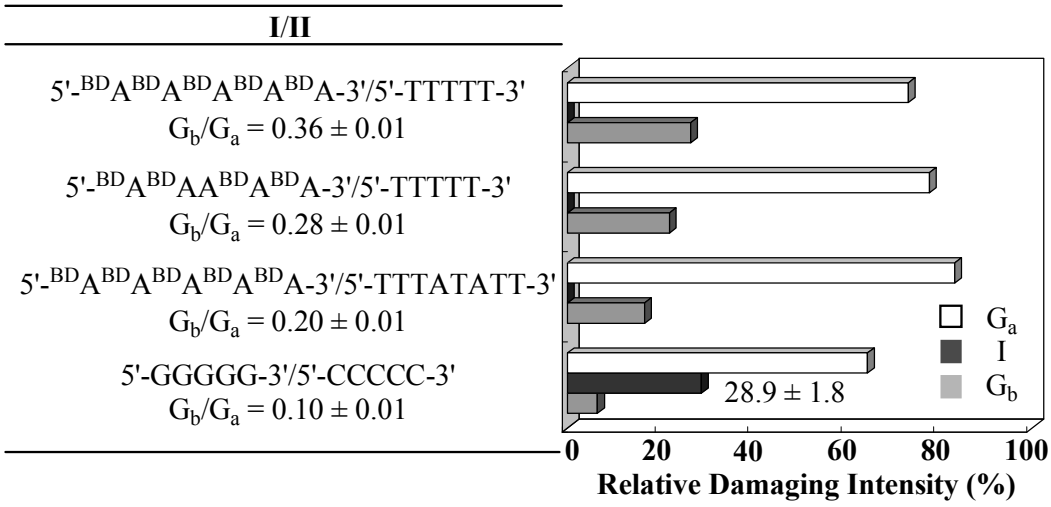

Figure 1 (a) A DNA sequence for measuring the hole transport efficiency of sequence I/II. (b) The ratio G_b/G_a of oxidative damage at G_a and G_b, and the damaging intensity at hole-transporting sequence I/II. The duplexes (spacer m = 2) in 10 mM sodium cacodylate (pH 7.0) were irradiated (= 312 nm) at 0 ˚C for 45 min followed by a hot piperidine treatment. The relative damaging intensities show the percentage of strand breakages at G_a, G_b, and sequence I relative to the total strand cleavage obtained by densitometric analysis. The hole-trapping ratio (G_b/G_a) corresponding to the hole transport efficiency of sequence I/II was calculated from the relative intensities of the oxidative cleavage bands at G_a and G_b.

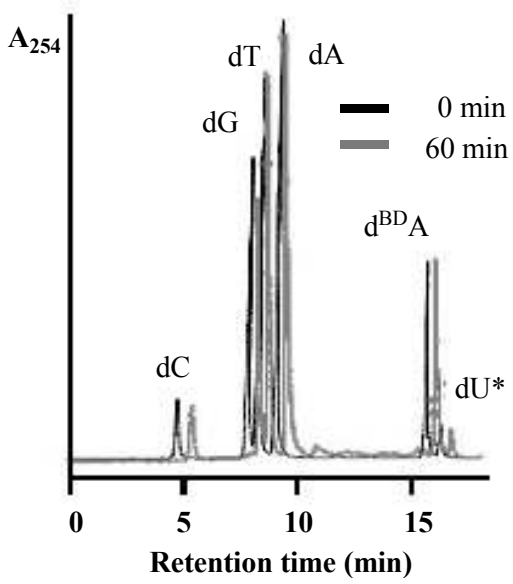

Figure 2. Enzymatic digestion of ODN after photoirradiation. An aliquot of photoirradiation ODN solution was fully digested with calf intenstine alkaline phosphatase (50 U/mL), snake venom phosphodiesterase (0.15 U/mL) and P1 nuclease (50 U/mL) at 37 ºC for 3 h. Digested solution was analyzed by HPLC on CHEMCOBOND 5-ODS-H column (4.6 × 150 mm), elution with a solvent mixture of 0.1 M triethylammonium acetate (TEAA), pH 7.0, linear gradient, 0-20% acetonitrile over 10 min and then 20-80% over another 10 min at a flow rate 1.0 mL/min). Decomposition of nucleosides was determined by the decrease of peak areas of each nucleosides.

Table 1. Decrease of dG and $d^{BD}A$ after photoirradiation (**I**/**II** = $^{MD}A_5/T_5$: spacer, $m = 2$)

Time (min)	$d^{BD}A$ (%)	dG (%)
0	100	100
30	98±3	95±2
45	100±10	95±3
60	101±12	88±1

We next investigated the efficiency of hole transport through the ^{BD}A runs, by increasing the number (n) of ^{BD}A runs from 1 to 20 to know the effect of the length of the π-stacking array of the ^{BD}A runs on the hole transport efficiency. Figure 3 shows the resulting G_b/G_a damaging ratio plotted against n. The G_b/G_a ratio increased with an increasing number of ^{BD}A units in the $^{BD}A_n$ runs (for n = 1-5). This result is in sharp contrast to the hole transport behavior generally observed in natural DNA, which drops off rapidly with increasing distance.[9] Furthermore, G_b/G_a became saturated at a value of ca. 0.4, when the number of ^{BD}A units was greater than five. It has been proposed that stationary polarons in DNA can extend over 5-7 base pairs,[2e,10] and, hence, the influence of the length of the ^{BD}A runs on the hole transport efficiency would possibly relate to the polaron width generated in the DNA. PAGE analysis of these reactions did not show any oxidative degradation of ^{BD}A, regardless of the number of ^{BD}A units in the ^{BD}A runs. Such an effective long-range hole transport without any degradation of the G units is very difficult to achieve in natural DNA.

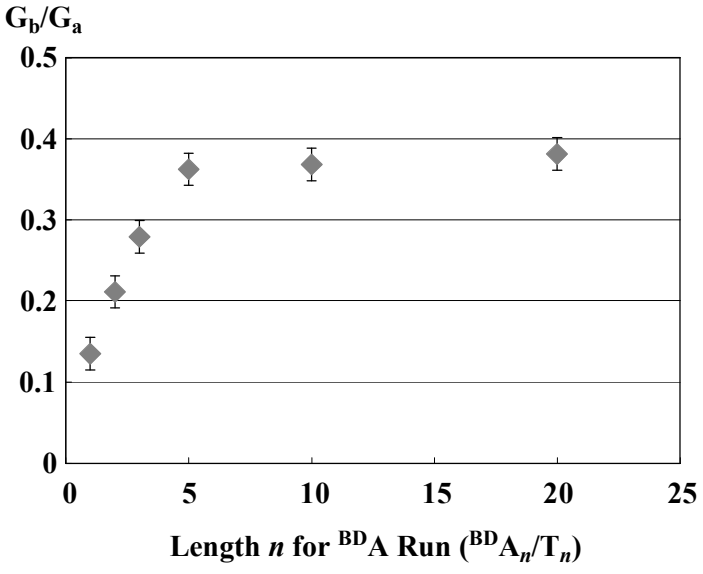

Figure 3. Correlation of the hole transport efficiency to the length of the ^{BD}A runs (spacer m = 2). Estimated error for G_b/G_a was ±0.02.

We next prepared two ^{BD}A derivatives, methoxy-substituted ^{MD}A and naphthalene-fused NDA[11], to elucidate the influence of the oxidation potential and the stacking surface area on the hole transport efficiency. Both the ionization potential[12] and the base stacking[3,13] of the bridge sequence have been discussed as important factors for hole transport efficiency through DNA. The synthesis of ^{MD}A-containing DNA was readily achieved from 4-chloro-6-methoxy-1*H*-pyrimido[4,5-*b*]indole[5] as shown in Scheme 2. The G_b/G_a damaging ratios for ^{MD}A and $^{MD}A_2$ were 0.43 and 0.67, respectively, showing a remarkable increase in the hole transport efficiency (Table 2). In addition, in NDA, the hole transport efficiency was higher than that observed for ^{BD}A. Both ^{MD}A and NDA had lower oxidation potentials than that of ^{BD}A, and the stacking surface areas of dimers $^{MD}A_2/T_2$ and $^{ND}A_2/T_2$ obtained from the calculation of the water-accessible surface were enhanced by 18 and 22%, respectively, when compared to that calculated for ^{BD}A. These results indicate that both the oxidation potential and the stacking of the nucleobases play a key role in mediating a hole transport.

Scheme 2[a]

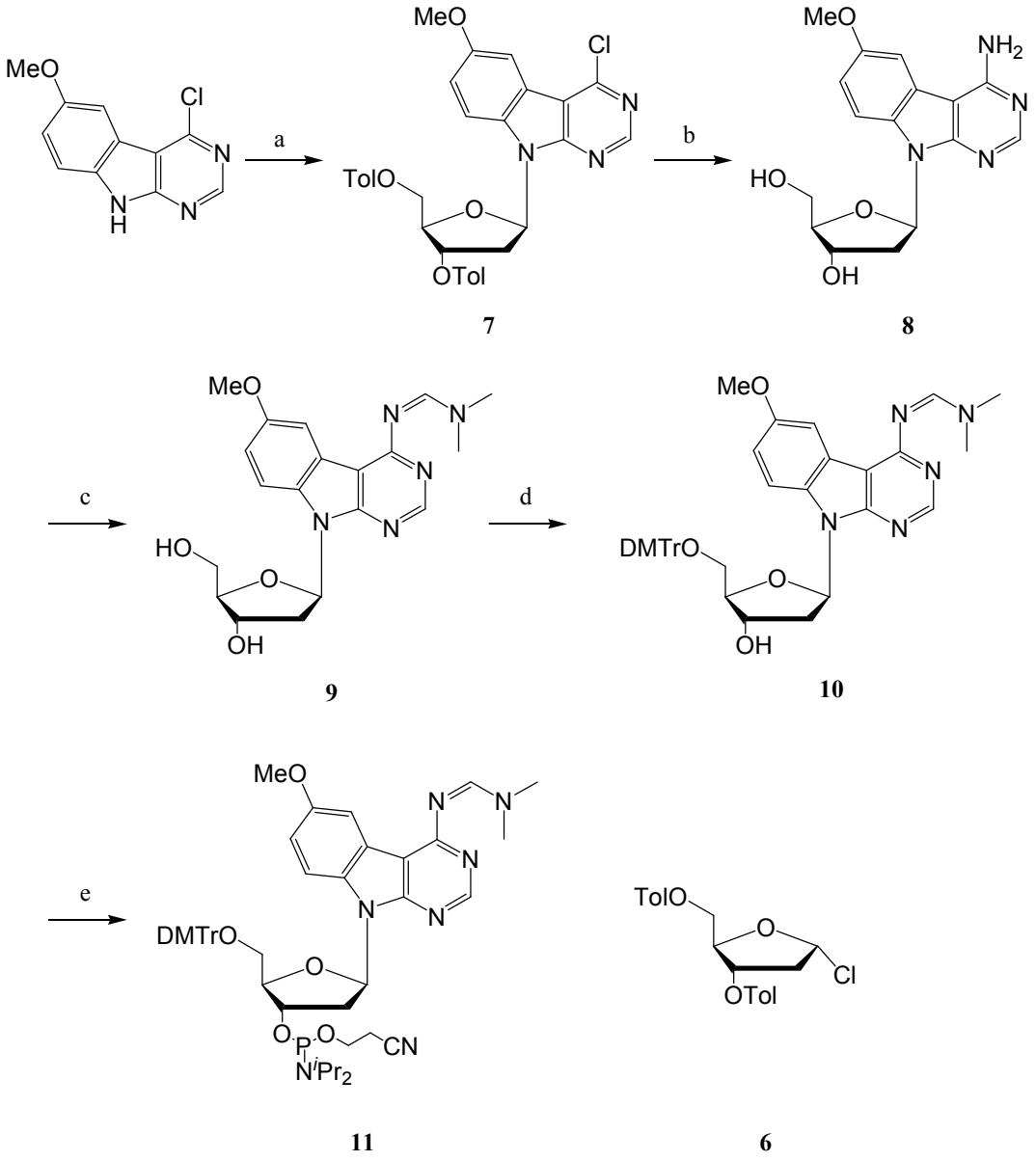

[a]*Reagents*: (a) Sodium hydride, acetonitrile, room temperature, 82%; (b) methanolic ammonia, 150 ˚C, 75%; (c) DMF-dimethylacetal, DMF, 60 ˚C, 88%; (d) 4,4'-dimethoxytrityl chloride, pyridine, room temperature, 75%; (e) 2-cyanoethyl tetraisopropylphosphorodiamidite, tetrazole, acetonitrile, room temperature, quant.

Table 2. Hole transport efficiencies (G_b/G_a) of adenine and ^{BD}A analogues

Bases (**X**)	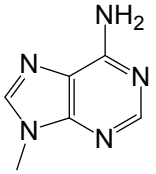 **A**	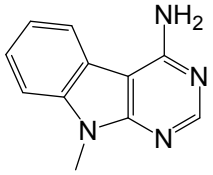 **^{BD}A**	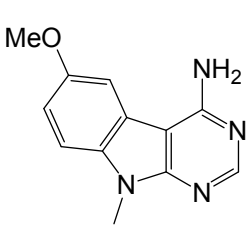 **^{MD}A**	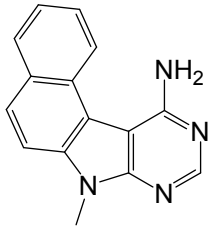 **NDA**
Oxidation Potential (E_p)[a]	1.45 V	1.32 V	1.10 V	1.03 V
Stacking Surface Area[b]	137.1 Å^2	160.1 Å^2	188.3 Å^2	194.7 Å^2
G_b/G_a (**I/II** = **X**/T)	~0	0.14±0.02	0.43±0.04	0.50±0.05
G_b/G_a (**I/II** = **X**$_2$/T$_2$)	–[c]	0.21±0.02	0.64±0.05	0.53±0.08

[a]Oxidation potentials (E_p vs SCE) of nucleosides (R = 2'-deoxyribos-1'-yl) were obtained from cyclic voltarnmograms. The E_p of G was 1.15 V. [b]The stacking surface area of **X**$_2$/T$_2$ (R = H) was caluculated by AMBER* (water set) in MacroModel 6.0. [c]Experiment was not carried out.

On the basis of these results, we designed a DNA sequence containing $^{MD}A_{20}$ and investigated the hole transport efficiency. As shown in Figure 4, the G_b/G_a damaging ratio was 0.99 ± 0.04, implying that a hole in the DNA was effectively free to migrate between two GGG sites (a distance of ca. 7.6 nm). Although ^{MD}A has a smaller oxidation potential than G, no damage of the $^{MD}A_{20}$ was observed from either PAGE analysis or HPLC analysis after enzyme digestion of photoirradiated DNA (Table 3). HPLC analysis for the enzyme-digested DNA after photoirradiation showed 7% destruction of G with almost no ^{MD}A decomposition. This is quite different from the behavior seen in the G runs. As is needed for a molecular wire, the ^{MD}A run behaved as a good mediator for hole transport and was not oxidatively decomposed.

(a)

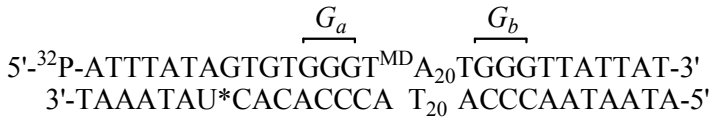

(b)

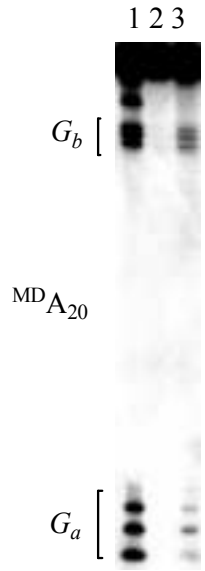

(C)

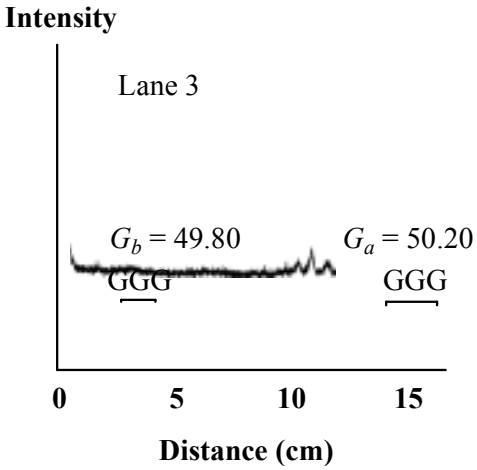

Figure 4. Effective hole transport through an ^{MD}A run. (a) The sequence of duplex DNA containing $^{MD}A_{20}/T_{20}$. (b) An autoradiogram of a denaturing gel electrophoresis of ^{32}P-5'-end-labeled DNA after photoirradiation of the duplex. Lane 1, Maxam-Gilbert G + A sequencing lane; lane 2, control lane (no photoirradiation); lane 3, duplex DNA photoirradiated as described in Figure 1. (c) Densitometric analysis of lane 3 of Figure 3b. The G_b/G_a ratio obtained from the peak areas of the cleavage bands at both GGG sites was 0.99 ± 0.04.

Table 3. Decrease of dG and $d^{MD}A$ after photoirradiation (**I**/**II** = $^{MD}A_{20}/T_{20}$: m = 1)

Time (min)	$d^{MD}A$ (%)	dG (%)
0	100	100
30	101±3	95±5
45	99±2	93±5
60	101±9	88±6

Conclusions

In conclusion, we have demonstrated a protocol for building a DNA nanowire. We indicated three important factors that are prerequisites for designing real DNA nanowires: (i) a highly ordered π-stacking array, (ii) low oxidation potentials, and (iii) suppressed oxidative degradation. In particular, the ^{MD}A runs developed according to this principle showed a remarkably high hole transport ability, similar to that expected for a molecular wire. These DNA wires are suitable for further development encompassing site-specific fabrication and functionalization, which are difficult and troublesome for known conductive materials, such as carbon nanotubes and conductive polymers. In addition, they are expected to constitute a new, well-regulated bionanomaterial that will be widely applicable to electronic devices and biosensors.

Experimental Section

General. ^{1}H NMR spectra were measured with Varian Mercury 400 (400 MHz) spectrometer. ^{13}C NMR spectra were measured with JEOL JNM a-500 (500 MHz) spectrometer. Coupling constants (*J* value) are reported in hertz. The chemical shifts are expressed in ppm downfield from tetramethylsilane, using residual chloroform (δ = 7.24 in ^{1}H NMR, δ = 77.0 in ^{13}C NMR) and dimethyl sulfoxide (δ = 2.48 in ^{1}H NMR, δ = 39.5 in ^{13}C NMR) as an internal standard. FAB mass spectra were recorded on a JEOL JMS DX-300 spectrometer or JEOL JMS SX-102A spectrometer. HPLC was performed on a Cosmosil 5C-18AR or CHEMCOBOND 5-ODS-H column (4.6 × 150 mm) with a Gilson chromatography model 305 using a UV detector model 118 at 254 nm.

4-Chloro-7-(2-deoxy-3,5-di-*O*-*p*-toluoyl-β-$_{D}$-*erythro*-pentofuranosyl)-7*H*-pyrimido[4,5-b]indole (1). 4-Chloro-1*H*-pyrimido[4,5-*b*]indole (360 mg, 1.77 mmol) was suspended in dry acetonitrile (250 mL) at ambient temperature. To this suspension was added sodium hydride (60% in oil; 142 mg, 3.54 mmol), and the mixture was stirred at reflux for 10 min. The ribose **6** (687 mg, 1.77 mmol) was added, and the mixture was stirred for 1 h at ambient temperature. The reaction mixture was concentrated and purified by column chromatography on silica gel, eluting with 20% ethyl acetate in hexane to give compound 1 (890 mg, 91%). ^{1}H NMR ($CDCl_3$): δ 8.71 (s, 1H), 8.36 (d, 1H, *J* = 7.9 Hz), 7.99 (d, 2H, *J* = 8.2 Hz), 7.95 (d, 2H, *J* = 6.6 Hz), 7.79 (d, 1H, *J* = 8.4 Hz), 7.37 (dt, 1H, *J* = 8.1, 0.7 Hz), 7.28 (d, 2H, *J* = 8.1 Hz), 7.27 (dt, 1H, *J* = 8.2, 1.1 Hz), 7.23 (d, 2H, *J* = 8.4 Hz), 7.03 (dd, 1H, *J* = 8.8, 6.2 Hz), 5.93 (dt, 1H, *J* = 6.2, 2.7 Hz), 4.86 (dd, 2H, *J* = 11.1, 3.5 Hz), 4.59 (dd, 1H, *J* = 7.2, 3.9 Hz), 3.56 (ddd, 1H, *J* = 16.1, 7.5, 7.2 Hz), 2.59 (ddd, 1H, *J* = 14.4, 6.2, 2.4 Hz), 2.43 (s, 3H), 2.41 (s, 3H). ^{13}C NMR ($CDCl_3$): δ 166.2, 166.1, 155.6, 153.5, 152.7, 144.4, 144.0, 137.8, 129.8, 129.7, 129.3, 129.2, 128.3, 126.9, 126.5, 123.4, 122.6, 119.1, 112.8, 112.1, 83.6, 81.8, 74.4, 63.8, 35.3, 21.73, 21.70. MS (FAB,

NBA/CH_2Cl_2): m/z (%) 556 [(M + H)$^+$]. HRMS (FAB) calcd for $C_{31}H_{27}ClN_3O_7$ [(M + H)$^+$] 556.1639, found 556.1638.

4-Amino-9-(2'-deoxy-β-$_D$-*erythro*-pentofuranosyl)-7*H*-pyrimido[4,5-*b*]indole (2, ^{BD}A). A suspension of **1** (300 mg, 0.54 mmol) in 20 mL of methanolic ammonia (saturated at -76 ˚C) was stirred at 150 ˚C in a sealed bottle for 10 h. The turbid solution was concentrated and purified by column chromatography on silica gel, eluting with 10% methanol in chloroform to give compound **2** (117 mg, 72%). ^{1}H NMR (DMSO-d_6): δ 8.31 (d, 1H, *J* = 7.7 Hz), 8.27 (s, 1H), 7.84 (d, 1H, *J* = 8.2 Hz), 7.37 (dt, 1H, *J* = 8.2, 1.1 Hz), 7.32-7.25 (3H), 6.82 (dd, 1H, *J* = 8.8, 6.0 Hz), 5.32 (d, 1H, *J* = 4.4 Hz), 5.28 (t, 1H, *J* = 4.9 Hz), 4.46 (m, 1H), 3.86 (dd, 1H, *J* = 7.3, 3.8 Hz), 3.66 (m, 2H), 2.88 (ddd, 1H, *J* = 15.6, 8.8, 6.6 Hz), 2.05 (ddd, 1H, *J* = 15.4, 6.0, 2.2 Hz). ^{13}C NMR (DMSO-d6): δ 157.7, 154.7, 154.4, 135.5, 124.7, 121.3, 121.0, 120.2, 111.8, 87.1, 82.8, 70.9, 61.9, 37.5, 31.5. MS (FAB, NBA/DMSO): m/z (%) 301 [(M + H)$^+$]. HRMS (FAB) calcd for $C_{15}H_{17}N_4O_3$ [(M + H)$^+$] 301.1301, found 301.1297.

4-(*N,N'*-Dimethylaminomethylidene)amino-9-(2'-deoxy-β-$_D$-*erythro*-pentofuranosyl)-9*H*-pyrimido[4,5-*b*]indole (3). A solution of **2** (130 mg, 0.43 mmol) and *N,N*-dimethylformamide dimethylacetal (5 mL, 28.3 mmol) in *N,N*-dimethylformamide (5 mL) was stirred for 18 h at 55 ˚C. The reaction mixture was concentrated to a brown oil and purified by column chromatography on silica gel, eluting with 10% methanol in chloroform to give compound **3** (134 mg, 87%). ^{1}H NMR ($CDCl_3$): δ 8.94 (s, 1H), 8.53 (s, 1H), 8.41 (d, 1H, *J* = 7.1 Hz), 7.49 (d, 1H, *J* = 8.1 Hz), 7.44 (dt, 1H, *J* = 7.1, 1.1 Hz), 7.30 (dt, 1H, *J* = 7.8, 0.9 Hz), 6.73 (dd, 1H, *J* = 8.9, 5.5 Hz), 4.83 (d, 1H, *J* = 5.1 Hz), 4.23 (s, 1H), 4.01 (dd, 1H, *J* = 2.9, 1.4 Hz), 3.82 (m, 1H), 3.31 (s, 3H), 3.29-3.22 (m, 2H), 3.21 (s, 3H), 2.23 (dd, 2H, *J* = 15.4, 5.7 Hz). ^{13}C NMR ($CDCl_3$): δ 161.9, 156.8, 155.2, 153.1, 137.9, 125.9,123.7, 121.4, 121.0, 108.9, 88.8, 85.7, 74.0, 63.8, 41.2, 39.9, 35.2, 31.4. MS (FAB, NBA/CH_2Cl_2): m/z (%) 356 [(M + H)$^+$]. HRMS (FAB)

calcd for $C_{18}H_{22}N_5O_3$ [$(M + H)^+$] 356.1723, found 356.1722.

4-(*N,N′*-Dimethylaminomethylidene)amino-9-(2'-deoxy-5'-*O*-dimethoxytrityl-β-D-*erythro*-pentofuranosyl)-9*H*-pyrimido[4,5-*b*]indole (4). A solution of **3** (60 mg, 0.18 mmol) and 4,4'-dimethoxytrityl chloride (8.0 mg, 0.24 mmol) was stirred in anhydrous pyridine (10 mL) for 2 h at ambient temperature. The reaction mixture was concentrated to a brown oil and purified by column chromatography on silica gel, eluting with a mixed solution of 50:50:5 (v/v/v) hexane, ethyl acetate, and triethylamine to give compound **4** (80 mg, 72%). ^{1}H NMR ($CDCl_3$): δ 8.91 (s, 1H), 8.53 (s, 1H), 8.39 (d, 1H, *J* = 7.7 Hz), 7.70 (d, 1H, *J* = 8.3 Hz), 7.43 (dd, 2H, *J* = 8.6, 1.5 Hz), 7.31 (dd, 4H, *J* = 9.0, 1.5 Hz), 7.27-7.13 (5H), 6.94 (t, 1H, *J* = 7.3 Hz), 6.75 (dt, 4H, *J* = 9.9, 3.1 Hz), 4.85 (dt, 1H, *J* = 7.7, 4.4 Hz), 4.04 (q, 1H, *J* = 4.6 Hz), 3.747 (s, 3H), 3.745 (s, 3H), 3.48 (d, 1H, *J* = 4.6 Hz), 3.30 (s, 3H), 3.21 (s, 3H), 3.25-3.19 (m, 1H), 2.29 (ddd, 1H, *J* = 13.7, 7.0, 3.8 Hz). ^{13}C NMR ($CDCl_3$): δ 161.3, 158.4, 156.52, 156.47, 154.0, 144.7, 136.8, 135.8, 130.14, 130.11, 128.2, 127.8, 126.8, 125.6, 123.5, 121.8, 121.4, 113.1, 111.7, 105.6, 86.5, 84.5, 82.7, 72.6, 63.6, 60.4, 55.2, 45.6, 41.0, 37.7, 35.1, 21.1, 14.2. MS (FAB, NBA/CH_2Cl_2): m/z (%) 658 [$(M + H)^+$]. HRMS (FAB) calcd for $C_{39}H_{40}N_5O_5$ [$(M + H)^+$] 658.2951, found 658.3038.

4-(*N,N′*-Dimethylaminomethylidene)amino-9-(2'-deoxy-5'-*O*-dimethoxytrityl-β-D-*erythro*-pentofuranosyl-3'-*O*-cyanoethyl-*N,N′*-diisopropylphosphoramidite)-9*H*-pyrimido[4,5-*b*]indole (5). A solution of **4** (10 mg, 15.2 μmol), 2-cyanoethyl tetraisopropylphosphorodiamidite (5.3 μL, 16.7 μmol), and tetrazole (1.2 mg, 16.7 μmol) in acetonitrile (400 μL) was stirred at ambient temperature for 2 h. The mixture was filtered off and used without further purification.

4-Chloro-6-methoxy-7-(2-deoxy-3,5-di-*O*-*p*-toluoyl-β-D-*erythro*-pentofuranosyl)-7*H*-pyrimido[4,5-*b*]indole (7). 4-Chloro-6-methoxy-1*H*-pyrimido[4,5-*b*]indole (100 mg, 0.43 mmol) was

suspended in dry acetonitrile (10 mL) at ambient temperature. To this suspension was added sodium hydride (60% in oil; 19 mg, 0.47 mmol), and the mixture was stirred at reflux for 10 min. The ribose 6 (184 mg, 0.47 mmol) was added, and the mixture was stirred for 1 h at ambient temperature. The reaction mixture was concentrated and purified by column chromatography on silica gel, eluting with 20% ethyl acetate in hexane to give compound **7** (210 mg, 82%). ^{1}H NMR ($CDCl_3$): δ 8.69 (s, 1H), 7.97 (d, 2H, *J* = 14.8 Hz), 7.96 (d, 2H, *J* = 14.8 Hz), 7.82 (d, 1H, *J* = 2.6 Hz), 7.68 (d, 1H, *J* = 4.0 Hz), 7.27 (d, 2H, *J* = 16.8 Hz), 7.24 (d, 2H, *J* = 15.7 Hz), 7.00 (dd, 1H, *J* = 8.8, 6.1 Hz), 6.82 (dd, 1H, *J* = 9.0, 2.6 Hz), 5.90 (dt, 1H, *J* = 7.0, 3.3 Hz), 4.85 (dd, 1H, *J* = 12.1, 3.3 Hz), 4.70 (dd, 1H, *J* = 12.1, 4.0 Hz), 4.57 (dt, 1H, *J* = 7.1, 3.6 Hz), 3.87 (s, 3H), 3.48 (ddd, 1H, *J* = 16.3, 8.8, 5.7 Hz), 2.57 (ddd, 1H, *J* = 14.3, 6.0, 2.9 Hz), 2.43 (s, 3H), 2.41 (s, 3H). ^{13}C NMR ($CDCl_3$): δ 166.2, 166.1, 155.8, 155.7, 153.4, 152.7, 144.4, 144.0, 132.2, 129.8, 129.7, 129.3, 129.2, 126.9, 126.5, 119.9, 117.1, 113.0, 112.7, 106.1, 83.6, 81.7, 74.4, 63.8, 55.9, 35.4, 21.74, 21.71. MS (FAB, NBA/CH_2Cl_2): m/z (%) 634 [(M + H)$^+$]. HRMS (FAB) calcd for $C_{32}H_{29}ClN_3O_8$ [(M + H)$^+$] 634.2552, found 634.2553.

4-Amino-6-methoxy-9-(2'-deoxy-β-$_D$-*erythro*-pentofuranosyl)-7*H*-pyrimido[4,5-*b*]indole (8, ^{MD}A). A suspension of **7** (500 mg, 0.85 mmol) in 20 mL of methanolic ammonia (saturated at -76 ˚C) was stirred at 150 ˚C in a sealed bottle for 10 h. The turbid solution was concentrated and purified by column chromatography on silica gel, eluting with 10% methanol in chloroform to give compound **8** (420 mg, 75%). ^{1}H NMR (DMSO-d_6): δ 8.23 (s, 1H), 7.86 (d, 1H, *J* = 2.4 Hz), 7.73 (d, 1H, *J* = 8.8 Hz), 7.29 (br, 2H), 6.97 (dd, 1H, *J* = 9.0, 2.6 Hz), 6.78 (dd, 1H, *J* = 9.0, 6.2 Hz), 5.26 (d, 1H, *J* = 4.4 Hz), 5.20 (t, 1H, *J* = 5.8 Hz), 4.43 (m, 1H), 3.85 (s, 3H), 3.65 (m, 2H), 3.27 (s, 3H), 2.82 (ddd, 1H, *J* = 13.0, 6.8, 2.8 Hz), 2.01 (ddd, 1H, *J* = 13.1, 6.2, 2.3 Hz). ^{13}C NMR (DMSO-d_6): 157.6, 154.8, 154.7, 154.3, 129.9, 120.8, 113.0, 112.4, 104.9, 95.6, 86.9, 82.7, 70.8, 61.8, 55.9, 37.4. MS (FAB, NBA): m/z (%) 331 [(M + H)$^+$]. HRMS (FAB) calcd for

$C_{16}H_{19}N_4O_4$ [$(M + H)^+$] 331.1406, found 331.1402.

4-(*N,N'*-Dimethylaminomethylidene)amino-6-methoxy-9-(2'-deoxy-β-$_D$-*erythro*-pentofuranosyl)-9*H*-pyrimido[4,5-*b*]indole (9). A solution of **8** (90 mg, 0.27 mmol) and *N,N*-dimethylformamide dimethylacetal (10 mL) in *N,N*-dimethylformamide (10 mL) was stirred for 3 h at 60 ˚C. The reaction mixture was concentrated to a brown oil and purified by column chromatography on silica gel, eluting with 10% methanol in chloroform to give compound **9** (120 mg, 88%). ^{1}H NMR ($CDCl_3$): δ 8.93 (s, 1H), 8.50 (s, 1H), 7.97 (d, 1H, *J* = 2.8 Hz), 7.39 (d, 1H, *J* = 9.0 Hz), 7.06 (dd, 1H, *J* = 8.8, 2.6 Hz), 6.66 (dd, 1H, *J* = 9.9, 5.5 Hz), 4.82 (d, 1H, *J* = 4.9 Hz), 4.22 (s, 1H), 4.02 (d, 1H, *J* = 1.6 Hz), 3.90 (s, 3H), 3.82 (m, 1H), 3.31 (s, 3H), 3.22 (s, 3H), 2.94 (s, 1H), 2.86 (s, 1H), 2.21 (dd, 1H, *J* = 13.5, 5.7 Hz). ^{13}C NMR ($CDCl_3$): δ 161.8, 156.8, 155.3, 155.0, 153.1, 132.6, 121.7, 114.3, 109.6, 107.1, 106.8, 88.8, 85.9, 74.0, 63.8, 55.8, 41.2, 39.4, 35.1. MS (FAB, NBA/CH_2Cl_2): m/z (%) 386 [$(M + H)^+$]. HRMS (FAB) calcd for $C_{19}H_{24}N_5O_4$ [$(M + H)^+$] 386.1828, found 386.1827.

4-(*N,N'*-Dimethylaminomethylidene)amino-6-methoxy-9-(2'-deoxy-5'-*O*-dimethoxytrityl-β-$_D$-*erythro*-pentofuranosyl)-9*H*-pyrimido[4,5-*b*]indole (10). A solution of **9** (120 mg, 0.1 mmol) and 4,4'-dimethoxytrityl chloride (137.0 mg, 0.41 mmol) was stirred in anhydrous pyridine (10 mL) for 2 h at ambient temperature. The reaction mixture was concentrated to a brown oil and purified by column chromatography on silica gel, eluting with a mixed solution of 90:3:5 (v/v/v) chloroform, methanol, and triethylamine to give compound **10** (161 mg, 75%). ^{1}H NMR ($CDCl_3$): δ 8.89 (s, 1H), 8.50 (s, 1H), 7.94 (dt, 1H, *J* = 2.9, 2.2 Hz), 7.62 (d, 1H, *J* = 9.0 Hz), 7.31 (dd, 2H, *J* = 8.8, 1.9 Hz), 7.25-7.15 (8H), 6.94 (t, 1H, *J* = 5.3 Hz), 6.75 (d, 4H, *J* = 8.6 Hz), 6.68 (dd, 2H, *J* = 6.9, 2.7 Hz), 4.84-4.80 (m, 1H), 4.05 (q, 1H, *J* = 4.4 Hz), 3.83 (s, 3H), 3.76 (s, 3H), 3.48 (d, 2H, *J* = 4.4 Hz), 3.28 (s, 3H), 3.19 (s, 3H), 3.16-3.11 (m, 1H), 2.93 (dt, 1H, *J* = 14.2, 6.9 Hz), 2.27 (ddd, 1H, *J* = 13.5, 6.8, 3.5 Hz). ^{13}C NMR ($CDCl_3$): δ 161.3,

158.5, 156.6, 156.5, 155.0, 153.9, 144.7, 135.8, 135.76, 131.4, 130.17, 130.14, 129.8, 129.1, 128.2, 127.8, 126.8, 122.6, 113.7, 113.1, 112.6, 107.0, 105.6, 86.5, 84.6, 82.7, 72.4, 63.5, 55.2, 45.5, 41.0, 37.8, 35.0, 9.0. MS (FAB, NBA/CH2Cl2): m/z (%) 688 [(M + H)+]. HRMS (FAB) calcd for C40H42N5O6 [(M + H)+] 688.3135, found 688.3134.

4-(*N,N′*-Dimethylaminomethylidene)amino-6-methoxy-9-(2'-deoxy-5'-*O*-dimethoxytrityl-β-$_D$-*erythro*-pentofuranosyl-3'-*O*-cyanoethyl-*N,N′*-diisopropylphosphoramidite)-9*H*-pyrimido[4,5-*b*]indole (11). A solution of **10** (50 mg, 72.7 μmol), 2-cyanoethyl tetraisopropylphosphorodiamidite (25 μL, 79.9 μmol), and tetrazole (7 mg, 0.1 mmol) in acetonitrile (500 μL) was stirred at ambient temperature for 2 h. The mixture was filtered and used without further purification.

Modified ODN Synthesis. Modified ODNs were synthesized by the conventional phosphoramidite method using an Applied Biosystems 392 DNA/RNA synthesizer. Synthesized ODNs were purified by reversed phase HPLC on a 5-ODS-H column (10 × 150 mm, elution with a solvent mixture of 0.1 M triethylammonium acetate (TEAA), pH 7.0, linear gradient over 30 min from 5 to 20% acetonitrile at a flow rate 3.0 mL/min) or 15% denaturing polyacrylamide gel electrophoresis (PAGE). Mass spectra of ODNs purified by HPLC were determined with ESI-TOF mass spectroscopy or MALDI-TOF mass spectroscopy (acceleration voltage 21 kV, negative mode) with 2',3',4'-trihydroxyacetophenone as matrix, using T8 ([M - H]$^-$ 2370.61) and T17 ([M - H]$^-$ 5108.37) as an internal standard. The ODNs purified by PAGE were characterized by Maxam-Gilbert sequencing reactions.

5'-d(ATTTATAGTGTGGGTTBDABDABDABDABDATTGGGTTATTAT)-3': MALDI-TOF [(M - H)$^-$] calcd 10 511.00, found 10 511.80. 5'-d(ATTTATAGTGTGGGTTBDABDAABDABDATTGGGTTATTAT)-3': MALDI-TOF [(M - H)$^-$] calcd 10 461.93, found 10 461.20.

5'-d(ATTTATAGTGTGGGTBDABDABDABDABDATGGGTTATTAT)-3' : MALDI-TOF [(M - H)$^-$] calcd 9901.61, found 9903.96. 5'-d(ATTTATA-GTGTGGGTTBDATTGGGTTATTAT)-3': MALDI-TOF [(M - H)$^-$] calcd 9060.89, found 9059.34. 5'-d(ATTTATAGTGTGGGTTBDABDATTGGGTTATTAT)-3': MALDI-TOF [(M - H)$^-$] calcd 9424.17, found 9425.89. 5'-d(ATTTATAGTGTGGGTTBDABDABDATTGGGTTATTAT)-3': MALDI-TOF [(M - H)$^-$] calcd 9786.45, found 9788.19. 5'-d(ATTTATAGTGTGGGTTBDA10TTGGGTTATTAT)-3': MALDI-TOF [(M - H)$^-$] calcd 12 322.39, found 12 322.50. 5'-d(ATTTATAGTGTGGGTTBDA20TTGGGTTATTAT)-3': PAGE purification. 5'-d(ATTTATAGTGTGGGTTMDATTGGGTTATTAT)-3': MALDI-TOF [(M - H)$^-$] calcd 9091.92, found 9093.31. 5'-d(ATTTATAGTGTGGGTTMDAMDATTGGGTTATTAT)-3': MALDI-TOF [(M - H)$^-$] calcd 9484.22, found 9482.20. 5'-d(ATTTATAGTGTGGGTTNDATTGGGTTATTAT)-3': MALDI-TOF [(M - H)$^-$] calcd 9111.95, found 9112.59. 5'-d(ATTTATAGTGTGGGTTNDANDATTGGGTTATTAT)-3': MALDI-TOF [(M - H)$^-$] calcd 9524.29, found 9524.74. 5'-d(ATTTATAGTGTGGGTMDA20TGGGTTATTAT)-3': ESI-TOF [(M - 9H)9$^-$] calcd 1773.4693, found 1773.4647.

Measurement of Cyclic Voltammetry (CV) Spectra. Oxidation potentials (E_p) of nucleosides (saturated in water, ca. 200 μM) were measured with an ALS electrochemical analyzer model 660-A in 100 mM $LiClO_4$ solution at room temperature. The scan rate was 100 mV/s. The working electrode was glassy carbon. The counter electrode was Pt wire. The reference electrode was SCE.

Calculation of Stacking Surface Area of Adenine and ^{BD}A Analogues. The interior X_2/T_2 of the duplex 5'-d(AAXXXXAA)-3'/5'-d(TTTTTTTT)-3', as calculated by AMBER* (water set) in MacroModel 6.0, was used for

calculating the stacking surface area of X_2/T_2 (R = H in Table 1). The stacking surface area was calculated from (stacking surface area of X_2/T_2) = {(water-accessible surface area of X/T) × 2 - (water-accessible surface area of X_2/T_2)}/2. A probe radius value of 1.4 Å was used for calculating the water-accessible surface area.

Preparation of ^{32}P-5'-End-Labeled Oligomers. The ODNs (400 pmol-strand) were 5'-end-labeled by phosphorylation with 4 μL of [γ-^{32}P]ATP (Amersham) and T4 polynucleotide kinase using a standard procedure. The 5'-end-labeled ODN was recovered by ethanol precipitation and further purified by 15% denaturing polyacrylamide gel electrophoresis (PAGE) and isolated by the crush and soak method.

Hole Transport Experiment and PAGE Analysis. ^{32}P-5'-End-labeled ODNs were hybridized to the complementary strand containing cyanobenzophenone-substituted uridine in 10 mM sodium cacodylate buffer (pH 7.0). Hybridization was achieved by heating the sample at 90 ˚C for 3 min and slowly cooling to room temperature. Photoirradiation was then carried out in a 100 μL total volume containing 30 kcpm of ^{32}P-5'-end-labeled ODNs and their complementary strands (2 μM strand concentration) in 10 mM sodium cacodylate buffer at pH 7.0. The reaction mixtures were irradiated with a transilluminator (312 nm) at a distance of 3 cm at 0 ˚C for 45 min. After irradiation, all reaction mixtures were precipitated with the addition of 10 μL of 3 M sodium acetate, 20 μL of herring sperm DNA (1 mg/ mL), and 800 μL of ethanol. The precipitated ODN was washed with 100 μL of 80% cold ethanol and dried *in vacuo*. The precipitated ODN was resolved in 50 μL of 10% aniline (v/v), heated at 50 ˚C for 20 min, evaporated by vacuum rotary evaporation to dryness, and resuspended in 5-20 μL of 80% formamide loading buffer (a solution of 80% v/v formamide, 1 mM EDTA, 0.1% xylenecyanol, and 0.1% bromophenol blue). All reactions, along with Maxam-Gilbert G + A sequencing reactions, were conducted with heating at 90 ˚C for 1 min and

quickly chilled on ice. The samples (1 μL, 3-10 kcpm) were loaded onto 15% denaturing 19:1 acrylamide:bisacrylamide gel containing 7 M urea, electrophoresed at 1900 V for approximately 1.5 h, and transferred to a cassette and stored at -80 ˚C with Fuji X-ray film.

Enzymatic Digestion of ODN after Photoirradiation. An aliquot of photoirradiated ODN solution was fully digested with calf intestine alkaline phosphatase (50 U/mL), snake venom phosphodiesterase (0.15 U/mL), and P1 nuclease (50 U/mL) at 37 ˚C for 3 h. The digested solution was analyzed by HPLC on a CHEMCOBOND 5-ODS-H column (4.6 × 150 mm, elution with a solvent mixture of 0.1 M triethylammonium acetate (TEAA), pH 7.0, linear gradient, 0-20% acetonitrile over 10 min, and then 20-80% over another 10 min at a flow rate 1.0 mL/min). The decomposition of nucleosides was determined by the decrease of peak areas of each nucleoside.

References

1. (a) Fink, H.-W.; Schönenberger, C. *Nature* **1999**, *398*, 407–410. (b) Porath, D.; Bezryadin, A.; de Vries, S.; Dekker, C. *Nature* **2000**, *403*, 635–638. (c) Cai, L.; Tabata, H.; Kawai, T. *Appl. Phys. Lett.* **2000**, *77*, 3105–3106. (d) Kasumov, A. Y.; Kociak, M.; Guéron, S.; Reulet, B.; Volkov, V. T.; D. V. Klinov, D. V.; Bouchiat, H. *Science* **2001**, *291*, 280–281.
2. (a) Hall, D. B.; Holmlin, R. E.; Barton, J. K. *Nature* **1996**, *382*, 731–735. (b) Burrows, C. J.; Muller, J. G. *Chem. Rev.* **1998**, *98*, 1109–1154. (c) Grinstaff, M. W. *Angew. Chem. Int. Ed.* **1999**, *38*, 3629–3635. (d) Núñez, M. E.; Barton, J. K. *Curr. Opin. Chem. Biol.* **2000**, *4*, 199–206. (e) Schuster, G. B. *Acc. Chem. Res.* **2000**, *33*, 253–260. (f) Giese, B. *Acc. Chem. Res.* **2000**, *33*, 631–636. (g) Lewis, F. D.; Letsinger, R. L.; Wasielewski, M. R. *Acc. Chem. Res.* **2001**, *34*, 159–170.
3. Recently, A runs have been reported to be a less distance-dependent mediator for hole transport. (a) Giese, B.; Amaudrut, J.; Köhler, A.-K.; Spormann, M.; Wessely, S. *Nature* **2001**, *412*, 318–320. (b) Kendrick, T.; Giese, B. *Chem. Commun.* **2002**, 2016–2017.
4. Cadet, J.; Berger, M.; Buchko, G. W.; Joshi, P. C.; Raoul, S.; Ravanat, J.-L. *J. Am. Chem. Soc.* **1994**, *116*, 7403–7404.
5. Showalter, H. D. H.; Bridges, A. J.; Zhou, H.; Sercel, A. D.; McMichael, A.; Fry, D. W. *J. Med. Chem.* **1999**, *42*, 5464–5474.
6. Nakatani, K.; Dohno, C.; Saito, I. *J. Org. Chem.* **1999**, *64*, 6901–6904.
7. Saito, I.; Nakamura, T.; Nakatani, K.; Yoshioka, Y.; Yamaguchi, K.; Sugiyama, H. *J. Am. Chem. Soc.* **1998**, *120*, 12686–12687.
8. Rosen, M. A.; Shapiro, L.; Patel, D. J. *Biochemistry* **1992**, *31*, 4015–4026.
9. (a) Bixon, M.; Giese, B.; Wessely, S.; Langenbacher, T.; Michel-Beyerle M. E.; Jortner, J. *Proc. Natl. Acad. Sci. U.S.A.* **1999**, *96*, 11713–11716. (b) Grozema, F. C.; Berlin, Y. A.; Siebbeles, L. D. A.

J. Am. Chem. Soc. **2000**, *122*, 10903–10909.

10. (a) Conwell, E. M.; Rakhmanova, S. V. *Proc. Natl. Acad. Sci. U.S.A.* **2000**, *97*, 4556–4560. (b) Rakhmanova, S. V.; Conwell, E. M. *J. Phys. Chem. B* **2001**, *105*, 2056–2061.
11. (a) Saito, I.; Nakamura, T.; Nakatani, K.; Yoshioka, Y.; Yamaguchi, K.; Sugiyama, H. *J. Am. Chem. Soc.* **1998**, *120*, 12686–12687. (b) Nakatani, K.; Dohno, C.; Saito, I. *J. Am. Chem. Soc.* **2000**, *122*, 5893–5894.
12. (a) Holmlin, R. E.; Dandliker, P. J.; Barton, J. K. *Angew. Chem. Int. Ed.* **1997**, *24*, 2715–2730. (b) Treadway, C. R.; Hill, M. G.; Barton, J. K. *Chem. Phys.* **2002**, *281*, 409–428.

CHAPTER 2

Protocol for the Construction of Logic Gates Using DNA

Abstract: We evaluated the modulation of the hole transport efficiency of DNA by complementary bases. In the reaction for the duplex containing a methoxybenzodeazaadenine (^{MD}A)/T base pair, a reasonable hole transport was observed. On the other hand, in the reaction of a sequence where the base opposite ^{MD}A was replaced by C, the hole transport was strongly suppressed. The influence of complementary pyrimidine bases on hole transport efficiency of ^{MD}A is quite contrary to the selectivity observed for G that G/C base pair is a good hole carrier but G/T base pair strongly suppresses hole transport. These orthogonal hole-transporting properties can be an important key for making logic gate systems. We report on new molecular logic gates utilizing hole transport ability of designed short DNAs containing ^{MD}A. This logic gate has been designed in order to observe the output signal when hole transport occurred. We show a general protocol for the preparation of DNA logic gates and circuits. The advantages of DNA logic gates are, i) hole transport (*i.e.* charge transfer) is used, ii) the unit size per an input is only 1 nm, and iii) all types of logic gates can be easily prepared according to the protocol. As an example, one of combinational logic gate, full adder, was prepared according to the protocol.

Introduction

The design and construction of molecular and supramolecular systems that respond to chemical and/or photonic inputs by generating output signals that are in accordance with logic gate behavior has attracted considerable attention.[1] Only in the past few years scientists have realized key experimental demonstrations of molecules that serve as molecular logic gates, represented by switchable rotaxane systems and PET-based sensors.[2] However, despite the broadly based and encouraging recent progress, a set of technical challenges still must be overcome to make an easily designable, robust, and universal logic circuit integrated on the molecular scale. In addition, logic circuits must be produced that are molecular scale in their entirety, not just incorporating molecular-scale components. Clearly, the degree of complexity that can be achieved with only one molecular logic gate is limited. If a supramolecular system in which logic gates are integrated can be developed, then chemical circuits should also be within reach.

For new generation of molecular logic gates, we focused on DNA, which is a biomolecule possessing well-regulated structures and stores genetic information.[3] In the last decade it has been demonstrated that biochemical methods based on oligonucleotides can be successfully employed for solving hard computational problems.[4] This unique capability of nucleic acids has attracted attention in the context of molecular computing. In addition, DNA can form self-assembled monolayer on gold surface,[5] construct complicated geometric structure,[6] and be site-specifically modified by chemical reactions.[7] Valuable nature of DNA is that a long-range hole transport reaction through DNA occurs.[8] A number of mechanistic and physical studies on DNA hole transport have been reported. Recently, we have found that an artificial nucleobase ^{MD}A which is the first base transporting the hole efficiently in the duplex.[9] ^{MD}A run acts as a robust wire that facilitates an efficient long-range hole transport. This property is contrast to the hole transport property observed for G that the

hole transports only when G forms a base pair with C. The orthogonality of these hole transport properties will be very promising for the design of a new molecular logic gate.

Here, we report on brand-new molecular logic gates utilizing hole transport ability of designed short DNAs containing ^{MD}A. This logic gate has been designed in order to observe the output signal when hole transport occurred. We showed a general protocol for the preparation of DNA logic gates and circuits. The advantages of DNA logic gates are, i) hole transport (*i.e.* charge transfer) is used, ii) the unit size per an input is only 1 nm, and iii) all types of logic gates can be easily prepared according to the protocol.

Results and Discussion

The sequence designed for the ^{MD}A-mediated logic gate is shown in Figure 1A. The duplex includes cyanobenzophenone-substituted uridine (**S**) as a photosensitizer and two GGG steps as detectors of hole in DNA.[10] GGG steps, which are known as an effective hole trap, were incorporated into both sides of the logic gate sequence **I**/**II** separated by T/A spacers. Hole transport reaction was triggered by photoirradiation with a transilluminator (312 nm) at 0 °C. To visualize the hole transport results, the resulting ODN was heated in 10% piperidine at 90 °C, and then the oxidative strand cleavage at GGG steps was analyzed by polyacrylamide gel electrophoresis (PAGE).[9] The hole transport efficiency of the logic gate sequence **I**/**II** was defined by the ratio of oxidative strand cleavage at the distal GGG (G_b) *vs* the proximal GGG (G_a).

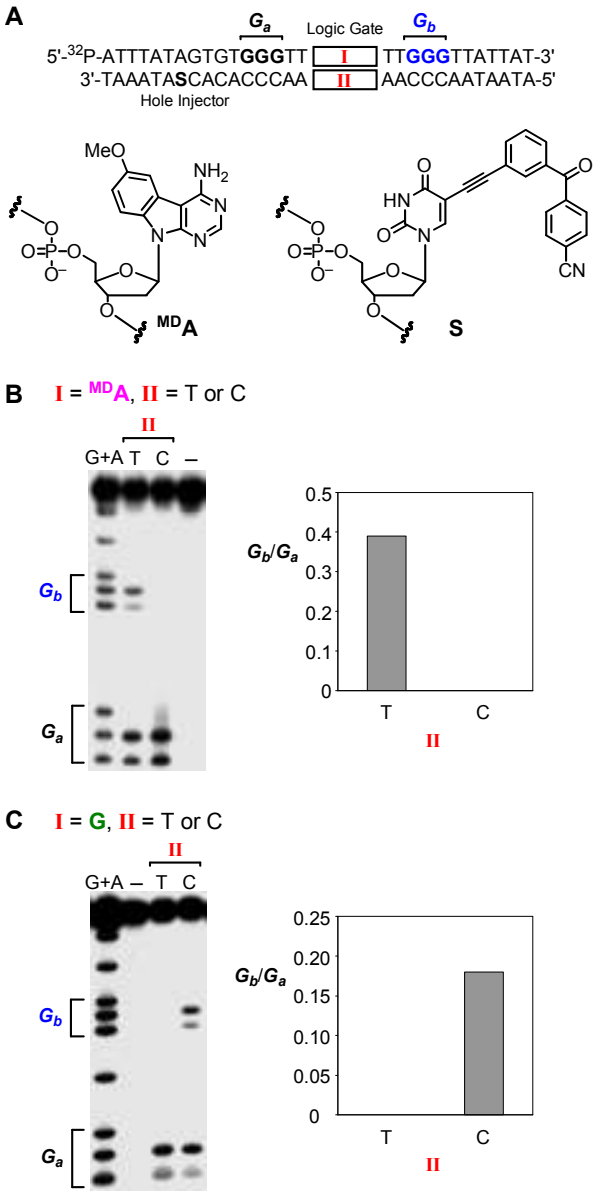

Figure 1. Basic logic gates, YES and NOT using DNA. (A) DNA sequence in this experiment. **S** represents cyanobenzophenone-tethered uridine ($d^{CNBP}U$); (B) autoradiogram of a denaturing gel electrophoresis of ^{32}P-5'-end-labeled DNA after photooxidation of the duplexes. Lane 1, Maxam-Gilbert G+A sequencing lane; lane 2, **I**=^{MD}**A**, **II**=T; lane 3, **I**=^{MD}**A**, **II**=C; lane 4, control (**I**=^{MD}**A**, **II**=T) without irradiation; (C) lane 1, Maxam-Gilbert G+A sequencing lane; lane 2, control (**I**=G, **II**=C) without irradiation; lane 3, **I**=G, **II**=T; lane 4, **I**=G, **II**=C. Output signals obtained from densitometric analysis were shown at the side of autoradiogram, and they represented YES and NOT logic gate, respectively.

Initially, we evaluated the modulation of the hole transport efficiency of ^{MD}A-containing DNA occurred by pyrimidines forming a base pair with ^{MD}A. The experimental result is shown in Figure 1B. In the reaction for the duplex containing an ^{MD}A/T base pair, a reasonable hole transport value (damaging ratio, G_b/G_a = 0.39) was observed. On the other hand, in the reaction of a sequence where the base opposite ^{MD}A was replaced by C, the G_b/G_a damaging ratio was negligible ($G_b/G_a < 0.01$), suggesting that the hole transport was strongly suppressed when ^{MD}A formed a base pair with C. It is probably due to the disturbance of the π-stacking of base pairs that plays a key role in efficient hole transport.[9] The influence of complementary pyrimidines on hole transport efficiency of ^{MD}A is quite contrary to the selectiveity observed for G that G/C base pair is a good hole carrier but G/T base pair strongly suppresses hole transport (Figure 1C). These orthogonal hole-transporting properties can be an important key for making logic gate systems. In other words, if input signals "1" and "0" are applied to T and C in sequence **II**, respectively, then the result of the hole transport mediated by ^{MD}A is like a YES logic and that by G is like a NOT logic that performs inversions. Thus, the ease with which ^{MD}A/T and ^{MD}A/C base pairs can modulate hole transport is a useful starting point for designing DNA-based logic gates. Systems which respond to a given combination of hole transport-controllable base pairs open the way to more complex logic gates at the molecular scale.

Addition of extra base pairs modulating hole transport through DNA would be a rational approach to logic systems which handle two or more inputs. We built an AND logic by arranging two ^{MD}A in single logic sequence. To the AND sequence containing two ^{MD}A bases in series (It denotes ^{MD}A-^{MD}A.), we hybridised the input sequence containing two input pyrimidines (Y_1-Y_2) (Figure 2A). In these sequences designed for AND logic, the input pyrimidines have been separated by two T/A base pairs to independently work. The size of one input region including a input and spacers is three base pairs, *i.e.* only 1 nm length. As results of hole transport experiments for these sequences, when the strand where both

input pyrimidines are T was used, the strand cleavage at G_b site as an output signal, indicating that effective hole transport occurred, was observed ($G_b/G_a = 0.43$), as shown in Figure 2A. When Y_1 and/or Y_2 are C, hole transport to G_b site was strongly suppressed ($G_b/G_a < 0.01$). The sequence containing multiple ^{MD}A bases in series can provide the basis for a sharp AND logic action.

Next, we designed an OR DNA logic gate, which is expressed by sum of inputs, and converted the OR equation to a standard sum-of-product (SOP) expression, which is the one when all the variables in the domain appear in each product term in the expression. Standard SOP expressions facilitate the sequence design of DNA logic gates. We designed three sequences for OR logic, ^{MD}A-^{MD}A, ^{MD}A-G and G-^{MD}A, according to each product term in the standard SOP expression of OR logic, and simultaneously analyzed their hole transport reactions in single cuvette (Figure 2B). The resulting PAGE exhibited the strand cleavage bands at the G_b site when the input sequence Y_1-Y_2 is T-T, T-C and C-T (G_b/G_a = 0.12, 0.10 and 0.08, respectively). For C-C input, the strand cleavage at the G_b site was not observed ($G_b/G_a < 0.01$). The cleavage pattern observed for this mixed sample exhibited an OR logic behavior under sequence conditions designed according to standard SOP expression. NOT, AND and OR gates are the basic logic gates from which all logic functions are constructed, and we can create any combinational logic circuits when these gates are assembled in DNA sequence. We have found that specific sequences of YES, NOT, OR, and AND operations can be programmed in a single cuvette by applying standard SOP expressions. Combination of these operators would offer the possibility of obtaining any combinational logic circuit.

Equation 1. The protocol for design of DNA sequences. The values, m, n, and X are determined according to standard SOP expression.

m = (the number of Boolean multiplication in minterm) + 1
X: A$\rightarrow$^{MD}A, $\overline{\text{A}}\rightarrow$G
n = the number of minterm

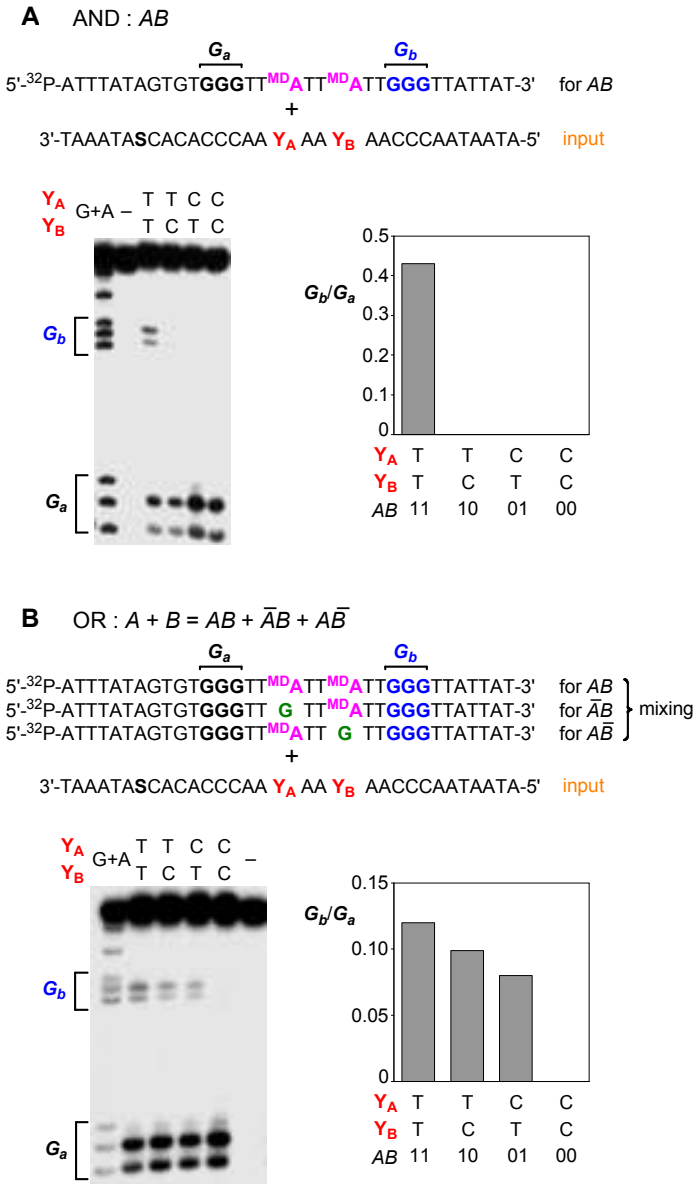

Figure 2. Band intensities of the AND and OR gates**.** (A) autoradiogram of a denaturing gel electrophoresis of ^{32}P-5'-end-labeled DNA after photooxidation of the duplexes. Lane 1, Maxam-Gilbert G+A sequencing lane; lane 2, control without irradiation; lane 3, $\mathbf{Y_A}$=T, $\mathbf{Y_B}$=T; lane 4, $\mathbf{Y_A}$=T, $\mathbf{Y_B}$=C; lane 5, $\mathbf{Y_A}$=C, $\mathbf{Y_B}$=T; lane 6, $\mathbf{Y_A}$=C, $\mathbf{Y_B}$=C; (B) lane 1, Maxam-Gilbert G+A sequencing lane; lane 2, $\mathbf{Y_A}$=T, $\mathbf{Y_B}$=T; lane 3, $\mathbf{Y_A}$=T, $\mathbf{Y_B}$=C; lane 4, $\mathbf{Y_A}$=C, $\mathbf{Y_B}$=T; lane 5, $\mathbf{Y_A}$=C, $\mathbf{Y_B}$=C; lane 6, control without irradiation. Output signals obtained from densitometric analysis were shown at the side of autoradiogram, and they represented AND and OR logic gate, respectively.

The assembled forms of DNA logic gates should lead to a more complicated system capable of performing as an adder, one of combinational logics. A full-adder, as the basic component of computational arithmetic in semiconductor technology, is a digital circuit that adds three inputs (A, B and C_{in}) to produce two outputs (Σ and C_{out}). On the basis of the results described above, we created a full-adder logic, according to their standard SOP expression. Figure 3A shows a schematic representation of circuits that can perform the full-adder operations. We prepared two cuvettes for Σ calculation and output carry calculation. Logic strands in each cuvette were designed according to the standard SOP expression of the full-adder logic. As results of photoirradiation and PAGE analysis for each cuvette, the hole transport efficiency shown in Figure 3B was obtained for each input strand. The strand cleavage efficiencies were in good agreement with the truth table of full adder as shown in Figure 3C. This DNA logic circuit system designed according to protocols described above satisfied full adder logic.

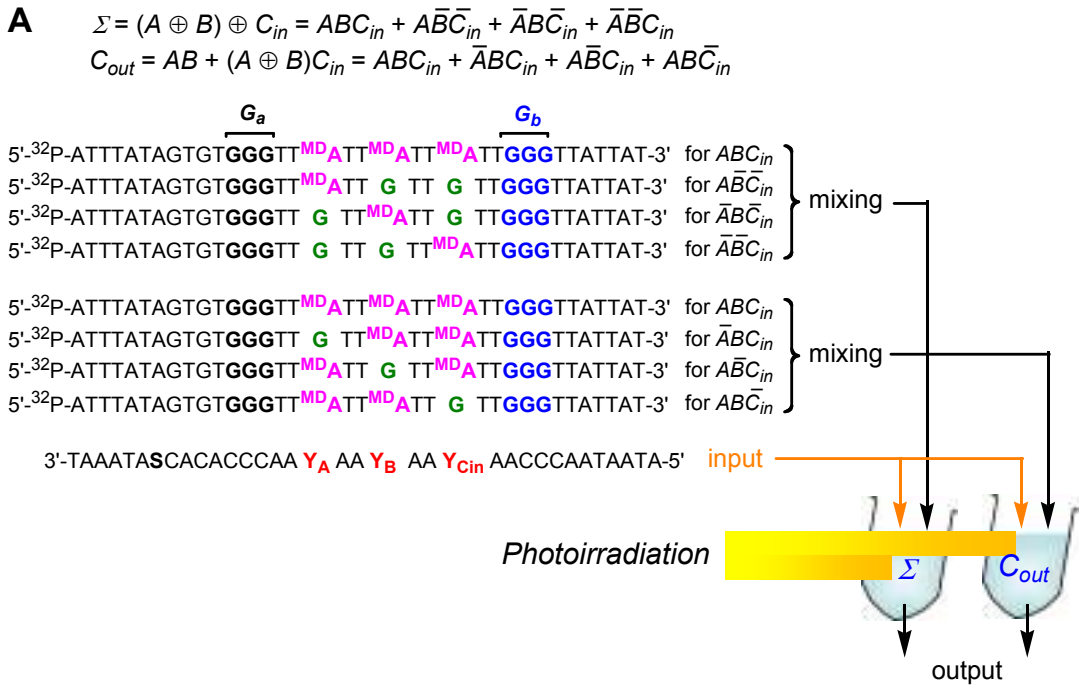

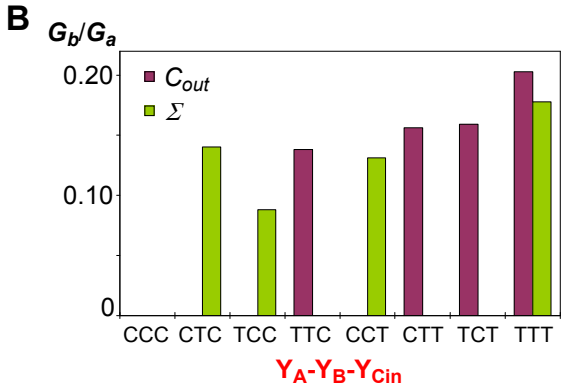

C

Input Seq.			Inputs			Outputs	
Y_1	Y_2	Y_3	A	B	C_{in}	C_{out}	Σ
C	C	C	0	0	0	0	0
C	T	C	0	1	0	0	1
T	C	C	1	0	0	0	1
T	T	C	1	1	0	1	0
C	C	T	0	0	1	0	1
C	T	T	0	1	1	1	0
T	C	T	1	0	1	1	0
T	T	T	1	1	1	1	1

Figure 3. Preparation of the Full Adder gate. (A) Standard SOP expression of Full Adder gate and ODNs used in this experiment. Logic strands were designed according to the standard SOP expression of the full-adder logic. As results of photoirradiation and PAGE analysis, the hole transport efficiency was obtained for each input strand. (B) Comparison between observed outputs and expected outputs. (C) The truth table of Full Adder gate.

Conclusion

In conclusion, we have demonstrated a design of a DNA logic gate. We indicated four important rational factors that are prerequisite for designing real DNA logic gates: (i) modulation bases of ^{MD}A and G-mediated hole transport by complementary pyrimidines results in a remarkably complementary base-selective hole transport ability. In addition, if output is obtained as digital electronic signals instead of the band intensity of G_b in PAGE analysis, it could be easy to joint this DNA nanotechnology to known silicon tip technology; (ii) multiple input pyrimidine sites are arranged in series for AND operation; (iii) DNA logic gates are in nanometer scale (1 nm/ gate); and (iv) equations for OR logic and combinational logic are converted to standard SOP expressions to design DNA logic gates. Any logic gates can be prepared by designing sequences according to the protocol. In addition, it means that every set of YES and NOT gates which can generate output signals by same input signals is prepared by complicated logic gates according to eq. 1. The DNA logic gates developed by this principle are easily applicable to complicated combinational logic circuits such as a full-adder. Our DNA logic circuits was produced in a molecular scale in their entirety, not just incorporating molecular-scale components. These DNA logic gates are suitable for further development encompassing well-regulated assembly and site-specific fabrication, which are other difficult and troublesome for known molecular logic gates. In addition, they are expected to constitute a new, well-regulated bionanomaterial that will be widely applicable to electronic devices and biosensors.

Experimental Section

General. The reagents for the DNA synthesizer such as A, G, C, and T-β-cyanoethyl phosphoramidite, and CPG support were purchased from Applied Biosystem, or GLEN RESEARCH. HPLC was performed on a Cosmosil 5C-18AR or CHEMCOBOND 5-ODS-H column (4.6 × 150 mm) with a Gilson chromatography model 305 using a UV detector model 118 at 254 nm. Calf intestine alkaline phosphatase (AP) (100 units/mL), snake venom phosphodiesterase (sv PDE) (3 units/mL) and nuclease P1 (P1) were purchased from Boehringer Mannheim. [γ-^{32}P] ATP (370 Mbq / μL) was obtained from Amersham. Oligonucleotides were purchased from QIAGEN.

Modified ODN Synthesis. Modified ODNs containing ^{MD}A were synthesized by the conventional phosphoramidite method using an Applied Biosystems 392 DNA/RNA synthesizer. Synthesized ODNs were purified by reversed phase HPLC on a 5-ODS-H column (10 × 150 mm, elution with a solvent mixture of 0.1 M triethylammonium acetate (TEAA), pH 7.0, linear gradient over 30 min from 5 to 20% acetonitrile at a flow rate 3.0 mL/min). Mass spectra of ODNs purified by HPLC were determined with MALDI-TOF mass spectroscopy (acceleration voltage 21 kV, negative mode) with 2',3',4'-trihydroxyacetophenone as matrix, using T8 ([M - H]$^-$ 2370.61) and T17 ([M - H]$^-$ 5108.37) as an internal standard.

Preparation of ^{32}P-5'-End-Labeled Oligomers. The ODNs (400 pmol-strand) were 5'-end-labeled by phosphorylation with 4 μL of [γ-^{32}P]ATP (Amersham) and T4 polynucleotide kinase using a standard procedure. The 5'-end-labeled ODN was recovered by ethanol precipitation and further purified by 15% denaturing polyacrylamide gel electrophoresis (PAGE) and isolated by the crush and soak method. After that, ODNs were mixed according to the protocol.

Detection of Output Signals with PAGE Analysis. ^{32}P-5'-End-labeled ODNs were hybridized to the complementary strand containing cyanobenzophenone-substituted uridine in 10 mM sodium cacodylate buffer (pH 7.0). Hybridization was achieved by heating the sample at 90 ˚C for 3 min and slowly cooling to room temperature. Photoirradiation was then carried out in a 100 μL total volume containing 30 kcpm of ^{32}P-5'-end-labeled ODNs and their complementary strands (2 μM strand concentration) in 10 mM sodium cacodylate buffer at pH 7.0. The reaction mixtures were irradiated with a transilluminator (312 nm) at a distance of 3 cm at 0 ˚C for 45 min. After irradiation, all reaction mixtures were precipitated with the addition of 10 μL of 3 M sodium acetate, 20 μL of herring sperm DNA (1 mg/ mL), and 800 μL of ethanol. The precipitated ODN was washed with 100 μL of 80% cold ethanol and dried *in vacuo*. The precipitated ODN was resolved in 50 μL of 10% aniline (v/v), heated at 50 ˚C for 20 min, evaporated by vacuum rotary evaporation to dryness, and resuspended in 5-20 μL of 80% formamide loading buffer (a solution of 80% v/v formamide, 1 mM EDTA, 0.1% xylenecyanol, and 0.1% bromophenol blue). All reactions, along with Maxam-Gilbert G + A sequencing reactions, were conducted with heating at 90 ˚C for 1 min and quickly chilled on ice. The samples (1 μL, 3-10 kcpm) were loaded onto 15% denaturing 19:1 acrylamide:bisacrylamide gel containing 7 M urea, electrophoresed at 1900 V for approximately 1.5 h, and transferred to a cassette and stored at -80 ˚C with Fuji X-ray film.

References

1. (a) Saghatelian, A.; Völcker, N. H.; Guckian, K. M.; Lin, V. S. –Y.; Ghadiri, M. R. *J. Am. Chem. Soc.* **2003**, *125*, 347-348. (b) Fahlman, R. P.; Sen, D. *J. Am. Chem. Soc.* **2003**, *125*, 4310-4316. (c) Bachtold, A.; Hadley, P.; Nakanishi, T.; Dekker, C. *Science* **2001**, *294*, 1317-1320. (d) Yao, Z.; Postma, H. W. C.; Balents, L.; Dekker C. *Nature* **1999**, *402*, 273-276. (e) Huang, Y.; Duan, X.; Cui, Y.; Lauhon, L. J.; Kim, K. –H.; Lieber, C. M. *Science* **2001**, *294*, 1313-1317. (f) Zhan, W.; Crooks, R. M. *J. Am. Chem. Soc.* **2003**, *125*, 9934-9935.
2. (a) Collier, C. P.; Wong, E. W.; Belohradsk´y, M.; Raymo, F. M.; Stoddart, J. F.; Kuekes, P. J.; Williams, R. S.; Heath, J. R. *Science*, **1999**, *285*, 391-394. (b) Guo, X.; Zhang, D.; Wang, T.; Zhu, D. *Chem. Commun*. **2003**, 914-915. (c) Balzani, V.; Venture, M.; Credi, A. *Molecular Devices and Machines, A Journey into the Nanoworld*; WILEY-VCH: Weinheim, Germany, 2003, pp. 235-263. (d) Feringa, B. *Molecular Switches*; WILEY-VCH: Weinheim, Germany, 2002.
3. Clelland, C. T.; Risca, V.; Bancroft, C. *Nature* **1999**, *399*, 533-534.
4. Adleman, L. *Science* **1994**, *266*, 1021-1025.
5. (a) Boon, E. M.; Ceres, D. M.; Drummond, T. G.; Hill, M. G.; Barton, J. K. *Nature Biotechnol.* **2000**, *18*, 1096-1100. (b) Kelley, S. O.; Boon, E. M.; Barton, J. K.; Jackson, N. M.; Hill, M. G. *Nucleic Acids Res.* **1999**, *27*, 4830-4837. (c) Kelley, S. O.; Jackson, N. M.; Hill, M. G.; Barton, J. K. *Angew. Chem. Int. Ed. Engl.* **1999**, *38*, 941-945.
6. Seeman, N. C. *Biochemistry* **2003**, *42*, 7259-7269.
7. Okamoto, A.; Tainaka, K.; Saito, I. *Tetrahedron Lett.* **2002**, *43*, 4581-4583.
8. Murphy, C. J.; Arkin, M. R.; Jenkins, Y.; Ghatlia, N. D.; Bossmann, S. H.; Turro, N. J.; Barton, J. K. *Science* **1993**, *262*, 1025-1029.
9. Okamoto, A., Tanaka, K., Saito, I. *J. Am. Chem. Soc.* **2003**, *125***,** 5066-5071.
10. Nakatani, K., Dohno, C., Saito, I. *J. Org. Chem*. **1999**, *64*, 6901-6904.

CHAPTER 3

Enzymatic Synthesis of DNA Nanowire

Abstract: We have recently reported an artificial nucleobase, methoxy-benzodeazaadenine (^{MD}A), that can effectively mediate hole transport and is not oxidatively decomposed. These results suggest a possible application of ^{MD}A-containing DNA as a molecular wire. We report here that DNA wire consisting of ^{MD}A was enzymatically connectable, and photo-induced hole transport reaction proceeded efficiently through a ligated long DNA duplex. 5'-triphosphate of ^{MD}A (^{MD}ATP) was synthesized and evaluated as a substrate for various DNA polymerases. All enzymes except Deep Vent DNA polymerase revealed a full-length primer extension on the template containing a single thymine site. Especially, KOD Dash DNA polymerase showed a greatest activity in this experiment. Furthermore, The addition of Mn^{2+} improved the yields in all enzymes. In the presence of Mn^{2+}, ^{MD}ATP was incorporated into the complementary strand of T_{10} sequence with KOD Dash DNA polymerase, and, photo-induced hole transport also proceeded through the synthesized duplex. These techniques should be applicable for manufacturing programmable molecular circuits from building blocks consisting of ^{MD}A and functional molecules.

Introduction

Manipulating matters at the nanometer scale is important for many electronic, chemical and biological advances, but presently available methods do not reproducibly achieve the dimensional control at the nanometer scale. Challenges remain both in the formation of nanostructures that constitute the active parts of devices and in the construction of small connecting wires. There has been reported the supramolecular systems containing the structure of π-stack array.[1,2] The aromatic crystals and liquid crystalline materials can be used in optical and electronic applications.[3,4] Recently, carbon nanotubes are widely known as a promising molecule for the nanoscale electronics.[5,6] However, the construction of nanoscale electronic devices from the molecules remains problematic due to the difficulties of achieving inter-element wiring and electrical interfacing to macroscopic electrode. The remarkable recognition properties of DNA are appropriate for the molecularly designed and controlled nanostructure.[7] Furthermore, self-assembly of DNA is suitable for further development encompassing site-specific fabrication and functionalization,[8] which are difficult and troublesome for known conductive materials, such as carbon nanotubes or conductive polymers. Using DNA as the building blocks of electronic circuits has motivated the study of development of DNA wire.[9] However, when natural DNA is used as a molecular wire, unavoidable oxidative degradation of G bases occurs.[10] In addition, the hole transport in natural DNA is strongly influenced by the sequence and the transport distance.[11] We have recently reported an artificial nucleobase, methoxy-benzodeazaadenine (^{MD}A), that can effectively mediate hole transport and is not oxidatively decomposed.[9] These results suggest a possible role of using ^{MD}A-containing DNA as a molecular wire. Herein, we report the enzymatic connection and synthesis of ^{MD}A-containing DNA wires, and the hole transport efficiency of the duplexes was examined.

Results and Discussion

Connection of DNA wire with ligase.

The synthesis of oligodeoxynucleotides (ODNs) containing ^{MD}A and cyanobenzophenone-substituted uridine (U*) has previously been reported (Table 1).[9,12]

Table 1. Oligodeoxynucleotides (ODNs) used in ligation reaction

	Sequence
ODN 1	5'-ATTTATAGTGTGGGTT^{MD}A^{MD}A^{MD}A^{MD}A^{MD}ATTTTT-3'
ODN 2	3'-TAAATAU*CACACCCAAp-5'
ODN 3	5'-pTTGGGTTATTAT-3'
ODN 4	3'-TTTTT^{MD}A^{MD}A^{MD}A^{MD}A^{MD}AAACCCAATAATA-5'

The reaction mixture containing **ODNs 1–4** was incubated for 10 h at 14 °C in the presence of T4 DNA ligase. The reaction products were separated on a denaturing 15 % polyacrylamide gel. As shown in Figure 1, the ligated 38-mer product was obtained after the ligation reaction (lane 1). The product yield calculated by densitometric analysis was 37 %. Although the ODN contained an ^{MD}A run, the ligation reaction proceeded with remarkably high efficiency.

After the ligated ODN was isolated from the gel, we examined the photo-induced hole transport reaction through a ligated duplex in 10 mM sodium cacodylate buffer at pH 7.0. The reaction mixtures were irradiated with a transilluminator (312 nm) at 0 ºC for 45 min. The hole transport efficiency was defined by the ratio of oxidative damage at the proximal and distal GGG, as quantified by PAGE (Figures 2 and 3). The hole transport efficiency of a ligated duplex was 0.59. This result indicates that the ligated duplex has a high hole transport ability.

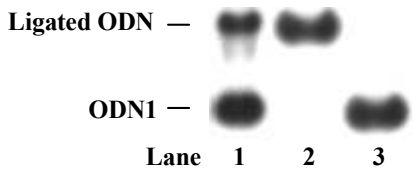

Figure 1. Autoradiogram of native polyacrylamide gel electrophoresis showing the ligation of **ODNs 1–4** by T4 DNA ligase. The reaction mixture containing **ODNs 1–4** (5 μM each), 66 mM Tris-HCl (pH 7.6), 6.6 mM $MgCl_2$, 10 mM DTT, and 0.1 mM ATP was incubated at 14 °C for 10 h. The mixture was electrophored in 10% native polyacrylamide gel. Lane 1, ligation reaction products; lane 2, 38-mer control; lane 3, intact ODN.

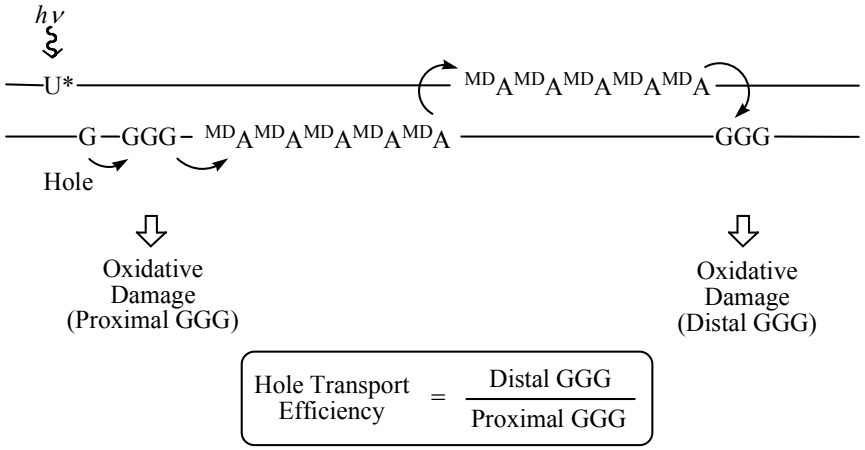

Figure 2. Photo-induced hole transport reaction through a ligated duplex. The hole transport efficiency was defined by the ratio of oxidative damage at the proximal and distal GGG, as quantified by PAGE.

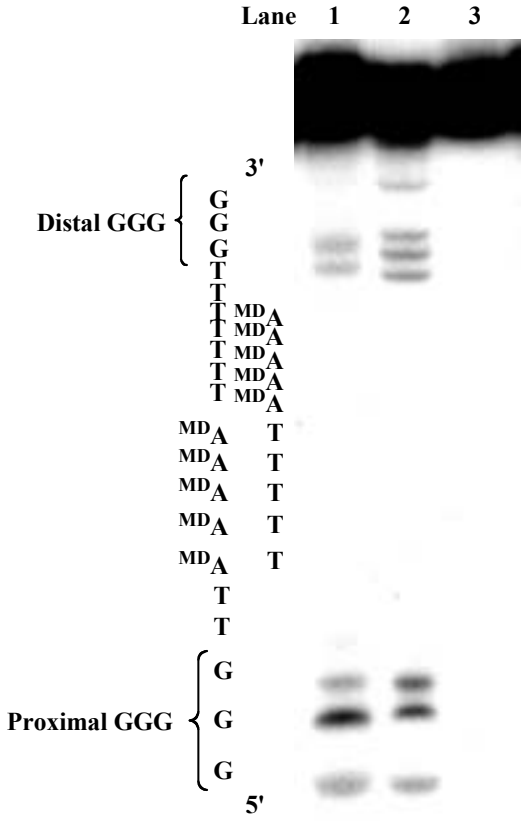

Figure 3. Autoradiograms of a denaturing 15% polyacrylamide/7 M urea gel for the ^{32}P-5' end labeled ODN 5'-ATT TAT AGT GTG GGT T^{MD}A^{MD}A ^{MD}A^{MD}A^{MD}A TTT TTT TGG GTT ATT AT-3' sequence which was synthesized by T4 DNA ligase after photoirradiation. Hybridization was achieved by heating the sample at 90 °C for 5 min and slowly cooling to room temperature. The ^{32}P-5' end labeled ODN duplex was irradiated at 312 nm with transilluminator at 0 °C for 45 min. After piperidine treatment (90 °C, 5 min), the samples were suspended in denaturing loading buffer and electrophoresed through a denaturing 15% polyacrylamide/7 M urea gel. Lane 1, photoirradiated ODN; lane 2, Maxam-Gilbert sequencing reactions G+A; lane 3, control.

Enzymatic synthesis of DNA wire.

Next, we synthesized ^{MD}A-containing DNA wire using polymerase. ^{MD}A triphosphate (d^{MD}ATP) was synthesized, and primer extension with d^{MD}ATP was executed. Synthetic procedure of d^{MD}ATP was outlined in Scheme 1. The resulting crude solution was lyophilized, and purification via reverse phase HPLC (0%-60% acetonitrile in 0.1 M TEAA, pH 7.0) afford d^{MD}ATP as a white solid.

Scheme 1[a]

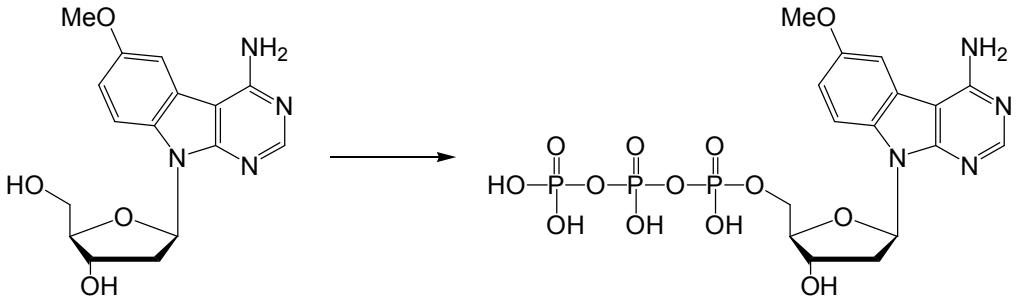

[a]*Reagents*: *N,N,N',N'*-Tetramethyl-1,8-naphthalenediamine, trimethyl phosphate, $POCl_3$, tributylammonium pyrophosphate, DMF, 29%.

Table 2. ODNs used in primer extension reaction

ODN 1	5'-^{32}P-GACGGAACAAGACGGGA-3'
ODN T_1	3'-CTGCCTTGTTCTGCCCTCGCCTCGGCAGAACCGGAGGACAAAC-5'
ODN T_{10}	3'-CTGCCTTGTTCTGCCCTCGCCTTTTTTTTTTCGGCAGAACCGGAGGACAAAC-5'
ODN 2	5'-^{32}P-ATTTATAGTGTGGG
extended ODN 2	5'-^{32}P-ATTTATAGTGTGGGTT^{MD}A^{MD}A^{MD}A^{MD}A^{MD}A^{MD}A^{MD}A^{MD}A^{MD}ATTGGGTTTCTTTGT-3'
ODN 3	3'-TAAATATCACACCCAATTTTTTTTTTAACCCAAAGAAACA-5'

As an initial step, we examined ^{MD}A-containing DNA synthesis by a variety of DNA polymerases in a primer extension assay. Templates were constructed containing a primer binding site, followed by 4 natural nucleotides and thymine base which was expected to be the template for constructing ^{MD}A-runs in complementary strand. Thus, each polymerase was given a normal DNA substrate for initial binding and a "running start" of 4 nucleotides before being challenged to continue ^{MD}A-runs synthesis. A broad range of DNA polymerases were surveyed for activity in this assay.

First, primer-extension reaction was executed with various polymerases and **ODN T_1** as a template. The results of our screen for DNA polymerase recognition of d^{MD}ATP are shown in Figure 4. All enzyme except M-MLV R.T. and Deep Vent revealed full-length primer extension. Especially, the enzyme possessing the greatest activity was KOD Dash DNA polymerase, which can extend DNA chain and incorporate modified nucleotides into DNA.[13]

In an effort to improve the efficiency of the synthesis of DNA containing long ^{MD}A runs, we explored the change of the incubation conditions. The presence of Mn^{2+} ions is known to relax the specificity of many DNA polymerases.[14-16] We found that supplementing standard polymerase reaction mixtures with 1.5 mM $MnCl_2$ had a dramatic effect on the activity of polymerases. The effect was most pronounced among SS II (Figure 4, lanes 11-12, from 20 to 71%). In the case of M-MLV, the fraction of full-length product increased from 3% in the absence of Mn^{2+} to as much as 46% in the presence of Mn^{2+}. The presence of Mn^{2+} also had slight effects on the thermophilic polymerase Deep Vent (Figure 4, lane 13-14, from 0 to 9%).

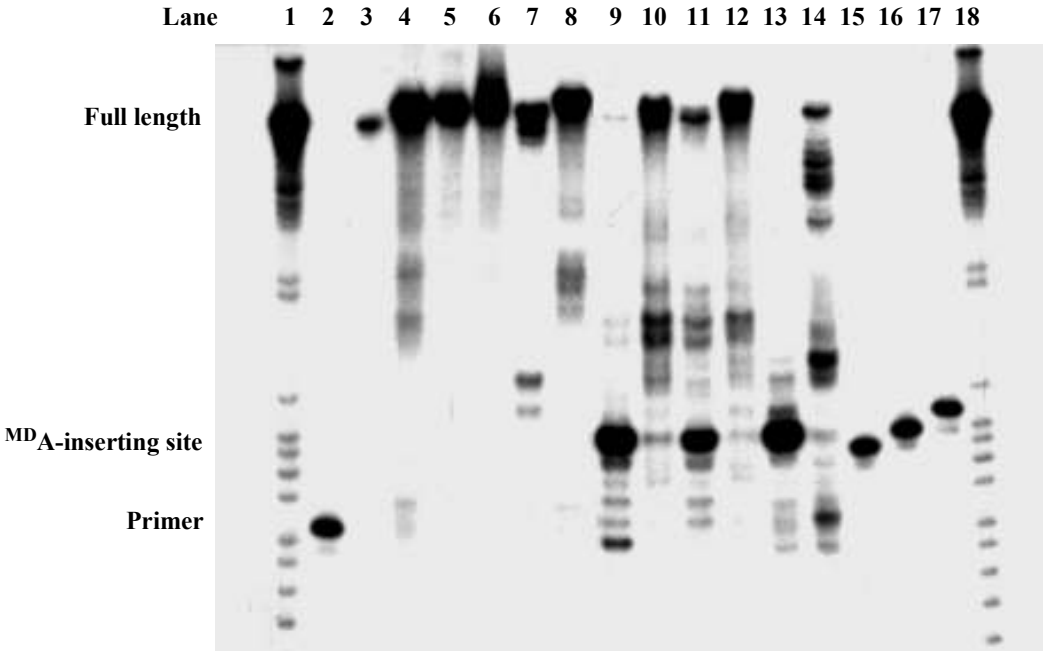

Figure 4. Primer-extension experiments. **ODN 1** as primer was 5'-labeled with ^{32}P and hybridized with **ODN T_1**. Polymerization reactions were performed with 33 μM template and equimolar ratios of $d^{MD}ATP$, dGTP, dCTP, and dTTP (833 μM) by incubating under conditions optimal for each enzyme. Reactions were analyzed by denatured polyacrylamide gel electrophoresis. Lane 1 and 18, Maxam-Gilbert G+A sequencing lane; lane 2, control lane (**ODN 1**); lane 3, and 15-17, marker lane (43, and 21-23, respectably); lane 4, positive control lane (reaction with four native dNTPs and KOD Dash DNA polymerase); lane 5-14, reaction with KOD Dash DNA polymerase in the absence (lane 5) and presence (lane 6) of Mn^{2+}, Bst in the absence (lane 7) and presence (lane 8) of Mn^{2+}, M-MLV R.T. in the absence (lane 9) and presence (lane 10) of Mn^{2+}, SS II R.T. in the absence (lane 11) and presence (lane 12) of Mn^{2+}, and Deep Vent in the absence (lane 13) and presence (lane 14) of Mn^{2+}, respectively.

Table 3. Yields of primer extension on **ODN T_1** using various polymerases

Enzyme	Yield (%)		
Mn^{2+}	-	+	Δ^a
KOD Dash	94	96	+2
Bst	71	97	+26
M-MLV R. T.	3	46	+43
SS II R. T.	20	71	+51
Deep Vent	0	9	+9

[a]The increasing (Δ) of reaction yield equals reaction yields in the presence (+) of Mn^{2+} minus in the absence (-) of Mn^{2+}.

Next, the extension of the primer on T_{10} template was examined with KOD Dash DNA polymerase which showed the greatest activity in above experiment. In a previous report, it was shown that KOD Dash DNA polymerase can tolerate the modification of the substrates.[13] The fraction of full-length product increased from 0% in the absence of Mn^{2+} to as much as 8% in the presence of Mn^{2+}.

For the execution of the hole transport reaction through extended DNA, the duplex containing U* and $^{MD}A_{10}$ runs was synthesized with T_{10} template and KOD Dash DNA polymerase in the presence of Mn^{2+}. From Maxam-Gilbert G+A and C+T, incorporation of ^{MD}A on the complementary of T was confirmed. After the extended ODN was isolated from the gel, we examined photo-induced hole transport reaction (Figure 6). The hole transport efficiency (G_{Dist}/G_{Proxy}) of a extended duplex was 37/63 = 0.60. This result suggests that the extended duplex also has a high hole transport ability.

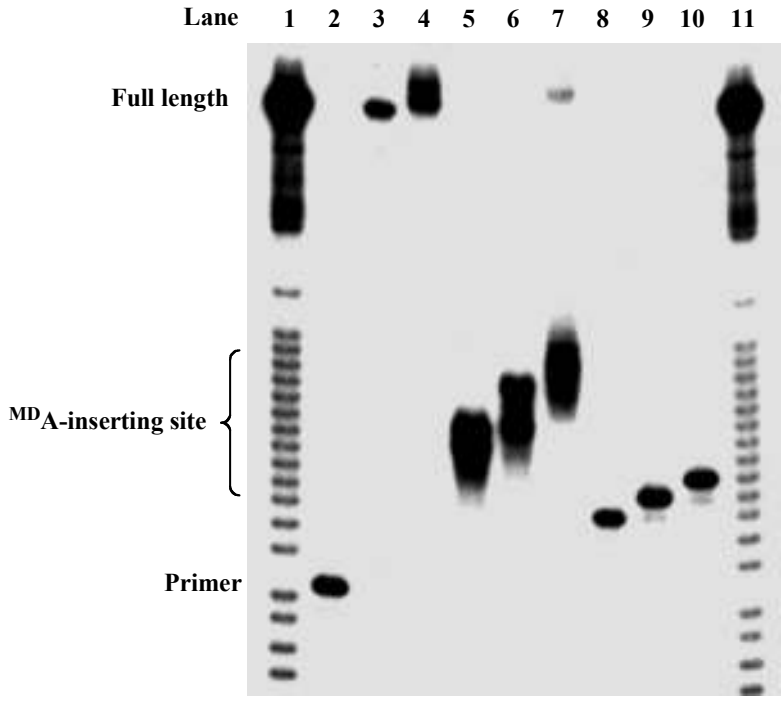

Figure 5. Primer extension experiments. **ODN 1** as primer was 5'-labeled with ^{32}P and hybridized with **ODN T_{10}**. Polymerization reactions were performed with 33 μM template and equimolar ratios of $d^{MD}ATP$, dGTP, dCTP, and dTTP (833 μM) by thermal cycling (initial 2min, 37 °C; 30 s, 72 °C; 30 sec) 30 times. Reactions were analyzed by denatured polyacrylamide gel electrophoresis. Lane 1 and 11, Maxam-Gilbert G+A sequencing lane; lane 2, control lane (**ODN 1**); lane 3, and 8-10, marker lane (43, and 21-23, respectably); lane 4, positive control lane (reaction with four native dNTP); lane 5, negative control lane (in the absence of $d^{MD}ATP$); lane 6-7, reaction with KOD Dash DNA polymerase in the absence (lane 6) and presence (lane 7) of Mn^2, respectively.

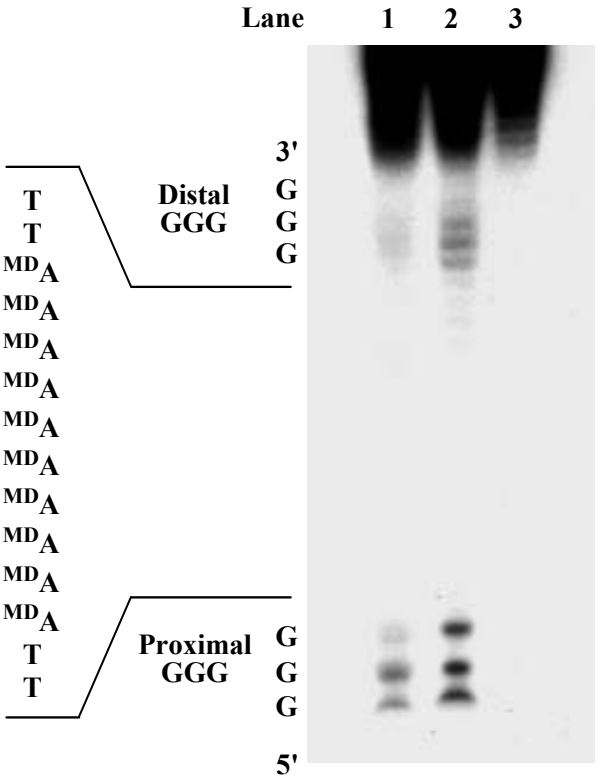

Figure 6. Autoradiograms of a denaturing 15% polyacrylamide/7 M urea gel for the ^{32}P-5' end labeled ODN 5'-ATT TAT AGT GTG GGT T^{MD}A^{MD}A ^{MD}A^{MD}A^{MD}A ^{MD}A^{MD}A ^{MD}A^{MD}AT TGG GTT TCT TGT-3' sequence which was synthesized by KOD Dash DNA polymerase after photoirradiation. Hybridization was achieved by heating the sample at 90 °C for 5 min and slowly cooling to room temperature. The ^{32}P-5' end labeled ODN duplex was irradiated at 312 nm with transilluminator at 0 °C for 45 min. After piperidine treatment (90 °C, 5 min), the samples were suspended in denaturing loading buffer and electrophoresed through a denaturing 15% polyacrylamide/7 M urea gel. Lane 1, photoirradiated ODN; lane 2, Maxam-Gilbert G+A sequencing lane; lane 3, control lane (no photoirradiation).

Conclusion

In conclusion, it was shown that ^{MD}A-containing DNA nanowires can be recognized by enzymes. First, ^{MD}A-containing ODNs were connected with DNA ligase. It was confirmed that hole transport proceeded smoothly through this synthetic ODNs. Next, a broad range of DNA polymerases was surveyed for the activity in primer extansion experiments. All enzymes revealed full-length primer extension in the presence of Mn^{2+}. Especially, the enzyme with the greatest activity was KOD Dash DNA polymerase. Lastly, ^{MD}A-containing DNA wires can be synthesized with the KOD Dash DNA polymerase, and hole transport also proceeded through synthetic DNA wire. These technologies provide powerful methods for preparing well-regulated bionanomaterials that will be widely applicable to electronic devices and biosensors.

Experimental Section

General. Chemical shift values (δ) are reported relative to H_3PO_4 (85%) for ^{31}P NMR (external standard). The reagents for the DNA synthesizer such as A, G, C, and T-β-cyanoethyl phosphoramidite, chemical phosphorylation reagent and CPG support were purchased from Applied Biosystem, or GLEN RESEARCH. Masses of oligonucleotides were determined with a MALDI-TOF MS (acceleration voltage 21 kV, negative mode) with 2', 3', 4'-trihydroxyacetophenone as matrix, using T8 mer ($[M - H]^-$ 2370.61) and T17 mer ($[M - H]^-$ 5108.37) as an internal standard. JASCO V-500 UV/VIS spectorometer was used for UV measurement. HPLC was performed on a Cosmosil 5C-18AR or CHEMCOBOND 5-ODS-H column (4.6 × 150 mm) with a Gilson chromatography model 305 using a UV detector model 118 at 254 nm. Calf intestine alkaline phosphatase (AP) (100 units/mL), snake venom phosphodiesterase (sv PDE) (3 units/mL) and nuclease P1 (P1) were purchased from Boehringer Mannheim. [γ-^{32}P] ATP (370 Mbq / μL) was obtained from Amersham. Oligonucleotides were purchased from QIAGEN. A GIBCO BRL Model S 2 Sequencing Gel Electrophoresis Apparatus was used for polyacrylamide gel electrophoresis (PAGE). T4 DNA ligase was purchased from *TaKaRa*. dNTP mix (PCR grade) was purchased from Roche Diagnostic. KOD Dash DNA polymerase was purchased from TOYOBO. M-MuLV Reverse Transferase, Deep $Vent_R^{®}$ (exo^-) DNA polymerase and *Bst* DNA polymerase Large Fragment were purchased from NEW ENGLAND BioLabs Inc. SuperScript™ II Rnase H^- Reverse Transcriptase was purchased from Invitorogen™.

Oligonucleotide Synthesis and Characterization. Oligodeoxynucleotide sequences were synthesized by conventional phosphoramidite method by using an Applied Biosystems 392 DNA/RNA synthesizer. Oligonucleotides were purified by reverse phase HPLC on a 5-ODS-H column (10 × 150 mm, elution with a solvent mixture of 0.1 M

triethylamine acetate (TEAA), pH 7.0, linear gradient over 30 min from 5 % to 35 % acetonitrile at a flow rate 3.0 mL/min). Oligonucleotides were fully digested with calf intestine alkaline phosphatase (50 U/mL), snake venom phosphodiesterase (0.15 U/mL) and P1 nuclease (50 U/mL) at 37 °C for 3 h. Digested solutions were analyzed by HPLC on a cosmosil 5C-18AR or CHEMCOBOND 5-ODS-H column (4.6 × 150 mm), elution with a solvent mixture of 0.1 M triethylamine acetate (TEAA), pH 7.0, linear gradient over 20 min from 0 % to 40 % acetonitrile at a flow rate 1.0 mL/min). Concentration of each oligonucleotides were determined by comparing peak areas with standard solution containing dA, dC, dG and dT at a concentration of 0.1 mM.

Preparation of ^{32}P-5'-End-Labeled Oligomers. The ODNs (400 pmol-strand) were 5'-end-labeled by phosphorylation with 4 μL of [γ-^{32}P]ATP (Amersham) and T4 polynucleotide kinase using a standard procedure. The 5'-end-labeled ODN was recovered by ethanol precipitation and further purified by 15% denaturing polyacrylamide gel electrophoresis (PAGE) and isolated by the crush and soak method.

Enzymatic Ligation and Preparation of ODN for Long-Range Hole Transfer through DNA. Enzymatic ligation was examined in 30 μL of the reaction buffer, which contained 66 mM Tris-HCl (pH 7.6), 6.6 mM $MgCl_2$, 10 mM DTT, 0.1 mM ATP, 3.3 μM each ODN containing ^{32}P-labeled ODN 1, and 35 units of T4 DNA ligase (from *TaKaRa*, Japan). The mixture was incubated for 10 h at 14 °C. The reaction was terminated by addition of 80 % formamide loading buffer (a solution of 80 % v/v formamide, 1 mM EDTA, 0.1 % xylene cyanol and 0.1 % bromophenol blue) and further purified by 10 % native polyacrylamide gel electrophoresis (PAGE) and isolated by the crush and soak method. Long range hole transfer reaction was carried out with same procedure described in cleavage of ^{32}P-5'-end-labeled d^{CNBP}U-containing ODNs by photoirradiation.

Hole Transport Experiment in Ligated ODNs and PAGE Analysis. ^{32}P-5'-End-labeled ODNs obtained from gel purification were annealed by heating the sample at 90 ºC for 3 min and slowly cooling to room temperature in 10 mM sodium cacodylate buffer (pH 7.0). Photoirradiation was then carried out in a 100 μL total volume containing 30 kcpm of ^{32}P-5'-end-labeled ODNs in 10 mM sodium cacodylate buffer at pH 7.0. The reaction mixtures were irradiated with a transilluminator (312 nm) at a distance of 3 cm at 0 ˚C for 45 min. After irradiation, all reaction mixtures were precipitated with the addition of 10 μL of 3 M sodium acetate, 20 μL of herring sperm DNA (1 mg/ mL), and 800 μL of ethanol. The precipitated ODN was washed with 100 μL of 80% cold ethanol and dried *in vacuo*. The precipitated ODN was resolved in 50 μL of 10% aniline (v/v), heated at 50 ˚C for 20 min, evaporated by vacuum rotary evaporation to dryness, and resuspended in 5-20 μL of 80% formamide loading buffer (a solution of 80% v/v formamide, 1 mM EDTA, 0.1% xylenecyanol, and 0.1% bromophenol blue). All reactions, along with Maxam-Gilbert G + A sequencing reactions, were conducted with heating at 90 ˚C for 1 min and quickly chilled on ice. The samples (1 μL, 3-10 kcpm) were loaded onto 15% denaturing 19:1 acrylamide:bisacrylamide gel containing 7 M urea, electrophoresed at 1900 V for approximately 1.5 h, and transferred to a cassette and stored at -80 ˚C with Fuji X-ray film.

Preparation of ^{MD}A Triphosphate. d^{MD}A (0.21 mmol) and *N,N,N',N'*-tetramethyl-1,8-naphthalendiamine (dry proton sponge) (1.1 mmol, 5 eq.) were dissolved in anhydrous acetonitrile and coevapolated three times. Then, those were dissolved in 3.0 mL of trimethylphosphate. The reaction mixture was stirred at room temperature under Ar and then cooled to 0 °C. After 2 h of stirring at 0 °C, tributylamine (0.20 mL, 0.84 mmol, 4.0 eq.) was added to the solution followed by 1.0 g tributylammonium pyrophosphate (1.6 moles tributylammonium per 1.0 mole of pyrophosphate, 2.1 mmol, 10 eq.) in 3 mL of anhydrous DMF. After 5 min, the reaction mixture was poured into 40 mL of diethyl ether :

acetone : $NaClO_4$-saturated acetone (10 : 9 : 1) with stirring. The precipitates were washed with ether twice and collected. The white solid was dried under vacuum, and redissolved in a small volume of 1 M TEAB buffer. The solution purified via reverse phase HPLC (0-60% acetonitrile over 20 min in 0.1 M TEAA buffer, pH 7.0) afford triphosphates as a white solid (yield 29%, determined by UV spectra). A 1 M solution of TEAB was prepare by bubbling CO_2 gas through a 1 M triethylamine solution in waer at 0 °C for five hours (pH approx. 7.4-7.6). ^{31}P NMR (D_2O) δ -5.11 (d, J = 18.3 Hz), -6.36 (d, J = 18.3 Hz), -18.0 (t, J = 18.3 Hz).

Primer Extension Reactions with ^{MD}A Triphosphate. For the full length extending, primer (5 μM each, 5'-^{32}P-labeled) and template (3.3 μM), as well as the appropriate dNTPs (0.8 mM each), were mixed with the reaction buffer, and each enzymes (KOD Dash: 2.5 U, Bst: 8 U, Deep Vent: 2 U, M-MLV R.T.: 200 U, SS II R.T.: 200 U, respectably) in the presence or absence of 1.5 mM $MnCl_2$, and adjusted to a final volume of 30 μL with water. In the case with KOD Dash DNA polymerase, Bst, and Deep Vent, the experiments were cycled (initial 2min, 37 ºC; 30 sec, 72 °C; 30 sec, 37 ºC) 30 times. In the case with M-MLV and SS II reverse transferase, the mixture was incubated at 37 °C for 1 h. The reaction was terminated by addition of 80 % formamide loading buffer (a solution of 80 % v/v formamide, 1 mM EDTA, 0.1 % xylene cyanol and 0.1 % bromophenol blue) and electrophoresed in 15% denatured polyacrylamide gel containing 7 M urea. The polyacrylamide gel was transferred to a cassette and stored at -80 °C with Fuji X-ray film.

Hole Transport Experiment with PAGE Analysis. ^{32}P-5'-End-labeled ODNs purified from polyacrylamide gel were hybridized to the complementary strand containing cyanobenzophenone-substituted uridine in 10 mM sodium cacodylate buffer (pH 7.0). Hybridization was achieved by heating the sample at 90 ºC for 3 min and slowly cooling to room temperature.

References

2. Inokuchi, H.; Imaeda, K.; Enoki, T.; Mori, T.; Maruyama, Y.; Saito, G.; Okada, N.; Yamochi, H.; Seki, K.; Higuchi, Y.; Yasuoka, N. *Nature* **1987**, *329*, 39-40.
3. Meibom, A.; Sleep, N. H.; Chamberlain, C. P.; Coleman, R. G.; Frei, R.; Hren, M. T.; Wooden, J. L. *Nature* **2002**, *419*, 702-705.
4. Guillon, D. *Adv. Chem. Phys.* **2000**, *113*, 1-49.
5. Kato, T. *Science* **2002**, *295*, 2414-2418.
6. (a) Bachtold, A.; Hadley, P.; Nakanishi, T.; Dekker, C. *Science* **2001**, *294*, 1317-1320. (b) Yao, Z.; Postma, H. W. C.; Balents, L.; Dekker C. *Nature* **1999**, *402*, 273-276.
7. Huang, Y.; Duan, X.; Cui, Y.; Lauhon, L. J.; Kim, K. –H.; Lieber, C. M. *Science* **2001**, *294*, 1313-1317.
8. Seeman, N. C. *Biochemistry* **2003**, *42*, 7259-7269.
9. (a) Okamoto, A.; Taiji, T.; Tainaka, K.; Saito, I. *Bioorg. Med. Chem. Lett.* **2002**, *12*, 1895-1896. (b) Okamoto, A.; Tainaka, K.; Saito, I. *Tetrahedron Lett.* **2002**, *43*, 4581-4583.
10. Okamoto, A., Tanaka, K., Saito, I. *J. Am. Chem. Soc.* **2003**, *125***,** 5066-5071.
11. Kasai, H., Yamaizumi, Z., Berger, M., Cadet, J. *J. Am. Chem. Soc.* **1992**, *114***,** 9692-9694.
12. Giese, B., Amaudrut, J., Köhler, A.-K., Spormann, M., Wessely, S., *Nature*, **2001**, *412*, 318-320.
13. Nakatani, K., Dohno, C., Saito, I. *J. Org. Chem*. **1999**, *64*, 6901-6904.
14. Obayashi, T.; Masud, M. M.; Ozaki, A. N.; Ozaki, H.; Kuwahara, M.; Sawai, H. *Bioorg. Med. Chem. Lett.* **2002**, *12*, 1167-1170.
15. Cadwell, R. C.; Joyce, G. F. *PCR Methods Appl.* **1992**, *2*, 28-33.
16. Tabor, S.; Richardson, C. C. *Proc. Natl. Acad. Sci. U.S.A.* **1989**, *86*, 4076-4080. Chaput, J. C.; Ichda, J. K.; Szostak, J. W. *J. Am. Chem. Soc.* **2003**, *125***,** 856-857.

CHAPTER 4

Unique Hole-Trapping Property of a Novel Degenerate Base, 2-Amino-7-Deazaadenine

Abstract: Development of an efficient hole-trapping nucleobase that can be incorporated into any DNA sequence, regardless of the presence of AT or GC base pairs, is very important to the study of long-range hole migration in DNA containing diverse sequences. We have identified an artificial degenerate nucleobase, 2-amino-7-deazaadenine (**1**) that can control long-range hole migration through an ODN by its unique hole-trapping capacity. The hole-trapping efficiency of **1** is superior to that of the GGG step and similar to that of ^{Z}G, regardless of the pyrimidine base that base-pairs with **1**. We also found that a hole can effectively migrate via a **1**–T base pair without decomposition of the GGG bridge, whereas the **1**–C base pair suppressed hole migration. The formation of the **1**–C base pair in duplex DNA would cause a decrease in π-stacking with the flanking base on the 3' side, because of the sliding of **1** in the base pair into the major groove of the duplex. Systematic π-stacking in duplex DNA is an important factor in hole migration in DNA. Therefore, disruption of π-stacking by the formation of a **1**–C base pair is unfavorable for effective hole migration in DNA, and leads to the suppression of hole migration.

Introduction

Long-range hole migration in duplex DNA has recently become a topic of interest at the interface of chemistry and biology. Long-range hole migration in DNA has been extensively investigated, especially the kinetics of hole generation and migration.[1-6] A conventional method for investigating the efficiency of hole migration in DNA involves the analysis of the band intensities of the products of oxidative DNA cleavage at multiple G steps (i.e., GG and GGG steps).[1,4-8] However, with such a detection method, the oligonucleotides to be used are limited to especially designed sequences containing GG and GGG steps as a hole trap. As an alternative base for efficient hole trapping at multiple G nucleotides, G analogue 7-deazaguanine (^{Z}G) has often been used.[9,10] This nucleobase can act as a surrogate for G but not for AT base pairs. Development of an efficient hole-trapping nucleobase that can be incorporated into any DNA sequence, regardless of the presence of AT or GC base pairs, is very important for the study of long-range hole migration in DNA containing diverse sequences.

We have already reported a highly effective degenerate nucleobase, 2-amino-7-deazaadenine (**1**, Figure 1 and Figure 4), which can form stable base pairs with both T and C.[11] If **1** acts as an effective hole trap like ^{Z}G, it would be a useful indicator for hole migration studies of DNA.

We herein report that **1** is the first hole-trapping degenerate base to be identified. The hole-trapping efficiency of **1** in duplex DNA is superior to GGG step and similar to that of ^{Z}G. We also demonstrate that the hole-trapping efficiency of **1** varies with the base-pairing pyrimidine base.

Results and Discussion

First, hole-trapping was evaluated by means of remote oxidative DNA damage induced by photoirradiation of a cyanobenzophenone (**S**)-tethered oligodeoxynucleotide (ODN). ODNs containing **1** were prepared according to the method reported earlier.[12] The ^{32}P-labeled ODN, containing an **X–Y** base pair (**X**=A, G, ^{Z}A, ^{Z}G or **1**; **Y**=T or C) and two GGG steps (*prox*-G_3 and *dist*-G_3), was annealed with an ODN containing **S** as an electron-accepting photosensitizer (Figure 2a). The duplexes were irradiated at 312 nm for 15 min at 0 ˚C, then treated with hot piperidine (90˚C, 20 min). DNA cleavage with alkaline treatment was assayed by PAGE (Figure 2b). The values calculated by quantifying the intensities of the cleavage band are shown in Table 1. When **X** was G or 7-deazaadenine (^{Z}A), the cleavage bands were observed almost exclusively at both *prox*-G_3 and *dist*-G_3 (lanes 5 and 6), indicating that G and ^{Z}A act as bridging bases for hole migration from *prox*-G_3 to *dist*-G_3. In contrast, strong cleavage bands at **X** were observed when **X** was **1** (lanes 2 and 3) or ^{Z}G (lane 4). In both cases, cleavage at *prox*-G_3 and *dist*-G_3 was strongly suppressed. The ODNs containing **1** were cleaved effectively at **1** regardless of the pyrimidine base with which it was base-paired. Cleavage at **1** did not occur without light or in the absence of a photosensitizer, indicating that the cleavage was caused by remote oxidation through hole migration in a duplex ODN.

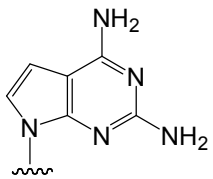

1

Figure 1. 2-Amino-7-deazaadenine (**1**) used in this study.

(a)

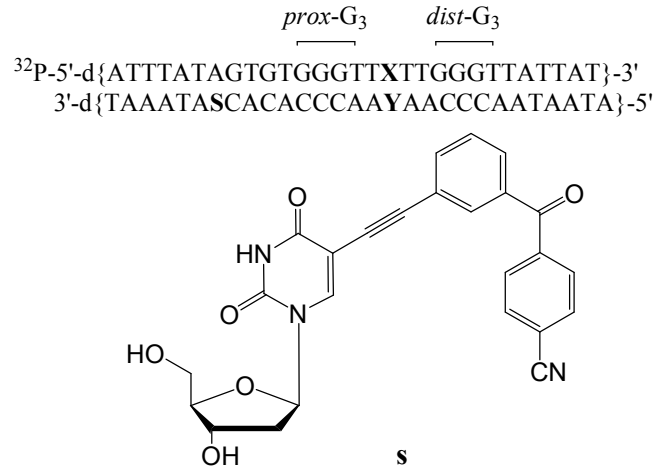

(b)

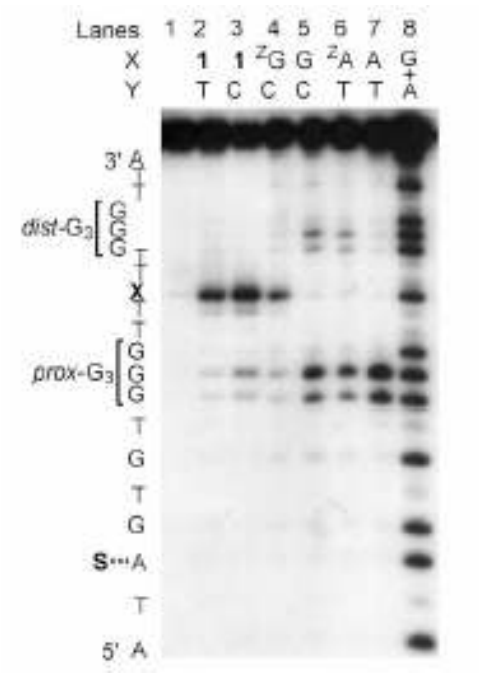

Figure 2. Remote oxidation of DNA containing **1**: (a) DNA sequence in this experiment. **S** represents cyanobenzophenone-tethered uridine ($d^{CNBP}U$); (b) autoradiogram of a denaturing gel electrophoresis of ^{32}P-5'-end-labeled DNA after photooxidation of the duplexes. The DNA duplexes were photoirradiated at 312 nm in 10 mM sodium cacodylate (pH 7.0) at 0 ˚C for 15 min, then treated with hot piperidine (90 ˚C, 20 min). Lane 1, control (**X**=**1**, **Y**=T) without irradiation; lane 2, **X**=**1**, **Y**=T; lane 3, **X**=**1**, **Y**=C; lane 4, **X**=^{Z}G, **Y**=C; lane 5, **X**=G, **Y**=C; lane 6, **X**=^{Z}A, **Y**=T; lane 7, **X**=A, **Y**=T; lane 8, Maxam-Gilbert G+A sequencing lane. ^{Z}G and ^{Z}A denote 7-deazaguanine and 7-deazaadenine, respectively.

Table 1. Efficiency of oxidative cleavage of DNA containing **1**[a]

X-Y		Cleavage band intensities (%)		
		proxy-G_3	**X**	*dist*-G_3
1-T	(Lane 2)	9	84	7
1-C	(Lane 3)	20	76	4
G-C	(Lane 4)	25	66	9
^{Z}G-C	(Lane 5)	73	2	25
^{Z}A-T	(Lane 6)	71	~0	29
A-T	(Lane 7)	>99	~0	~0

[a]The cleavage band intensities were calculated by densitometry, as show in Figure 2b. The numbers in the table represent the percentage strand cleavage at a given site relative to the strand cleavage. ^{Z}G and ^{Z}A denote 7-deazaguanine and 7-deazaadenine, respectively.

Having established the hole-trapping property of **1**, we estimated the ability of **1** to act as an electron-donating nucleobase. The oxidation potential of **1** was measured by cyclic voltammetry (CV), and compared with those of ^{Z}G and G. The peak potential (E_p) for the irreversible oxidation of **1** occurred at 0.79 V, whereas those of G and ^{Z}G were at 1.15 and 0.79 V *versus* SCE, respectively, indicating that **1** is a nucleobase more readily oxidized than G, and oxidized to a similar degree as ^{Z}G. Furthermore, the irreversiblity of the scanning wave of **1** suggests that the lifetime of **1** oxidized at the electrode surface is very short in aqueous medium. Its ready oxidation and subsequent rapid decomposition would be an important factor in the good hole-trapping properties of **1**.

To better evaluate the effect of the pyrimidine base opposite **1** on the efficiency of hole migration, we prepared ODNs containing two **1**'s ($\mathbf{X_1}$ and $\mathbf{X_2}$) located on either side of *dist*-G_3 as shown in Figure 3a. Photooxidation

and PAGE analysis was carried out using the methods described above. The efficiency of the cleavage at each **1** site is shown in Figure 3b and Table 2. The results can be divided into two categories according to the nature of the pyrimidine base ($\mathbf{Y_1}$) base-paired with $\mathbf{X_1}$. In the duplex ODN containing a **1**–T base pair at $\mathbf{X_1}$–$\mathbf{Y_1}$, we observed strong cleavage bands at both $\mathbf{X_1}$ and $\mathbf{X_2}$, indicating that a hole can migrate effectively from $\mathbf{X_1}$ to $\mathbf{X_2}$ (lanes 4 and 6). Cleavage was negligible at *dist*-G_3, which acts as a bridge for the hole migration between $\mathbf{X_1}$ and $\mathbf{X_2}$, although strong cleavage bands at GGG sites are observed in natural DNA (lane 7). This result suggests that the **1**–T base pair is a shallow hole trap and acts, not only as an effective hole trap suppressing the oxidation of G bases, but also as a good hole carrier. In contrast, when $\mathbf{X_1}$ formed a base pair with C, a strong cleavage band was observed at $\mathbf{X_1}$, whereas the cleavage band observed at $\mathbf{X_2}$ was 2–3 times weaker than that observed at $\mathbf{X_1}$ (lanes 3 and 5). This result shows that hole migration to the $\mathbf{X_2}$ site beyond the **1**–C base pair was not as effective as that beyond the **1**–T base pair, and that the **1**–C base pair suppresses hole migration.

(a)

prox-G_3 *dist*-G_3

^{32}P-5'-d{ATTTATAGTGTGGGTT**X$_1$**TTGGGTT**X$_2$**TTAT}-3'
3'-d{TAAATA**S**CACACCCAA**Y$_1$**AACCCAA**Y$_2$**AATA}-5'

(b)

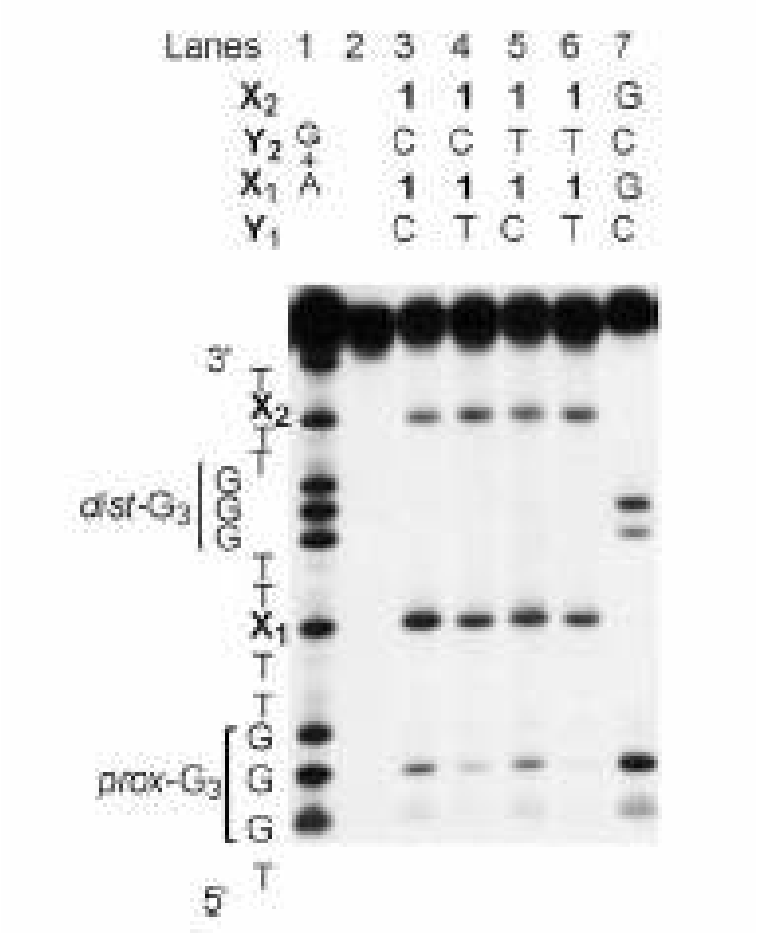

Figure 3. Remote oxidation of DNA containing two **1** sites. (a) DNA sequence in this experiment. **S** represents cyanobenzophenone-tethered uridine ($d^{CNBP}U$). (b) Autoradiogram of denaturing gel electrophoresis of ^{32}P-5'-end-labeled DNA after photooxidation of the duplexes. The DNA duplexes were photoirradiated at 312 nm in 10 mM sodium cacodylate (pH 7.0) at 0 ˚C for 45 min, then treated with hot piperidine treatment (90 ˚C, 20 min). Lane 1, Maxam–Gilbert G+A sequencing lane; lane 2, control (**X$_1$=1**, **Y$_1$**=T, **X$_2$=1**, **Y$_2$**=T); lane 3, **X$_1$=1**, **Y$_1$**=C, **X$_2$=1**, **Y$_2$**=C; lane 4, **X$_1$=1**, **Y$_1$**=T, **X$_2$=1**, **Y$_2$**=C; lane 5, **X$_1$=1**, **Y$_1$**=C, **X$_2$=1**, **Y$_2$**=T; lane 6, **X$_1$=1**, **Y$_1$**=T, **X$_2$=1**, **Y$_2$**=T; lane 7, **X$_1$**=G, **Y$_1$**=C, **X$_2$**=G, **Y$_2$**=C.

Table 2. Efficiency of oxidative cleavage of DNA containing two **1** sites[a]

Sequences		Cleavage band intensities (%)			
		proxy-G_3	**1** on $\mathbf{X_1}$	*dist*-G_3	**1** on $\mathbf{X_2}$
Y_1 = C, Y_2 = C	(Lane 3)	24	57	~0	19
Y_1 = T, Y_2 = C	(Lane 4)	8	47	~0	44
Y_1 = C, Y_2 = T	(Lane 5)	28	49	~0	23
Y_1 = T, Y_2 = T	(Lane 6)	3	48	~0	48

[a]The cleavage band intensities were calculated by densitometry, as show in Figure 3b. The numbers in the table represent the percentage strand cleavage at a given site relative to the total strand cleavage.

The reason for the suppression of hole migration by the **1**–C base pair probably involves the disruption of π-stacking by the formation of a non-Watson–Crick base pair. We also considered the electronic effect of the formation of a base pair with T or C on the oxidation of **1**. The HOMO energies of a Watson-Crick **1**-T base pair and a wobble **1**-C base pair, as drawn in Figure 4, were estimated as 4.54 and 4.57 eV, respectively, in the B3LYP/6-31G(d) calculation. The gap between **1**-T and **1**-C in HOMO energy was not wide enough to discuss any electronic effect of base-pairing on hole-trapping by **1**. Nucleobase **1** should form a wobble base pair with C at pH 7, as observed for the base pair formed between 2-aminopurine and C[13-15] (Figure 4). If so, the formation of the **1**–C base pair in duplex DNA would cause a decrease in π-stacking with the flanking base on the 3' side, because of the sliding of **1** in the base pair into the major groove of the duplex. Systematic π-stacking in duplex DNA is an important factor in hole migration in DNA.[9] Therefore, disruption of π-stacking by the formation of a **1**–C base pair is unfavorable for effective hole migration in DNA, and leads to the suppression of hole migration.

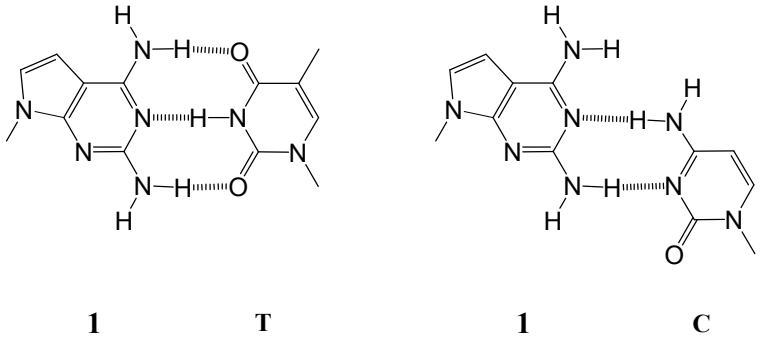

Figure 4. Watson–Crick **1**–T base pair (left) and wobble **1**–C base pair (right).

Conclusion

In conclusion, we have identified an artificial degenerate nucleobase **1** that can control long-range hole migration through an ODN by its unique hole-trapping capacity. The hole-trapping efficiency of **1** is superior to that of the GGG step and similar to that of ^{Z}G, regardless of the pyrimidine base that makes base-pairing with **1**. We also found that a hole can effectively migrate via a **1**–T base pair without decomposition of the GGG bridge, whereas the **1**–C base pair suppressed hole migration from $\mathbf{X_1}$ to $\mathbf{X_2}$. Consequently, **1** is a hole-trapping degenerate base, which can be incorporated at any site regardless of the AT or GC content, and can be used as a very effective tool for studying long-range hole migration in DNA containing diverse sequences.

Experimental Section

General. ^{1}H NMR spectra were measured with Varian Mercury 400 (400 MHz) spectrometer. ^{13}C NMR spectra were measured with JEOL JNM a-500 (500 MHz) spectrometer. Coupling constants (*J* value) are reported in hertz. The chemical shifts are expressed in ppm downfield from tetramethylsilane, using residual chloroform (δ = 7.24 in ^{1}H NMR, δ = 77.0 in ^{13}C NMR) and dimethyl sulfoxide (δ = 2.48 in ^{1}H NMR, δ = 39.5 in ^{13}C NMR) as an internal standard. FAB mass spectra were recorded on a JEOL JMS DX-300 spectrometer or JEOL JMS SX-102A spectrometer. HPLC was performed on a Cosmosil 5C-18AR or CHEMCOBOND 5-ODS-H column (4.6 × 150 mm) with a Gilson chromatography model 305 using a UV detector model 118 at 254 nm.

Measurement of Cyclic Voltammetry (CV) Spectra. Oxidation potentials (E_p) of nucleosides (saturated in water, ca. 200 μM) were measured with an ALS electrochemical analyzer model 660-A in 100 mM $LiClO_4$ solution at room temperature. The scan rate was 100 mV/s. The working electrode was glassy carbon. The counter electrode was Pt wire. The reference electrode was SCE.

Preparation of ^{32}P-5'-End-Labeled Oligomers. The ODNs (400 pmol-strand) were 5'-end-labeled by phosphorylation with 4 μL of [γ-^{32}P]ATP (Amersham) and T4 polynucleotide kinase using a standard procedure. The 5'-end-labeled ODN was recovered by ethanol precipitation and further purified by 15% denaturing polyacrylamide gel electrophoresis (PAGE) and isolated by the crush and soak method.

Hole Transport Experiment and PAGE Analysis. ^{32}P-5'-End-labeled ODNs were hybridized to the complementary strand containing cyanobenzophenone-substituted uridine in 10 mM sodium cacodylate buffer (pH 7.0). Hybridization was achieved by heating the sample at 90 ˚C

for 3 min and slowly cooling to room temperature. Photoirradiation was then carried out in a 100 μL total volume containing 30 kcpm of ^{32}P-5'-end-labeled ODNs and their complementary strands (2 μM strand concentration) in 10 mM sodium cacodylate buffer at pH 7.0. The reaction mixtures were irradiated with a transilluminator (312 nm) at a distance of 3 cm at 0 ˚C for 45 min. After irradiation, all reaction mixtures were precipitated with the addition of 10 μL of 3 M sodium acetate, 20 μL of herring sperm DNA (1 mg/ mL), and 800 μL of ethanol. The precipitated ODN was washed with 100 μL of 80% cold ethanol and dried *in vacuo*. The precipitated ODN was resolved in 50 μL of 10% aniline (v/v), heated at 50 ˚C for 20 min, evaporated by vacuum rotary evaporation to dryness, and resuspended in 5-20 μL of 80% formamide loading buffer (a solution of 80% v/v formamide, 1 mM EDTA, 0.1% xylenecyanol, and 0.1% bromophenol blue). All reactions, along with Maxam-Gilbert G + A sequencing reactions, were conducted with heating at 90 ˚C for 1 min and quickly chilled on ice. The samples (1 μL, 3-10 kcpm) were loaded onto 15% denaturing 19:1 acrylamide:bisacrylamide gel containing 7 M urea, electrophoresed at 1900 V for approximately 1.5 h, and transferred to a cassette and stored at -80 ˚C with Fuji X-ray film.

References

1. Hall, D. B., Holmlin, R. E., Barton, J. K. *Nature* **1996**, *382*, 731-734.
2. Burrows, C. J.; Muller, J. G. *Chem. Rev.* **1998**, *96*, 1109-1152.
3. Grinstaff, M. W. *Angew. Chem. Int. Ed.* **1999**, *38*, 3629-3635.
4. Núñez, M. E.; Barton, J. K. *Curr. Opin. Chem. Biol.* **2000**, *4*, 199-206.
5. Schuster, G. B. *Acc. Chem. Res.* **2000**, *33*, 253-260.
6. Giese, B. *Acc. Chem. Res.* **2000**, *33*, 631-636.
7. Nakatani, K.; Dohno, C.; Saito, I. *J. Am. Chem. Soc.* **1999**, *121*, 10854-10855.
8. Okamoto, A.; Tanabe, K.; Saito, I. *Bioorg. Med. Chem.* **2002**, *10*, 713-718.
9. Kelley, S. O.; Barton, J. K. *Chem. Biol.* **1998**, *5*, 413-425.
10. Nakatani, K.; Dohno, C.; Saito, I. *J. Am. Chem. Soc.* **2000**, *122*, 5893-5894.
11. Okamoto, A.; Tanaka, K.; Saito, I. *Bioorg. Med. Chem. Lett.* **2002**, 97-99.
12. Nakatani, K.; Dohno, C.; Saito, I. *J. Org. Chem.* **1999**, *64*, 6901-6904.
13. Sowers, L. C.; Eritja, R.; Chen, F. M.; Khwaja, T.; Kaplan, B.; Goodman, M. F.; Fazakerley, G. V. *Biochem. Biophys. Res. Commun.* **1989**, *165*, 89-92.
14. Fagan, P. A.; Fabrega, C.; Eritja, R.; Goodman, M. F.; Wemmer, D. E. *Biochemistry* **1996**, *35*, 4026-4033.
15. Sowers, L. C.; Boulard, Y.; Fazakerley, G.V. *Biochemistry* **2000**, *39*, 7613-7620.

CHAPTER 5

A Novel Nucleobase That Releases Reporter Tags upon DNA Oxidation

Abstract: We have developed a novel nucleosbase ethylenediamine-modified guanine, ^{eda}G, that efficiently releases various reporter units upon one-electron oxidation. The ^{eda}G-selective degradation of ODNs was achieved by various mild oxidizing agents. The major isolable photoproducts of the oxidation of benzoylated ^{eda}G-containing ODN were identified by mass spectrometric analysis as ODN fragments cleaved via an abasic site and benzamide possessing a guanidinium group. Next, we examined the detection of TAMRA released from ODN containing a TAMRA-tethered ^{eda}G via long-range hole transport through DNA. The photolyzed ODN was then removed from the sample solution by passing through a centrifugal filter, and fluorescence intensity of filtrates containing TAMRA released from ODN was measured. The result of the measurement of fluorescence intensity showed a good agreement with that of the evaluation of decomposed ratios at the site of TAMRA-tethered ^{eda}G, implying that the incorporation of TAMRA-^{eda}G into the duplex makes it possible to detect hole transport through DNA without PAGE analysis. The oxidant-dependent molecular releasing technique is quite useful not only for DNA-based drug releasing systems but also for the detection of long-range hole transport through DNA without time-consuming analysis.

Introduction

DNA biosensors offer considerable promise for extracting information from target genes in a quick and simple manner. Various DNA probes that give signals in a sequence-specific fashion, as represented by molecular beacons, have been widely used.[1] However, there are very few DNA probes that can release useful functional molecules.[2] A molecular releasing system that is triggered by external stimulation such as oxidation or photoirradiation would be a useful tool for gene analysis.

Herein, we report a novel nucleoside, ethylenediamine-modified G (^{eda}G), and a new molecular releasing system controllable by one-electron oxidation of oligodeoxynucleotides (ODNs). Reporter units tethered to ^{eda}G were easily released from ODNs by mild oxidation. In a long-range hole transport experiment, DNA duplex containing ^{eda}G efficiently and stoichiometrically released a fluorescent tag.

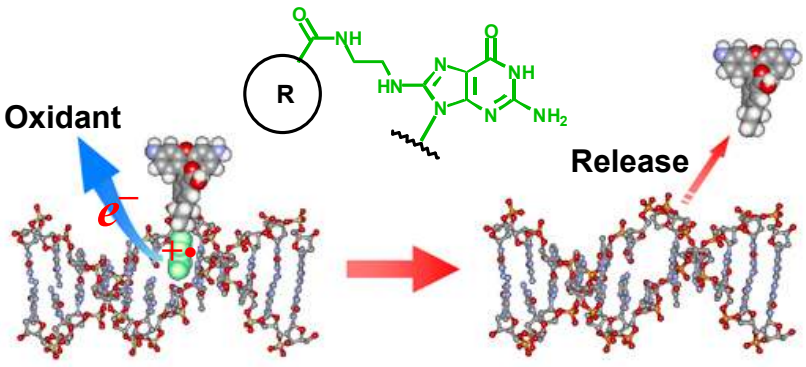

Results and Discussion

The synthesis of ^{eda}G-containing ODN is outlined in Scheme 1. 8-BromoG (**1**) protected by 4,4'-dimethoxytrityl group[3] was converted to **2** by refluxing in ethylenediamine, and the amino groups were protected to afford **3**. ^{eda}G phosphoramidite **4** was incorporated into ODNs by a conventional method. By the post-synthetic modification of ^{eda}G-containing ODNs using *N*-hydroxysuccinimidyl ester of carboxylic derivatives such as benzoic acid (Bz) and tetramethylrhodamine (TAMRA), reporter units were incorporated into the amino side chain of ^{eda}G in the ODNs.

We initially examined the photooxidation of single-stranded ODN containing Bz-^{eda}G, **ODN1(Bz-^{eda}G)** 5'-d(TATAATXTAATAT)-3' (**X** = Bz-^{eda}G), in the presence of a photosensitizer riboflavin (Figure 1).[4] A sample solution of 10 □M **ODN1(Bz-^{eda}G)** in 50 mM sodium cacodylate (pH 7.0) was irradiated at 366 nm in the presence of 50 □M riboflavin at 0 °C. Photoirradiation of **ODN1(Bz-^{eda}G)** resulted in a rapid decomposition of ODN ($t_{1/2}$ = 6.2 min).

Scheme 1[a]

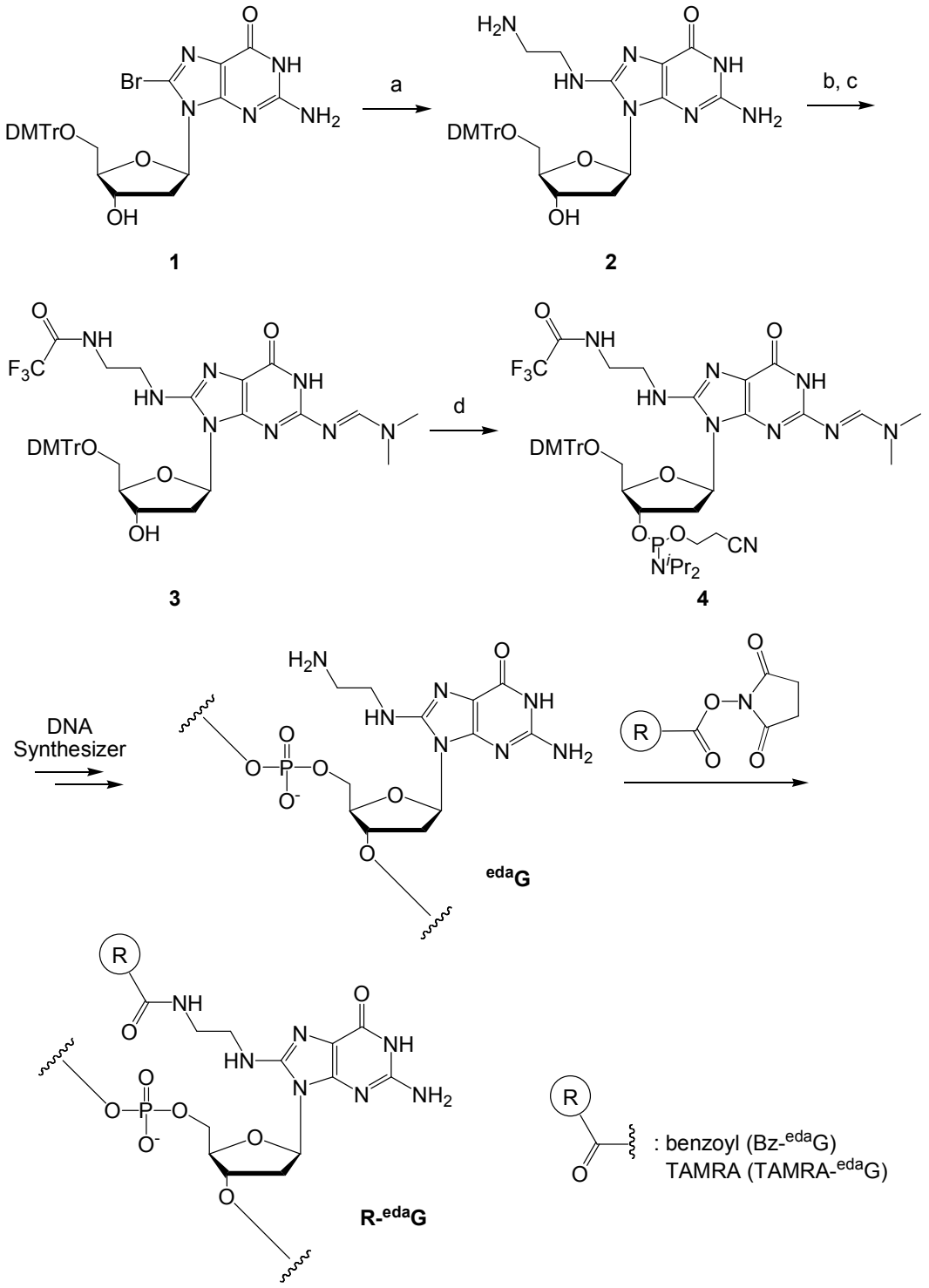

[a]*Reagents*: (a) ethylenediamene, reflux, 7 h; (b) ethyl trifluoroacetate, triethylamine, methanol, 0 °C, 2 h; (c) DMF-dimethylacetal, DMF, r.t., 2 h, 63% (three steps); (d) $(^{i}Pr_2N)_2PO(CH_2)_2CN$, tetrazole, acetonitrile, r.t., 2 h, *quant*.

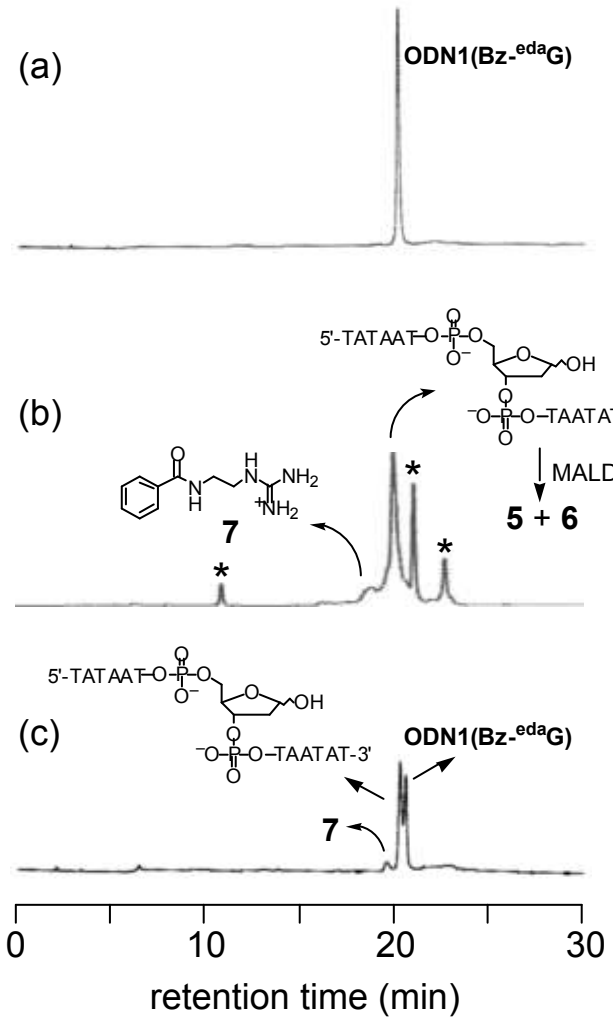

Figure 1. Typical HPLC profiles for the oxidation of Bz-^{eda}G-containing ODN. The reaction mixture was analyzed by HPLC on Cosmosil 5C-18AR or CHEMCOBOND 5-ODS-H column (4.6 × 150 mm), elution with a solvent mixture of 0.1 M triethylammonium acetate (TEAA), pH 7.0, linear gradient over 30 min from 0% to 30% acetonitrile at a flow rate 1.0 mL/min). (a) **ODN1(Bz-^{eda}G)**. (b) Photolysis of **ODN1(Bz-^{eda}G)** by photoirradiation in the presence of riboflavin. A solution of the modified ODN (10 μM) in sodium cacodylate buffer (pH 7.0) was irradiated at 366 nm at 0 °C for 30 min in the presence of riboflavin (50 μM). "*" denotes riboflavin and its photoproducts. (c) Oxidation of **ODN1(Bz-^{eda}G)** by Ir(IV). A solution of the modified ODN (10 μM) in sodium cacodylate buffer (pH 7.0) was incubated at room temperature for 15 min in the presence of sodium hexachloroiridate(IV) (20 μM).

The major isolable photoproducts of the oxidation of **ODN1(Bz-^{eda}G)** were identified by mass spectrometric analysis as ODN fragments **5**, cleaved via an abasic site, ([M–H]$^-$, calcd. 1968.32, found 1967.68 by MALDI-TOF), 5'-phosphate end 6 ([M–H]$^-$, calcd. 1870.22, found 1870.11 by MALDI-TOF), and benzamide **7** possessing a guanidinium group (M^+, 207 and its fragments 148, 105, 77 and 59 by LC-ESI/MS/MS) (Figure 2 and 3). The identified products strongly suggest that the rapid decomposition of ^{eda}G may proceed via the G cation radical decomposition mechanism proposed earlier[5] to result in a release of a function unit as typically represented by **7** (Scheme 2).

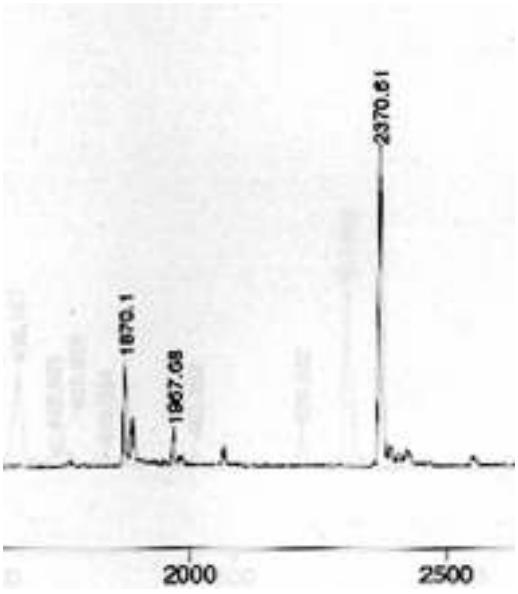

Figure 2. Mass spectroscopic analysis of UV-irradiated **ODN1(Bz-^{eda}G)**. The mass of photoirradiated ODN was determined by MALDI-TOF mass spectroscopy (acceleration voltage 21 kV, negative mode) with 2',3',4'-trihydroxyacetophenone (THAP) as matrix, using THAP ([M–H]$^-$ 167.04) and T_8 ([M–H]$^-$ 2370.61) as an internal standard. ODN fragments cleaved via an abasic nucleotide, **5** ([M–H]$^-$, calcd. 1968.32, found 1967.68) and **6** ([M–H]$^-$, calcd. 1870.22, found 1870.11) were found.

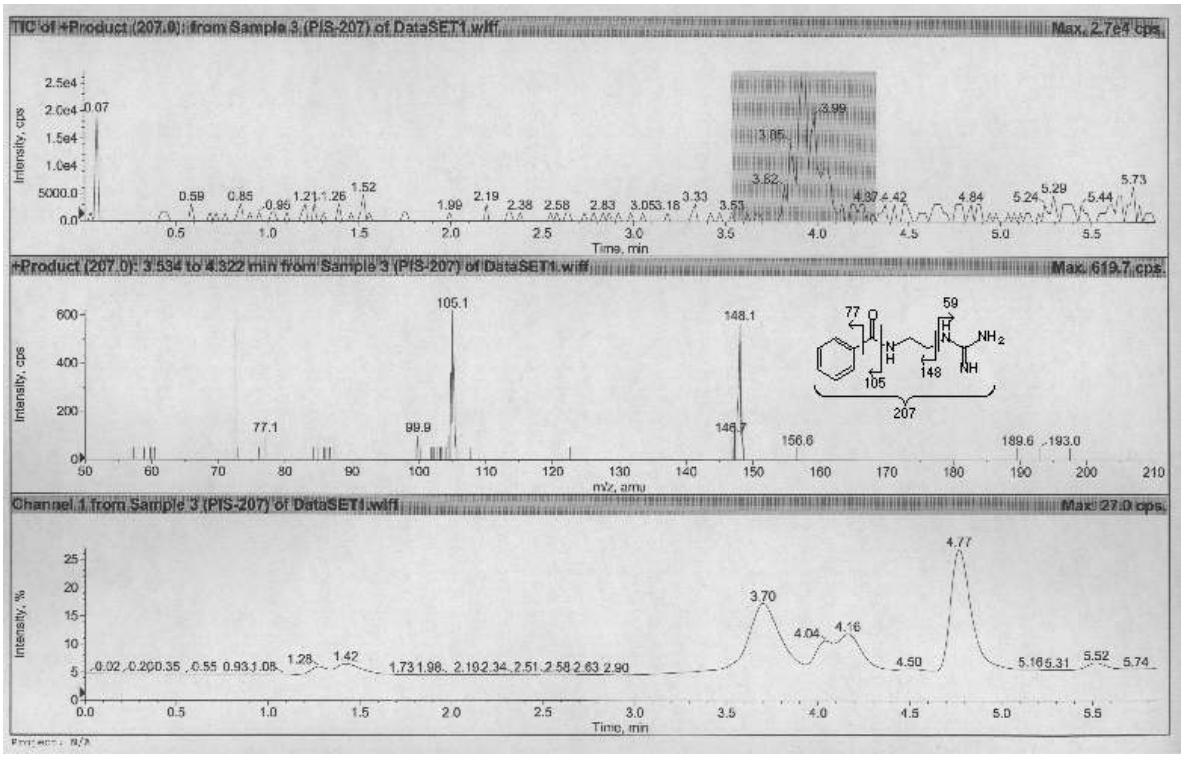

Figure 3. Mass spectroscopic analysis of UV-irradiated **ODN1(Bz-^{eda}G)**. The mass of photoirradiated ODN was determined by LC-ESI/MS/MS spectroscopy. Top, eluate containing MS 207; middle, fragments of MS 207; bottom, LC profile on a Intakt C-18 column (2.0 × 50 mm) detected at 254 nm; elution with a solvent mixture of 0.1 M triethylammonium acetate (pH 7.0), 0–90% acetonitrile for 5 min and 90% acetonitrile for 2 min at a flow rate 0.2 mL/min. The retention time for the product possessing MS 207 is 3.70 min. The peak of retention time of 4.77 min is riboflavin.

Scheme 2.

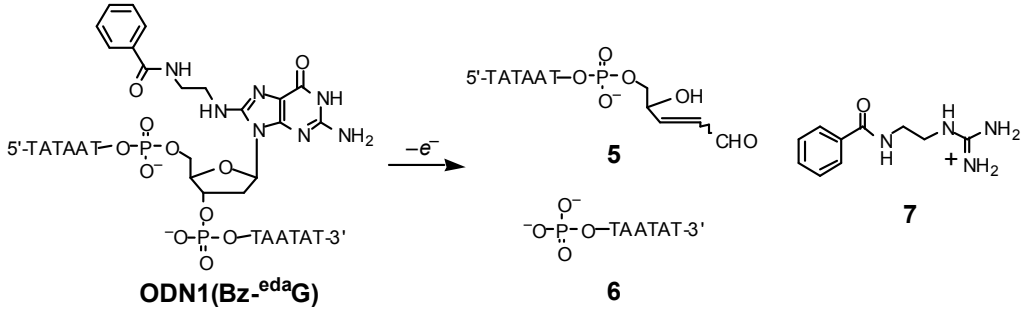

The site-selective oxidation of edaG-containing ODN was also observed with other one-electron oxidants. Ir(IV) is a highly selective oxidant that reacts exclusively with oxidized nucleobases such as 8-oxoG and 8-oxoA.[6] The oxidation potential ($E_{1/2}$) of Bz-edaG is 0.59 V (*vs* NHE), **7** which is close to that of 8-oxoG (0.56 V,[7] 0.60 V[8]). The ^{eda}G-containing **ODN ODN1(X)** (**X** = Bz- and TAMRA-^{eda}G) was mixed with Ir(IV).[6,9] A solution of single-stranded **ODN1(X)** (10 □M) in sodium cacodylate buffer (pH 7.0) was incubated at room temperature in the presence of sodium hexachloroiridate(IV) (20 □M). Oxidation with Ir(IV) resulted in a rapid degradation of **ODN1(X)** at the site of modified ^{eda}G (57% consumption for Bz-^{eda}G and 89% for TAMRA-^{eda}G in 15 min incubation, as determined by HPLC).

The method using ^{eda}G constitutes a facile strategy for detecting long-range hole transport through DNA without complicated and unwieldy analyzing processes such as quantification of oxidative guanine damage of labeled DNA[10] or the analysis of photodynamics.[11] We examined the detection of TAMRA released from **ODN2** containing a TAMRA-tethered ^{eda}G via long-range hole transport through DNA (Figure 4 and 5). The reaction sample containing the **ODN2/ODN2'(U*)** duplex possessing a cyanobenzophenone-modified uridine (**U***)[12] as a hole injector was irradiated at 312 nm (Figure 4a). The decrease of the fluorescence intensity of TAMRA by photobleaching was less than 5% after 312 nm photoirradiation for 90 min. The photolyzed ODN was then removed from the sample solution by passing through a centrifugal filter (Microcon YM-3). A strong fluorescence at 576 nm was observed from the filtrate of the **ODN2/ODN2'(U*)** sample after photoirradiation, and the fluorescence after 60 min irradiation was seven times stronger than that of the control **ODN2/ODN2'(T)** without **U*** (Figure 4b and 5). The fluorescence intensity of the **ODN2/ODN2'(U*)** sample increased in proportion to the irradiation time. The change of fluorescence intensity showed a good correlation with the strand cleavage at ^{eda}G site, which was independently quantified by PAGE for the experiment using the **ODN2/ODN2'(U*)** (Figure 4c and 6,

the 18% of TAMRA-^{eda}G in intact ODN was also damaged by hot piperidine treatment). In addition, in the PAGE analysis for the photoirradiated duplex, it was observed that lesions at the GGG sites, located between **U*** and ^{eda}G, were strongly suppressed. Thus, ^{eda}G acts as a very efficient hole trap, and the hole generated in the duplex by **U*** is selectively trapped at ^{eda}G site via a long-range hole transport to result in a release of TAMRA from the duplex. The fluorescence from the photoirradiated sample was visually detectable. As shown in Figure 4d, a strong visible emission was observable with the filtrate of photoirradiated **ODN2/ODN2'(U*)** sample, whereas the emission from the filtrate of photoirradiated **ODN2/ODN2'(T)**, a control sample, was negligible. The incorporation of TAMRA-^{eda}G into the duplex makes it possible to detect hole transport through DNA without PAGE analysis.

Conclusion

In conclusion, we have developed a novel nucleosbase, ^{eda}G, that efficiently releases reporter tags upon one-electron oxidation. The ^{eda}G-selective degradation of ODNs can be achieved by various mild oxidizing agents. This oxidant-dependent molecular releasing technique is useful not only for drug releasing systems but also for the release of fluorescent tag after gene analysis.

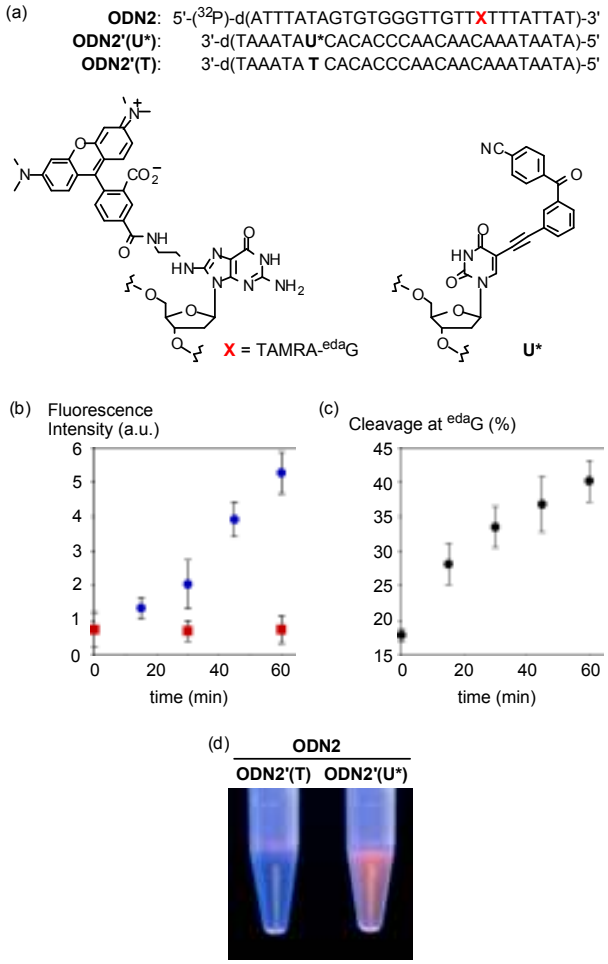

Figure 4. Release of TAMRA from TAMRA-^{eda}G via long-range DNA oxidation. (a) Sequences of duplex ODNs. (b) Fluorescence intensity of the reaction samples after photoirradiation and removal of ODN. The duplexes in 10 mM sodium cacodylate (pH 7.0) were irradiated (λ = 312 nm) at 0 ˚C followed by centrifugation with a centrifugal filter (Microcon YM-3). Fluorescence spectra were measured at 550 nm excitation. Fluorescence intensities at 576 nm were designated by □ (blue) for **ODN2**/**ODN2'(U*)** duplex and by □ (red) for **ODN2**/**ODN2'(T)**. (c) Cleavage of TAMRA-^{eda}G via hole transport. ^{32}P-labeled duplex in 10 mM sodium cacodylate (pH 7.0) was irradiated (λ = 312 nm) at 0 ˚C followed by a hot piperidine treatment. The relative damaging extents show the percentage of strand breakages at the ^{eda}G site relative to the total strand cleavage obtained by densitometric analysis. (d) Fluorescence image of the samples given by **ODN2**/**ODN2'(T)** duplex (left) and **ODN2**/**ODN2'(U*)** duplex (right) after 312 nm irradiation (60 min) followed by removal of ODN by filtration. The fluorescence image of the filtrate was taken using a transilluminator (312 nm).

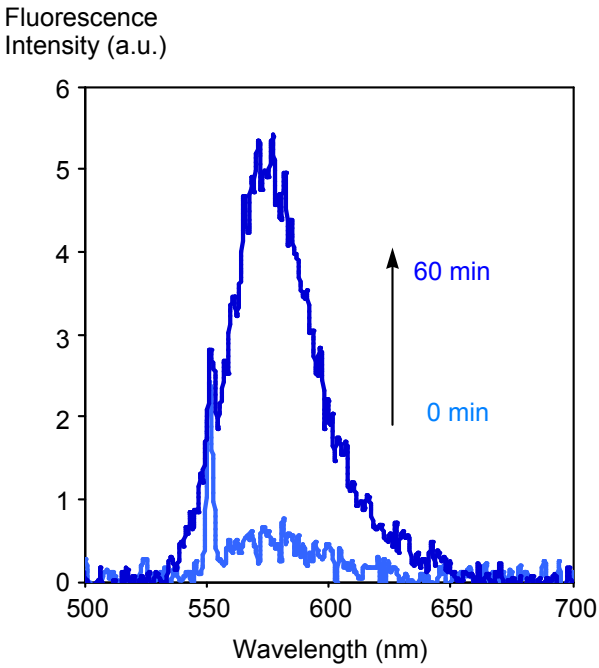

Figure 5. Fluorescence intensity of the reaction samples of **ODN2**/**ODN2'(U*)** after photoirradiation (λ = 312 nm) and removal of ODN. The duplexes in 10 mM sodium cacodylate (pH 7.0) were irradiated at 0 ˚C followed by centrifugation (15,000 rpm) with Microcon (YM-3, 3,000 MWCO), centrifugal filter devices, at 25 ˚C for 1 h. The fluorescence of the filtrate was measured with an excitation wavelength of 550 nm using a SHIMADZU RF-5300PC spectrofluorophotometer.

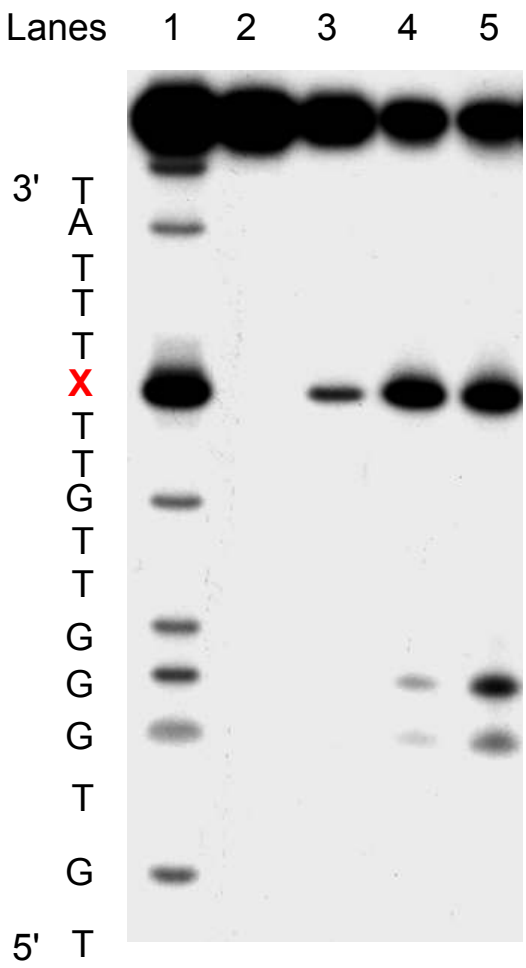

Figure 6. PAGE analysis of the photolysate. The ^{32}P-labeled **ODN2** was hybridized with **ODN2'(U*)** in 10 mM sodium cacodylate buffer (pH 7.0). Photoirradiation was then carried out on a solution containing duplex (1 μM strand concentration) in 10 mM sodium cacodylate buffer at pH 7.0. The mixture was irradiated with a transilluminator (312 nm) at a distance of 3 cm at 0 °C. The photoirradiated ODN was heated in 50 μL of 10% piperidine (*v*/*v*) at 90 °C for 20 min. **X** denotes TAMRA-^{eda}G. Lane 1, Maxam-Gilbert G+A sequencing reactions; lane 2, intact **ODN2**; lane 3, 0 min photoirradiation and hot piperidine treatment; lane 4, 30 min photoirradiation and hot piperidine treatment; lane 5, 60 min photoirradiation and hot piperidine treatment.

Experimental Section

General. ^{1}H NMR spectra were measured with Varian Mercury 400 (400 MHz) spectrometer. ^{13}C NMR spectra were measured with JEOL JNM α-500 (500 MHz) spectrometer. Coupling constants (*J* value) are reported in hertz. The chemical shifts are expressed in ppm downfield from tetramethylsilane, using residual chloroform (δ= 7.24 in ^{1}H NMR, δ= 77.0 in ^{13}C NMR) as an internal standard. FAB mass spectra were recorded on JEOL JMS DX-300 spectrometer or JEOL JMS SX-102A spectrometer. Masses of ODNs were determined with a MALDI-TOF mass spectroscopy (acceleration voltage 21 kV, negative mode) with 2',3',4'-trihydroxyacetophenone (THAP) as matrix, using T_8 ($[M–H]^-$ 2370.61) and T_{17} ($[M–H]^-$ 5108.37) as an internal standard. HPLC was performed on a cosmosil 5C-18AR or CHEMCOBOND 5-ODS-H column (4.6 × 150 mm) with a Gilson Chromatography Model 305 using a UV detector Model 118 at 254 nm.

8-[2-(*N*-Trifluoroacetylamino)ethyl]amino-2-(*N,N*-dimethylaminomethylidenyl)amino-5'-*O*-(4,4'-dimethoxytrityl)-2'-deoxyguanosine (3). A solution of 8-bromo-5'-*O*-(4,4'-dimethoxytrityl)-2'-deoxyguanosine **1** (2.0 g, 30.8 mmol) was stirred in ethylenediamine (100 mL) at 130 °C for 7 h. The reaction mixture was concentrated to give a crude product **2** as a brown oil. Crude **2** was dissolved in triethylamine (25 mL) and methanol (50 mL), and then 10 mL of ethyl trifluoroacetate was added to the mixture at 0 °C. The reaction mixture was stirred at 0 °C for 2 h, and then concentrated. Subsequently, *N,N*-dimethylformamide (25 mL) and *N,N*-dimethylformamide dimethylacetal (25 mL) were added to the residue. The reaction mixture was stirred at ambient temperature for 2 h. After concentration, the residue was purified by column chromatography on silica gel (chloroform : methanol = 30 : 1) to give compound **3** (1.5 g, 63%): ^{1}H NMR ($CDCl_3$) δ 9.77 (brs, 1 H), 9.56 (brs, 1 H), 8.54 (s, 1 H), 7.34–7.19 (m, 8 H), 6.83–6.80 (m, 5 H), 6.48 (dt, 1 H, *J* = 8.0, 4.0 Hz),

5.83 (brs, 1 H), 4.75 (d, 1 H, J = 5.8 Hz), 4.07 (d, 1 H, J = 2.4 Hz), 3.765 (s, 3 H), 3.763 (s, 3 H), 3.76–3.72 (m, 2 H), 3.38 (d, 1 H, J = 8.4 Hz), 3.10 (s, 3 H), 3.02 (s, 3 H), 3.01–2.95 (m, 2 H), 2.80–2.60 (m, 3 H), 2.33 (dd, 1 H, J = 13.3, 8.0 Hz); ^{13}C NMR ($CDCl_3$) δ 158.92, 158.91, 158.60, 157.56, 157.19, 156.55, 151.00, 143.55, 139.43, 134.61, 134.57, 130.29, 129.10, 128.42, 128.04, 127.82, 127.73, 127.55, 127.05, 120.27, 117.41, 114.55, 113.30, 113.27, 113.14, 87.01, 85.74, 82.80, 77.21, 71.87, 62.87, 55.27, 55.23, 42.65, 41.30, 40.77, 38.73, 35.11; MS (FAB, NBA/CH_2Cl_2) m/z (%) 779 [$(M+H)^+$]; HRMS (FAB) calcd for $C_{38}H_{42}N_8O_7F_3$ [$(M+H)^+$] 779.3129, found 779.3128.

3'-(*O*-Cyanoethyl-*N,N*-diisopropylphosphoramidite)-8-[2-(*N*-trifluoroacetylamino)ethyl]amino-2-(*N,N*-dimethylaminomethylidenyl)amino-5'-*O*-(4,4'-dimethoxytrityl)-2'-deoxyguanosine (4). To a solution of **3** (70 mg, 89.9 μmol), 2-cyanoethyl tetraisopropyldiphosphoramidite (31 μL, 98.9 μmol) and tetrazole (7 mg, 98.9 μmol) in acetonitrile (900 μL) were added. The reaction mixture was stirred at ambient temperature for 2 h. The mixture of **4** was filtered and used with no further purification.

ODN Synthesis and Characterization. ODNs were synthesized by the conventional phosphoramidite method by using an Applied Biosystems 392 DNA/RNA synthesizer. Synthesized ODNs were purified by reverse phase HPLC on a 5-ODS-H column (10 × 150 mm, elution with a solvent mixture of 0.1 M triethylammonium acetate (TEAA), pH 7.0, linear gradient over 30 min from 5% to 20% acetonitrile at a flow rate 3.0 mL/min). An aliquot of purified ODN solution was fully digested with calf intestine alkaline phosphatase (50 U/mL), snake venom phosphodiesterase (0.15 U/mL) and P1 nuclease (50 U/mL) at 37 °C for 3 h. Digested solution was analyzed by HPLC on Cosmosil 5C-18AR or CHEMCOBOND 5-ODS-H column (4.6 × 150 mm), elution with a solvent mixture of 0.1 M triethylammonium acetate (TEAA), pH 7.0, linear gradient over 20 min from 0% to 20% acetonitrile at a flow rate 1.0

mL/min). Concentration of each ODN was determined by comparing a given peak area with those of 0.1 mM standard solution containing dA, dC, dG and dT. Each ODN was characterized by MALDI-TOF MS; 5'-d(TATAAT^{eda}GTAATAT)-3', *m*/*z* 4027.33 (calcd for $[M–H]^-$ 4028.72); 5'-d(ATTTATAGTGTGGGTTGTT^{eda}GTTTATTAT)-3', *m*/*z* 8732.87 (calcd for $[M–H]^-$ 8732.69).

Postsynthetic Modification of ^{eda}G-Containing ODN and Its Characterization. To a 500 μL solution of ^{eda}G-containing ODNs (60 nmol) in 50 mM sodium phosphate buffer (pH 7.0) was added a solution of a *N*-hydroxysuccinimidyl ester of functional units (benzoic acid and tetramethylrhodamine 5-carboxylic acid) in DMSO (1 mg/mL, 150 μL), and the mixture was incubated at 4 °C for 18 h. Modified ODNs were purified by reverse phase HPLC on a 5-ODS-H column (10 × 150 mm, elution with a solvent mixture of 0.1 M triethylammonium acetate (TEAA), pH 7.0, linear gradient over 20 min from 0% to 20% acetonitrile at a flow rate 3.0 mL/min). Each ODN was characterized by MALDI-TOF MS; 5'-d(TATAAT[Bz-^{eda}G]TAATAT)-3' (**ODN1(Bz-^{eda}G)**), *m*/*z* 4132.39 (calcd for $[M–H]^-$ 4132.83); 5'-d(TATAAT[TAMRA-^{eda}G]TAATAT)-3' (**ODN1(TAMRA-^{eda}G)**), *m*/*z* 4442.34 (calcd for $[M–H]^-$ 4442.17); 5'-d(ATTTATAGTGTGGGTTGTT[TAMRA-^{eda}G]TTTATTAT)-3' (**ODN2**), *m*/*z* 9146.57 (calcd for $[M–H]^-$ 9146.12).

Oxidation of Bz-^{eda}G-Containing ODN by Photoirradiation in the Presence of Riboflavin. A solution of single-stranded ODN 5'-d(TATAAT**X**TAATAT)-3' (**X** = Bz-^{eda}G) (10 μM) in sodium cacodylate buffer (pH 7.0) was irradiated at 366 nm at 0 °C for 30 min in the presence of riboflavin (50 μM). After irradiation, the reaction mixture was analyzed by HPLC on Cosmosil 5C-18AR or CHEMCOBOND 5-ODS-H column (4.6 × 150 mm), elution with a solvent mixture of 0.1 M triethylammonium acetate (TEAA), pH 7.0, linear gradient over 30 min from 0% to 30% acetonitrile at a flow rate 1.0 mL/min). The modified

ODN was completely consumed within 30 min by photoirradiation. The reaction products were analyzed using MALDI-TOF MS and LC-ESI/MS/MS. ODN fragments **5**, $[M–H]^-$, calcd. 1968.32, found 1967.68 by MALDI-TOF; 5'-phosphate end **6**, $[M–H]^-$, calcd. 1870.22, found 1870.11 by MALDI-TOF; a benzamide **7**, M^+, 207 and its fragments 148, 105, 77 and 59 by LC-ESI/MS/MS.

Oxidation of Bz-^{eda}G-Containing ODN by Ir(IV). A solution of single-stranded ODN 5'-d(TATAAT**X**TAATAT)-3' (**X** = Bz-^{eda}G) (10 μM) in sodium cacodylate buffer (pH 7.0) was incubated at room temperature for 15 min in the presence of sodium hexachloroiridate(IV) (20 μM). After reaction, the reaction mixture was analyzed by HPLC on Cosmosil 5C-18AR or CHEMCOBOND 5-ODS-H column (4.6 × 150 mm), elution with a solvent mixture of 0.1 M triethylammonium acetate (TEAA), pH 7.0, linear gradient over 30 min from 0% to 30% acetonitrile at a flow rate 1.0 mL/min). HPLC profile is shown in Figure S1(c). 57% of modified ODN was consumed in 15 min incubation. In a similar manner, a solution of single-stranded ODN 5'-d(TATAAT**X**TAATAT)-3' (**X** = TAMRA-^{eda}G) (10 μM) in sodium cacodylate buffer (pH 7.0) was incubated at room temperature for 15 min in the presence of sodium hexachloroiridate(IV) (50 μM). 89% of modified ODN was consumed in 15 min incubation.

Hole Transport Experiment and Fluorescence Analysis. The ODN 5'-d(ATTTATAGTGTGGGTTGTT[TAMRA-^{eda}G]TTTATTAT)-3' was hybridized with the complementary strand containing cyanobenzophenone-substituted uridine (U*) in 10 mM sodium cacodylate buffer (pH 7.0). Hybridization was achieved by heating the sample at 90 °C for 5 min and slowly cooling to room temperature. Photoirradiation was then carried out for a solution containing duplex (1 μM strand concentration) in 10 mM sodium cacodylate buffer at pH 7.0. The mixture was irradiated with a transilluminator (312 nm) at a distance of 3 cm at 0 °C for 1 h. After irradiation, ODN was removed from samples by

centrifugation (15,000 rpm) with Microcon (YM-3, 3,000 MWCO), centrifugal filter devices, at 25 ˚C for 1 h. The fluorescence of the filtrate was measured with an excitation wavelength of 550 nm using a SHIMADZU RF-5300PC spectrofluorophotometer.

Preparation of ^{32}P-5'-End-Labeled Oligomers. The ODN 5'-d(ATTTATAGTGTGGGTTGTT[TAMRA-^{eda}G]TTTATTAT)-3' (400 pmol) was 5'-end labeled by phosphorylation with 4 μL of [γ-^{32}P]ATP (Amersham) and T4 polynucleotide kinase using a standard procedure. The 5'-end labeled ODN was recovered by ethanol precipitation and further purified by 15 % denaturing polyacrylamide gel electrophoresis (PAGE) and isolated by the crush and soak method.

Hole Transport Experiment and PAGE Analysis. The ODN 5'-^{32}P-d(ATTTATAGTGTGGGTTGTT[TAMRA-^{eda}G]TTTATTAT)-3' (2.0×10^5 cpm) was hybridized with the complementary strand containing cyanobenzophenone-substituted uridine (**U***) in 10 mM sodium cacodylate buffer (pH 7.0). Hybridization was achieved by heating the sample at 90 °C for 5 min and slowly cooling to room temperature. Photoirradiation was then carried out for a solution containing duplex (1 μM strand concentration) in 10 mM sodium cacodylate buffer at pH 7.0. The mixture was irradiated with a transilluminator (312 nm) at a distance of 3 cm at 0 °C for 1 h. After irradiation, all reaction mixtures were precipitated with the addition of 10 μL of 3 M sodium acetate, 20 μL of herring sperm DNA (50 μM base pair concentration) and 800 μL of ethanol. The precipitated ODN was washed with 100 μL of 80 % cold ethanol and dried *in vacuo*. The precipitated ODN was resolved in 50 μL of 10% piperidine (*v*/*v*), heated at 90 °C for 20 min., evaporated by vacuum rotary evaporation to dryness and resuspended in 5–20 μL of 80 % formamide loading buffer (a solution of 80 % *v*/*v* formamide, 1 mM EDTA, 0.1 % xylenecyanol and 0.1 % bromophenol blue). All reactions, along with Maxam-Gilbert G+A sequencing reactions, were conducted with heating at

90 °C for 1 min, and quickly chilled on ice. The samples (1 μL, 3–10 kcpm) were loaded onto 15 % denaturing 19:1 acrylamide-bisacrylamide gel containing 7 M urea and electrophoresed at 1900 V for approximately 1.5 h and transferred to a cassette and stored at –80 °C with Fuji X-ray film.

References

1. (a) Tyagi, S.; Kramer, F. R. *Nat. Biotechnol.* **1996**, *14*, 303–308. (b) Tyagi, S.; Btaru, D. P.; Kramer, F. R. *Nat. Biotechnol.* **1998**, *16*, 49–53. (c) Piatek, A. S.; Tyagi, S.; Pol, A. C.; Telenti, A.; Miller, L. P.; Kramer, F. R.; Alland, D. *Nat. Biotechnol.* **1998**, *16*, 359–363.
2. (a) Ma, Z.; Taylor, J.-S. *Proc. Natl. Acad. Sci. USA* **2000**, *97*, 11159–11163. (b) Ma, Z.; Taylor, J.-S. *Bioorg. Med. Chem.* **2001**, *9*, 2501–2510. (c) Okamoto, A.; Tanabe, K.; Inasaki, T.; Saito, I. *Angew. Chem., Int. Ed.* **2003**, *42*, 2502–2504.
3. Markiewicz, W. T.; Gröger, G.; Rösch, R.; Zebrowska, A.; Markiewicz, M.; Klotz, M.; Hinz, M.; Godzina, P.; Seliger, H. *Nucleic Acids Res.* **1997**, *25*, 3672–3680.
4. For photooxidation of DNA using riboflavin, see: (a) Ito, K.; Inoue, S.; Yamamoto, K.; Kawanishi, S. *J. Biol. Chem.* **1993**, *268*, 13221–13227. (b) Kino, K.; Saito, I.; Sugiyama, H. *J. Am. Chem. Soc.* **1998**, *120*, 7373–7374. (c) Saito, I.; Nakamura, T.; Nakatani, K.; Yoshioka, Y.; Yamaguchi, K.; Sugiyama, H. *J. Am. Chem. Soc.* **1998**, *120*, 12686–12687.
5. (a) Ikeda, H.; Saito, I. *J. Am. Chem. Soc.* **1999**, *121*, 10836–10837. (b) Cadet, J.; Berger, M.; Buchko, G. W.; Joshi, P. C.; Raoul, S.; Ravanat, J.-L. *J. Am. Chem. Soc.* **1994**, *116*, 7403–7404.
6. Muller, J. G.; Duarte, V.; Hickerson, R. P.; Burrows, C. J. *Nucleic Acids Res.* **1998**, *26*, 2247–2249.
7. Goyal, R. N.; Dryhurst, G. *J. Electroanal. Chem.* **1982**, *135*, 75–91.
8. Yanagisawa, H.; Ogawa, Y.; Ueno, M. *J. Biol. Chem.* **1992**, *267*, 13320–13326.
9. Hickerson, R. P.; Prat, F.; Mullar, J. G.; Foote, C. S.; Burrows, C. J. *J. Am. Chem. Soc.* **1999**, *121*, 9423–9428.
10. For selected examples, see: (a) Hall, D. B.; Holmlin, R. E.; Barton, J. K. *Nature* **1996**, *382*, 731–735. (b) Gasper, S. M.; Schuster, G. B. *J. Am. Chem. Soc.* **1997**, *119*, 12762–12771. (c) Meggers, E.; Kusch, D.;

Spichty, M.; Wille, U.; Giese, B. *Angew. Chem., Int. Ed. Engl.* **1998**, *37*, 460–462. (d) Núñez, M. E.; Hall, D. B.; Barton, J. K. *Chem. Biol.* **1999**, *6*, 85–97. (e) Nakatani, K.; Dohno, C.; Saito, I. *J. Am. Chem. Soc.* **2000**, *122*, 5893–5894. (f) Giese, B.; Amaudrut, J.; Köhler, A.-K.; Spormann, M.; Wessely, S. *Nature* **2001**, *412*, 318–320. (g) Okamoto, A.; Tanabe, K.; Dohno, C.; Saito, I. *Bioorg. Med. Chem.* **2002**, *10*, 713–718. (h) Okamoto, A.; Tanaka, K.; Saito, I. *J. Am. Chem. Soc.* **2003**, *125*, 5066–5071.

11. For selected examples, see: (a) Murphy, C. J.; Arkin, M. R.; Jenkins, Y.; Ghatlia, N. D.; Bossmann, S. H.; Turro, N. J.; Barton, J. K. *Science* **1993**, *262*, 1025–1029. (b) Meade, T. J.; Kayyem, J. F. *Angew. Chem., Int. Ed. Engl.* **1995**, *34*, 352–354. (c) Lewis, F. D.; Wu, T.; Zhang, Y.; Letsinger, R. L.; Greenfield, S. R.; Wasielewski, M. R. *Science* **1997**, *277*, 673–676. (d) Fukui, K.; Tanaka, K.; Fujitsuka, M.; Watanabe, A.; Ito, O. *J. Photochem. Photobiol. B* **1999**, *50*, 18–27. (e) Fiebig, T.; Wan, C.; Kelley, S. O.; Barton, J. K.; Zewail, A. H. *Proc. Natl. Acad. Sci. USA* **1999**, *96*, 1187–1192. (f) Kawai, K.; Takada, T.; Tojo, S.; Ichinose, N.; Majima, T. *J. Am. Chem. Soc.* **2001**, *123*, 12688–12689.
12. Nakatani, K.; Dohno, C.; Saito, I. *J. Org. Chem.* **1999**, *64*, 6901–6904.

CHAPTER 6

Design of Base-Discriminating Fluorescent Nucleoside and Its Application to T/C SNP Typing

Abstract: We report a novel method for base detection using a base-discriminating fluorescent (BDF) nucleoside. We developed BDF probes containing methoxybenzodeazaadenine ^{MD}A and methoxybenzodeaza-inosine ^{MD}I, which give strong fluorescence only when the base on the complementary strand is cytosine and thymine, respectively. Thus, the ^{MD}A- and ^{MD}I-containing ODNs can be used as a very effective BDF probe for the detection of single base alterations, such as SNPs and point mutations. The present method using BDF probes is a very powerful tool for SNP typing that does not require any enzymes and time-consuming steps, and can avoid hybridization errors. In addition, a combination of ^{MD}A- and ^{MD}I-containing BDF probes facilitates the T/C SNP typing of a heterozygous sample.

Introduction

The typing of single base alterations, such as single nucleotide polymorphisms (SNPs), using DNA probes is a rapidly developing area. Most of the presently available methods utilize the difference in hybridization efficiency between the target DNA and the probe oligodeoxynucleotides (ODNs),[1] or the difference in enzymatic recognition between full-matched and mismatched duplexes.[2] However, there are still problems, such as hybridization errors, the high cost of enzymes, and the time-consuming steps required. Thus, it is highly desirable to develop an alternative method for SNP typing that can easily determine single base alterations at target sites.

Here, we report a conceptually new method for the fluorescence assay of a single base alteration (Figure 1). We devised novel fluorescent oligonucleotide probes that contain base-discriminating fluorescent (BDF) nucleosides, methoxybenzodeazaadenine ^{MD}A and methoxybenzodeazainosine ^{MD}I, which emit strong fluorescence only when the base on the complementary strand is C and T, respectively. Thus, the ^{MD}A- and ^{MD}I-containing ODNs can be used as a very effective BDF probe for the detection of single base alterations, such as SNPs and point mutations.[3]

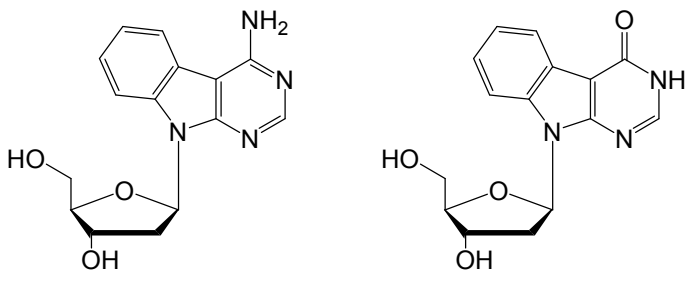

^{MD}A ^{MD}I

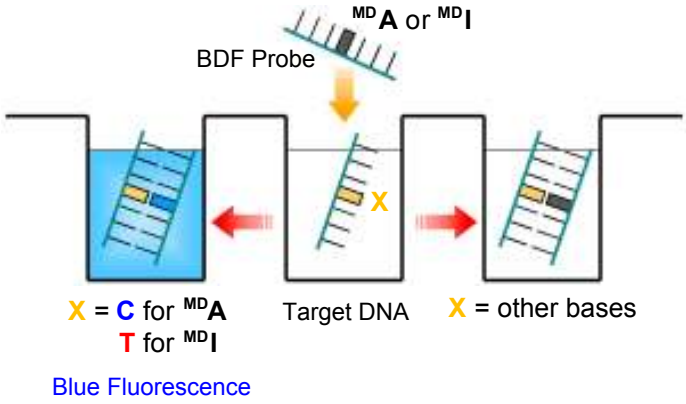

Figure 1. Schematic illustration of a new homogeneous SNP typing method using ^{MD}A- and ^{MD}I-containing base-discriminating fluorescent (BDF) probes.

Results and Discussion

The synthesis of ^{MD}A phosphoramidite unit and incorporation into ODNs were previously reported.[4,5] The syntheses of the novel fluorescent nucleosides, ^{MD}I, was readily achieved in a single step from 4-Chloro-7-(2-deoxy-3,5-di-*O*-*p*-toluoyl-β-$_D$-*erythro*-pentofuranosyl)-7*H*-pyrimido[4,5-b]indole (**1**) (Scheme 1).[5] Subsequently, nucleosides were protected and incorporated via the phosphoramidites into ODN, using a DNA synthesizer. The ODNs used in this study are summarized in Table 1. From melting temperature measurements with synthetic ODNs, it was revealed that ^{MD}A and ^{MD}I can form a stable base pair with T and C (Table 2).

Table 1. Oligodeoxynucleotides (ODNs) used in this study

	sequences
ODN(^{MD}A)	5'-d(CGCAAT^{MD}**A**TAACGC)-3'
ODN(^{MD}I)	5'-d(CGCAAT^{MD}**I**TAACGC)-3'
ODN(T)	5'-(GCGTTA**T**ATTGCG)-3'
ODN(C)	5'-(GCGTTA**C**ATTGCG)-3'
ODN(A)	5'-(GCGTTA**A**ATTGCG)-3'
ODN(G)	5'-(GCGTTA**G**ATTGCG)-3'
ODN$_{BRCA}$(^{MD}A)	5'-(GGTACCA^{MD}**A**TGAAATA)-3'
ODN$_{BRCA}$(^{MD}I)	5'-(GGTACCA^{MD}**I**TGAAATA)-3'
ODN$_{BRCA}$(T)	5'-(TATTTCA**T**TGGTACC)-3'
ODN$_{BRCA}$(C)	5'-(TATTTCA**C**TGGTACC)-3'

Scheme 1[a]

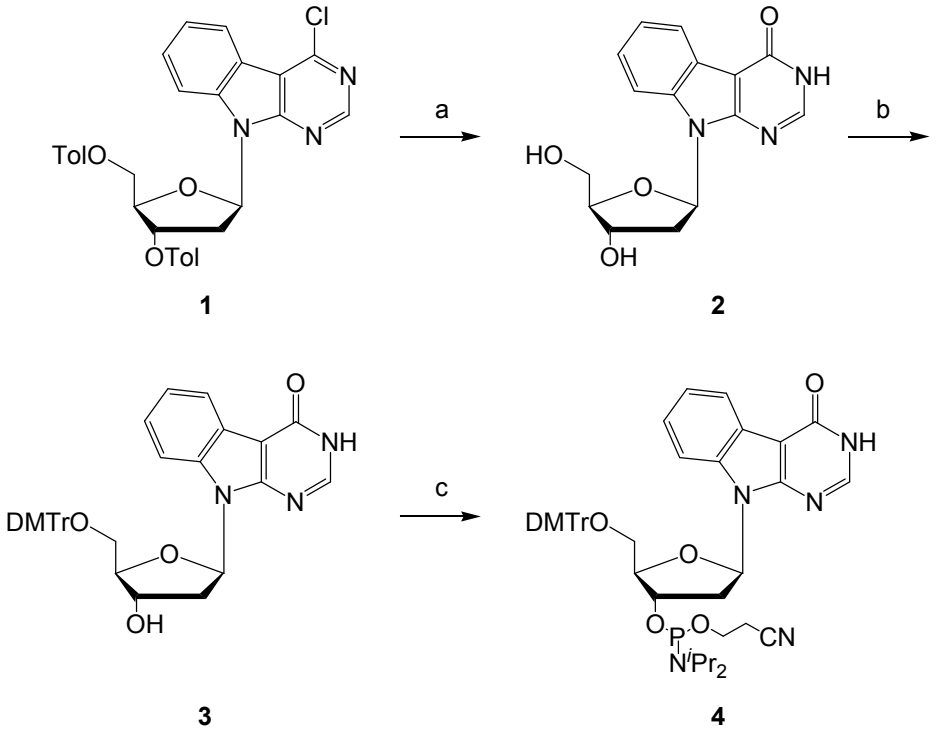

[a]*Reagents*: (a) 3 *N* NaOH-methanol-chloroform, reflux, 6 h, 94%; (b) 4,4'-dimethoxytrityl chloride, pyridine, r.t., 3 h, 91%; (c) (^{i}Pr$_2$N)$_2$PO(CH$_2$)$_2$CN, 1*H*-tetrazole, acetonitrile, r.t., 2 h, quant.

Table 2. Melting temperatures (T_m) for 5'-d(CGCAAT**X**TAACGC)-3'/5'-d(GCGTTA**Y**ATTGCG)-3' duplexes.[a]

X	T_m (°C)			
Y =	T	C	A	G
^{MD}I	51.0	51.4	47.4	42.9
^{MD}A	54.6	52.0	42.1	48.0
A	52.5	41.4	40.5	46.0

[a] Samples (2.5 μM duplex) were measured in 50 mM sodium phosphate / 0.1 M sodium chloride (pH 7.0)

The absorption maxima for ^{MD}A and ^{MD}I were initially observed at 327 nm (ε 2700) and 315 nm (ε 7800), respectively, where natural nucleosides have no absorption (Figure 2). Thus, ^{MD}A and ^{MD}I can be selectively excited with UV light above 300 nm. With excitation of ^{MD}A at 330 nm, we observed strong fluorescence (Φ = 0.118) at 397 and 427 nm. For ^{MD}I, strong fluorescence was observed at 442 nm (Φ = 0.117) with an excitation wavelength of 320 nm.

Next, the fluorescence of ^{MD}A-containing ODN (**ODN(^{MD}A)**) and ^{MD}I-containing ODN (**ODN(^{MD}I)**) was examined. In contrast to the strong fluorescence of ^{MD}A and ^{MD}I, the fluorescence intensities of their single-stranded ODNs and the "full-matched" duplexes with complementary strands (i.e., the strands containing T base opposite ^{MD}A and C base opposite ^{MD}I) were very weak (Figure 3a and 3b). Fluorescence quantum yields (Φ): a single-stranded **ODN(^{MD}A)**, 0.005; **ODN(^{MD}A)/ODN(T)**, <0.0005; **ODN(^{MD}A)/ODN(C)**, 0.081; **ODN(^{MD}A)/ODN(G)**, 0.020; **ODN(^{MD}A)/ODN(A)**, 0.0006; a single-stranded **ODN(^{MD}I)**, 0.006; **ODN(^{MD}I)/ODN(C)**, 0.002; **ODN(^{MD}I)/ODN(T)**, 0.011; **ODN(^{MD}I)/ODN(G)**, 0.007; **ODN(^{MD}I)/ODN(A)**, 0.003.[6] However, the fluorescence spectrum of the "mismatched" duplex **ODN(^{MD}A)/ODN(C)** showed a strong fluorescence at 424 nm (Φ = 0.081). It is noteworthy that the fluorescence of **ODN(^{MD}A)/ODN(C)** was 100 times stronger than that observed for **ODN(^{MD}A)/ODN(T)**. In contrast, when **ODN(^{MD}I)** was hybridized with the

complementary strand **ODN(T)**, a relatively strong fluorescence was observed at 424 nm (Φ = 0.011) that was 5.5 times stronger than that observed for **ODN(^{MD}I)/ODN(C)**. For the mismatched duplexes containing purine bases opposite ^{MD}A and ^{MD}I, the fluorescence intensities were much less than those of **ODN(^{MD}A)/ODN(C)** and **ODN(^{MD}I)/ODN(T)**.

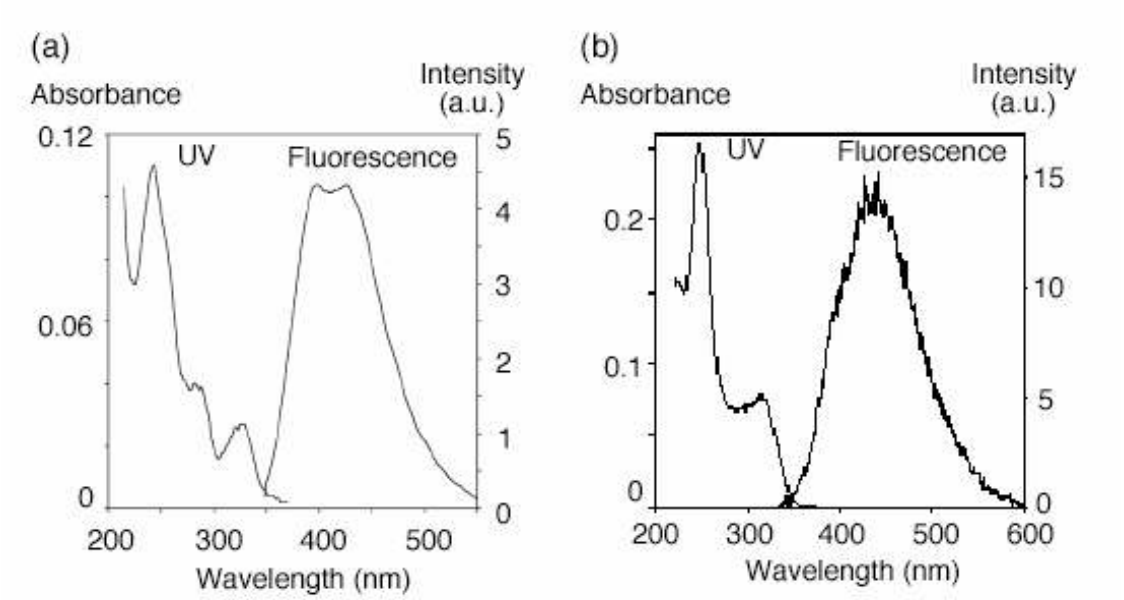

Figure 2. (a) Absorption and fluorescence spectra of 10 μM ^{MD}A nucleoside (50 mM sodium phosphate, 0.1 M sodium chloride, pH 7.0, r.t.) Excitation wavelength was 290 nm. (b) Absorption and fluorescence spectra of 10 μM ^{MD}I nucleoside (50 mM sodium phosphate, 0.1 M sodium chloride, pH 7.0, r.t.) Excitation wavelength was 330 nm.

The fluorescence spectra of **ODN(^{MD}A)/ODN(C)** and **ODN(^{MD}I)/ODN(T)** extended to 550 nm, as is shown in Figure 2a and 2b. Thus, the fluorescence emission from these solutions was visible to the human eye and clearly distinguishable from the solution of duplexes containing other base pairs (Figure 3c and 3d). The hybridization of BDF probes, **ODN(^{MD}A)** and **ODN(^{MD}I)**, with a target DNA facilitates the clear discrimination with the naked eye of C and T, respectively, located at a specific site of the target DNA.

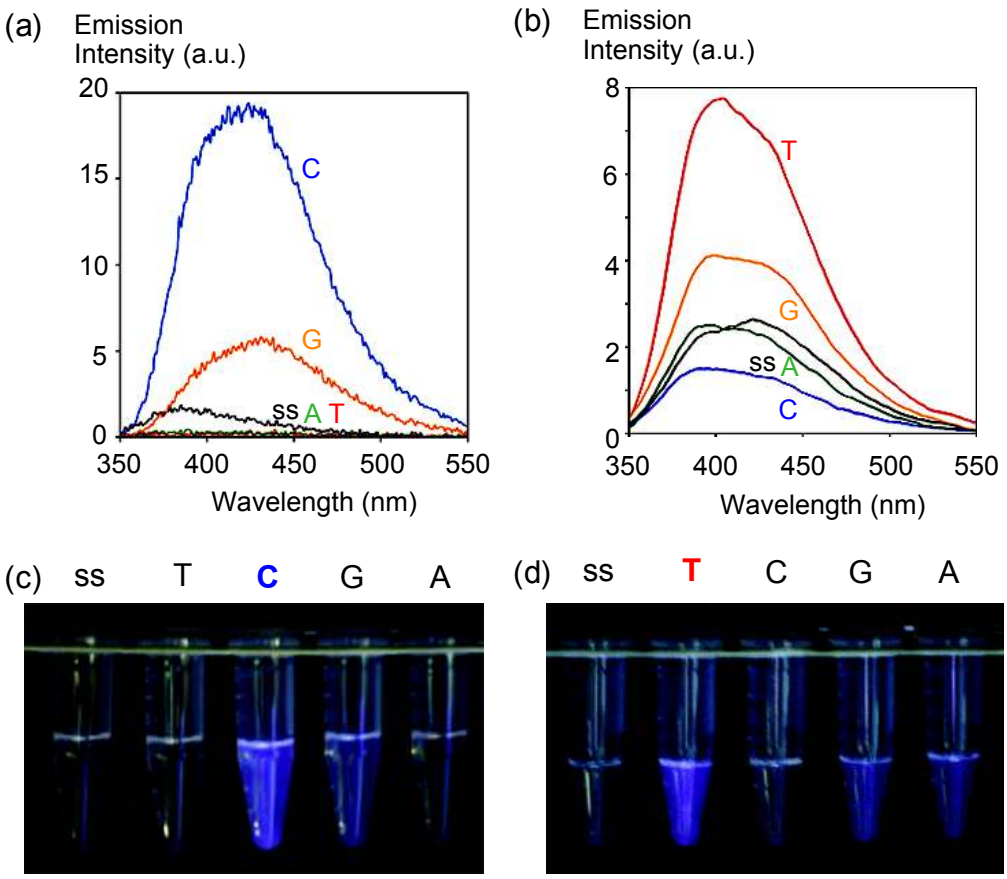

Figure 3. (a) Fluorescence spectra of 25 μM **ODN(**^{MD}**A)** hybridized with 25 μM **ODN(T)**, **ODN(C)**, **ODN(G)**, or **ODN(A)** (50 mM sodium phosphate, 0.1 M sodium chloride, pH 7.0, room temperature). Excitation was at 330 nm. (b) Fluorescence spectra of 25 μM **ODN(**^{MD}**I)** hybridized with 25 μM **ODN(T)**, **ODN(C)**, **ODN(G)**, or **ODN(A)** (50 mM sodium phosphate, 0.1 M sodium chloride, pH 7.0, room temperature). Excitation was at 330 nm. (c and d) Comparison of the fluorescence for the bases opposite ^{MD}A and ^{MD}I, respectively (25 μM strand concentration, 50 mM sodium phosphate, 0.1 M sodium chloride, pH 7.0, room temperature). "ss" denotes a single-stranded BDF probe. The sample solutions were illuminated with a 312 nm transilluminator.

Having established the fluorescence character of the ^{MD}A- and ^{MD}I-containing BDF probes, we tested the SNP detection of the T/C SNP sequence of the human breast cancer 1 gene (BRCA1)[6] by means of BDF probe hybridization. BDF probe, **ODN$_{BRCA1}$(^{MD}A)** or **ODN$_{BRCA1}$(^{MD}I)**, was mixed with a sample solution of the target sequence, **ODNBRCA1(T)**, **ODN$_{BRCA1}$(C)**, or a 1:1 mixture of **ODN$_{BRCA1}$(T)** and **ODN$_{BRCA1}$(C)**, to mimic the heterozygous state, and the fluorescence of the mixture was immediately read at room temperature with a fluorescence imaging instrument (Figure 4). As a result of the hybridization of BDF probes with **ODN$_{BRCA1}$(T)**, a strong emission was obtained for the addition of **ODN$_{BRCA1}$(^{MD}I)**, whereas the emission from the **ODN$_{BRCA1}$(^{MD}A)/ODN$_{BRCA1}$(T)** duplex was negligible. In contrast, for a sample solution containing **ODN$_{BRCA1}$(C)**, the addition of **ODN$_{BRCA1}$(^{MD}A)** showed a strong fluorescence, whereas a very weak fluorescence was observed for **ODN$_{BRCA1}$(^{MD}I)**. When BDF probes were added to a 1:1 mixture of **ODN$_{BRCA1}$(T)** and **ODN$_{BRCA1}$(C)**, a weak fluorescence emission was observed for both BDF probes and was clearly distinguishable from those of homozygous samples. Therefore, the present method using a combination of ^{MD}A- and ^{MD}I-containing BDF probes constitutes a very powerful tool for T/C SNP typing, although the general utility of our method is limited by the flanking base pairs of ^{MD}A and ^{MD}I. When the flanking base pair was a G/C base pair, then the fluorescences of ^{MD}A and ^{MD}I were considerably suppressed. Thus, the SNP typing method would be inaccurate for the sequence containing a G/C base pair flanking SNP site.

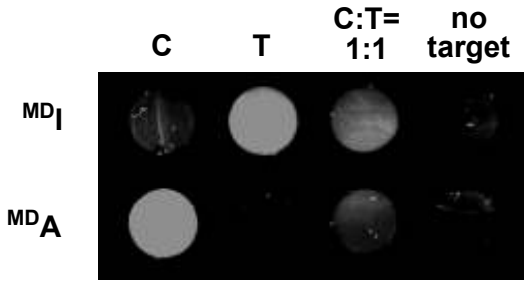

Figure 4. Determination of the T/C allele type of BRCA1 using the fluorescence change of BDF probes, **$ODN_{BRCA1}(^{MD}A)$** and **$ODN_{BRCA1}(^{MD}I)$**. A volume of 25 μM **$ODN_{BRCA1}(C)$** or **$ODN_{BRCA1}(T)$** was hybridized with 25 μM BDF probes (50 mM sodium phosphate, 0.1 M sodium chloride, pH 7.0, room temperature). Fluorescence was observed using a fluorescence imager Versa Doc Imaging System (BioRad) equipped with a 290-365 nm transilluminator. The image was taken through a 380 nm long pass emission filter.

Conclusion

In summary, we have devised a simple method for the detection of single nucleotide alteration by exploiting novel BDF probes. We designed new base-discriminating fluorescent nucleosides ^{MD}A and ^{MD}I, which can distinguish C and T, respectively, from other bases opposite the fluorescent base. The present SNP typing method using ^{MD}A- and ^{MD}I-containing BDF probes is a very powerful homogeneous assay that does not require enzymes or time-consuming steps, and avoids hybridization errors. In addition, a combination of these ^{MD}A- and ^{MD}I-containing BDF probes facilitates the T/C SNP typing of a heterozygous sample. Further work on the mechanistic aspects and more effective BDF probes is in progress in our laboratory.

Experimental Section

General. ^{1}H NMR spectra were measured with Varian Mercury 400 (400 MHz) spectrometer. ^{13}C NMR spectra were measured with JEOL JMN α-500 (500 MHz) spectrometer. Coupling constant (*J* value) are reported in hertz. The chemical shifts are expressed in ppm downfield from tetramethylsilane, using residual chloroform (δ = 7.24 in ^{1}H NMR, δ = 7.70 in ^{13}C NMR) and dimethylsulfoxide (δ = 2.48 in ^{1}H NMR, δ = 39.5 in ^{13}C NMR) as an internal standard. FAB Mass spectra were recorded on JEOL JMS DX-300 spectrometer or JEOL JMS SX-102A spectrometer. The reagents for the DNA synthesizer such as A, G, C, T-β-cyanoethyl phosphoramidite, and CPG support were purchased from Applied Biosystem, or GLEN RESEARCH. Masses of oligonucleotides were determined with a MALDI-TOF MS (acceleration voltage 21 kV, negative mode) with 2', 3', 4'-trihydroxyacetophenone as matrix, using T8 mer ([M - H]$^{-}$ 2370.61) and T17 mer ([M - H]$^{-}$ 5108.37) as an internal standard. HPLC was performed on a cosmosil 5C-18AR or CHEMCOBOND 5-ODS-H column (4.6 × 150 mm) with a Gilson Chromatography Model 305 using a UV detector Model 118 at 254 nm. ODNs were purchased from QIAGEN. Fluorescence measurements were using with BIO-RAD VersaDoc 3000. Fluorescence spectra were obtained using a SHIMADZU RF-5300PC spectrofluorophotometer.

1-Hydro-6-methoxy-9-(2'-deoxy-β-D-*erythro*-pentofuranosyl)-7*H*-pyrimido[4,5-β]indol-4-one (2). A suspension of **1** (100 mg, 0.17 mmol) in 3 *N* sodium hydroxide aqueous solution containing 10% ethanol and 1% chloroform was refluxed for 6 h. After cooling, the mixture was concentrated *in vacuo*, and the residue was pored into DMF (100 mL). The suspension was filtrated, and the filtrate was concentrated *in vacuo* to dryness, and the residue on purification by silica gel column chromatography (chloroform : methanol = 10 : 1) gave compound **2** (53 mg, 94%): ^{1}H NMR (DMSO-d_6) δ= 12.38 (br s, 1H), 8.30 (s, 1H), 7.86 (d, 1H,

J = 9.0 Hz), 7.51 (d, 1 H, *J* = 2.3 Hz), 6.95 (dd, 1H, *J* = 9.0, 2.4 Hz), 6.75 (dd, 1H, *J* = 8.6, 6.4 Hz), 5.32 (d, 1H, *J* = 4.2 Hz), 5.01 (t, 1H, *J* = 5.0 Hz), 4.43 (m, 1 H), 3.84 (dt, 1H, *J* =6.8, 3.1), 3.81 (s, 3H), 3.66 (m, 2 H), 2.75 (dt, 1H, *J* = 13.0, 6.8 Hz), 2.05 (ddd, 1H, *J* = 13.0, 5.5, 2.5 Hz); ^{13}C NMR (DMSO-d_6) δ=158.1, 155.1, 152.7, 147.3, 128.9, 122.9, 113.4, 102.9, 100.5, 87.0, 82.8, 70.5, 61.6, 55.4, 38.0; MS (FAB, NBA/DMSO-d_6) *m*/*z* (%) 332 [(M+H)$^+$]; HRMS (FAB) calcd for $C_{16}H_{17}N_3O_5$ [(M+H)$^+$] 332.1247, found 332.1246.

1-Hydro-6-methoxy-9-(2'-deoxy-5'-*O*-dimethoxytrityl-β-D-*erythro*-pentofuranosyl)-7*H*-pyrimido[4,5-*b*]indole (3). A solution of **2** (100 mg, 0.30 mmol), 4,4'-dimethoxytrityl chloride (133 mg, 0.39 mmol) was stirred in anhydrous pyridine (20 mL) for 2 h at ambient temperature. The reaction mixture was concentrated to a brown oil and purified by column chromatography on silica gel, eluting with a mixed solution of 90:3:5 (v/v/v) chloroform, methanol and triethylamine to give compound **3** (210 mg, 91%): ^{1}H NMR ($CDCl_3$) δ 11.10 (br s, 1H), 7.98 (d, 2H, *J* = 13.0 Hz), 7.69 (d, 1H, *J* = 2.5 Hz), 7.62 (d, 1H, *J* = 9.0 Hz), 7.43 (dt, 2H, *J* = 6.9, 1.7 Hz), 7.40-6.74 (m, 11H), 6.69 (dd, 1H, *J* = 9.0, 2.6 Hz), 4.80 (brs, 1H), 4.05 (dt, 1H, *J* = 4.3 Hz), 3.78 (s, 3H), 3.760 (s, 3H), 3.76 (m, 1H), 3.756 (s, 3H), 3.48 (q, 2H, *J* = 2.9), 3.08 (dt, 1H, *J* = 6.2 Hz), 2.29 (ddd, 1 H, *J* = 13.9, 7.1, 3.6 Hz); ^{13}C NMR ($CDCl_3$) δ 159.3, 158.4, 155.7, 153.1, 145.6, 144.7, 135.8, 135.7, 130.15, 130.13, 129.5, 128.2, 127.8, 126.8, 123.2, 114.2, 113.4, 113.1, 103.9, 101.7, 98.9, 86.5, 84.9, 83.1, 77.2, 72.1, 63.5, 55.8, 55.2, 45.8, 38.5; MS (FAB, NBA/CH_2Cl_2) *m*/*z* (%) 634 [(M+H)$^+$]; HRMS (FAB) calcd for $C_{37}H_{35}N_3O_7$ [M$^+$] 633.2475, found 633.2498.

1-Hydro-6-methoxy-9-(2'-deoxy-5'-*O*-dimethoxytrityl-β-D-*erythro*-pentofuranosyl-3'-*O*-cyanoethyl-*N,N'*-diisopropylphosphoramidite)-7*H*-pyrimido[4,5-*b*]indol-4-one (4). A solution of **3** (50 mg, 79.0 μmol), *N,N,N',N'* tetraisopropyl-2-cyanoethyl diphosphoramidite (28 μL, 86.9 mmol) and tetrazole (6 mg, 85.7 mmol) in acetonitrile (1 mL) was stirred at

ambient temperature for 2 h. The mixture was filtered and used with no further purification.

Oligonucleotide Synthesis and Characterization. Oligodeoxynucleotide sequences were synthesized by conventional phosphoramidite method by using an Applied Biosystems 392 DNA/RNA synthesizer. Oligonucleotides were purified by reverse phase HPLC on a 5-ODS-H column (10 × 150 mm, elution with a solvent mixture of 0.1 M triethylamine acetate (TEAA), pH 7.0, linear gradient over 30 min from 5 % to 35 % acetonitrile at a flow rate 3.0 mL/min). Oligonucleotides containing modified nucleobases were fully digested with calf intestine alkaline phosphatase (50 U/mL), snake venom phosphodiesterase (0.15 U/mL) and P1 nuclease (50 U/mL) at 37 °C for 3 h. Digested solutions were analyzed by HPLC on a cosmosil 5C-18AR or CHEMCOBOND 5-ODS-H column (4.6 × 150 mm), elution with a solvent mixture of 0.1 M triethylamine acetate (TEAA), pH 7.0, linear gradient over 20 min from 0 % to 10 % acetonitrile at a flow rate 1.0 mL/min). Concentration of each oligonucleotides were determined by comparing peak areas with standard solution containing dA, dC, dG and dT at a concentration of 0.1 mM.

UV and Fluorescence Measurements. All UV and fluorescence spectra of DNA duplex (25 μM) were taken in a buffer containing 50 mM sodium phosphate buffer (pH 7.0) and 100 mM NaCl at room temperature. Fluorescence spectra were obtained using a SHIMADZU RF-5300PC spectrofluorophotometer. Quantification of fluorescence intensity was obtained using with BIO-RAD VersaDoc 3000.

References

1. (a) Tyagi, S.; Bratu, D. P.; Kramer, F. R. *Nat. Biotechnol.* **1998**, *16*, 49-53. (b) Whitcombe, D.; Brownie, J.; Gillard, H. L.; McKechnie, D.; Theaker, J.; Newton, C. R.; Little, S. *Clin. Chem.* **1998**, *44*, 918-923. (c) Howell, W. M.; Jobs, M.; Gyllensten, U.; Brookes, A. J. *Nat. Biotechnol.* **1999**, *17*, 87-88. (d) Hacia, J. G. *Nat. Genet.* **1999**, *21*, 42-47. (e) Whitcombe, D.; Theaker, J.; Guy, S. P.; Brow, T.; Little, S. *Nat. Biotechnol.* **1999**, *17*, 804-807.
2. (a) Pastinen, T.; Raitio, M.; Lindroos, K.; Tainola, P.; Peltonen, L.; Syväen, A.-C. *Genome Res.* **2000**, *10*, 1031-1042. (b) Lizardi, P. M.; Huang, X.; Zhu, Z.; Bray-Ward, P.; Thomas, D. C.; Ward, D. C. *Nat. Genet.* **1998**, *19*, 225-232. (c) Lyamichev, V.; Mast, A. L.; Hall, J. G.; Prudent, J. R.; Kaiser, M. W.; Takova, T.; Kwiatkowski, R. W.; Sander, T. J.; de Arruda, M.; Arco, D. A.; Neri, B. P.; Brow, M. A. D. *Nat. Biotechnol.* **1999**, *17*, 292-296. (d) Fakhrai-Rad, H.; Pourmand, N.; Ronaghi, M. *Hum. Mutat.* **2002**, *19*, 479-485.
3. Okamoto, A.; Tainaka, K.; Saito, I. *J. Am. Chem. Soc.* **2003**, *125*, 4972-4973.
4. Showalter, H. D. H.; Bridges, A. J.; Zhou, H.; Sercel, A. D.; McMichael, A.; Fry, D. W. *J. Med. Chem.* **1999**, *42*, 5464-5474.
5. Okamoto, A.; Tanaka, K.; Saito, I. *J. Am. Chem. Soc.* **2003**, *125*, 5066-5071.
6. The fluorescence quantum yields were calculated according to: Morris, J. V.; Mahaney, M. A.; Huber, J. R. *J. Phys. Chem.* **1976**, *80*, 969-974.
7. (a) Haga, H.; Yamada, Y.; Ohnishi, Y.; Nakamura, Y.; Tanaka, T. *J. Hum. Genet.* **2002**, *47*, 605-610. (b) http://snp.ims.u-tokyo.ac.jp/cgi-bin/SnpInfo.cgi?SNP_ID=IMS-JST005851.

CHAPTER 7

Cytosine Detection by a Fluorescein-Labeled DNA Probe Containing Base-Discriminating Fluorescent Nucleoside

Abstract: A new technique for the clear detection of a C base on a complementary DNA strand, using fluorescent resonance energy transfer (FRET) between fluorescein and a novel fluorescent nucleoside, naphthodeazaadenine (NDA), has been described. The fluorescence spectrum of the duplex possessing a C base as a complementary base of NDA showed a fluorescence peak at 383 nm at 350 nm excitation. In contrast, when the complementary base of NDA was other bases than C, the fluorescence intensity was very low. If the fluorescence wavelength of BDF (base-discriminating fluorescent) nucleosides can be shifted to that of conventionally used fluorophores, then the BDF method will become a more powerful tool for the detection of single nucleotide alterations using a conventional fluorescence analyzer. By using FRET-BDF probes containing both NDA and fluorescein, the complementary base selective fluorescence of NDA was examined. The fluorescence emission from FRET-BDF probes was observed selectively when a complementary base was C. This system facilitates the detection of a single nucleotide alteration in a target sequence at the wavelength of fluorescein emission.

Introduction

Fluorescence-labeled nucleic acids are widely used for investigating the structure and dynamics of nucleic acids,[1] and for detecting nucleic acids containing target sequences.[2] At present, a large number of fluorophores, such as fluorescein, TAMRA, JOE, Alexa 594, BODIPY, and cyanine dyes, have been developed, and a variety of analyzers and imagers adjusted to the emission wavelength of these fluorophores are commercially available. However, the fluorescence of these known fluorophores is relatively insensitive to conjugated DNA sequences, with the exception that it is often decreased by a G base located in the neighborhood of an attached fluorophore.[3,4] Thus, such fluorophores are unsuitable for direct detection of a small change in DNA microenvironment.

We have recently reported a quite different type of fluorophore, base-discriminating fluorescent (BDF) nucleosides, which can distinguish bases on a complementary DNA strand by the fluorescence change.[5–8] For example, oligodeoxynucleotides (ODNs) containing a synthetic nucleoside benzopyridopyrimidine (BPP), one of the BDF nucleosides developed, selectively emit a strong fluorescence when the complementary base of BPP is A, and can be used as an effective BDF probe for the detection of a single nucleotide alteration where A base is concerned.[5] Such fluorescence behavior of BDF nucleosides has a remarkable advantage that is not observed for the commonly used fluorophores. However, the fluorescence wavelength of the BDF nucleosides is slightly shorter for the use of commercially available DNA fluorescence analyzers. If the fluorescence wavelength of BDF nucleosides can be shifted to that of conventionally used fluorophores, then the BDF method will become a more powerful tool for the detection of single nucleotide alterations using a conventional fluorescence analyzer.

Herein, we report on a new method for the detection of a base at a specific site in a DNA sequence by monitoring the fluorescence emission of fluorescein. To achieve this goal, we developed a new BDF nucleobase,

naphthodeazaadenine (NDA), which shows a fluorescence emission only when the complementary base of NDA is C. By using the fluorescence resonance energy transfer (FRET) from NDA to fluorescein a strong emission from fluorescein was observed selectively, *i.e.*, only when the base opposite NDA was C.

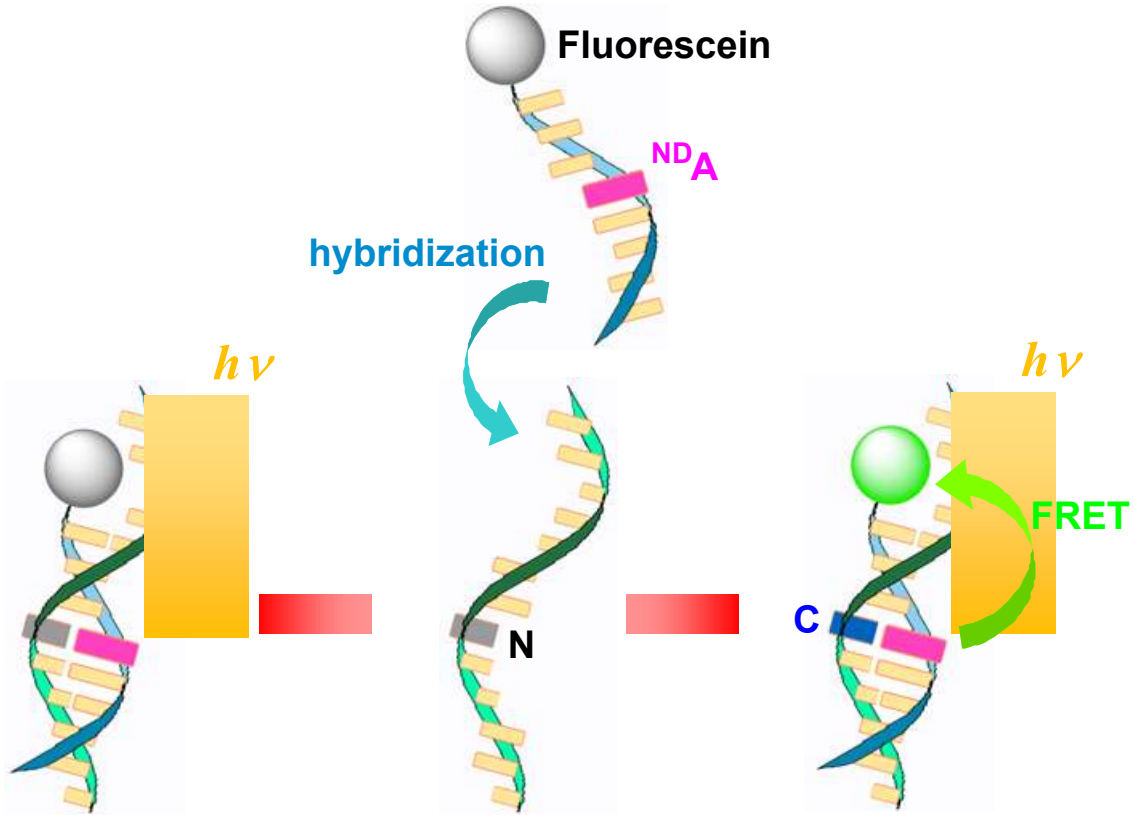

Results and Discussion

The novel BDF nucleoside NDA was synthesized from 1-chlorobenzo[*e*]pyrimidino[4,5-*b*]indole.[9] Subsequently, the nucleoside was protected and incorporated via phosphoramidites into the ODNs using a DNA synthesizer. The NDA-containing ODNs and the complementary ODNs used in this study are summarized in Table 1.

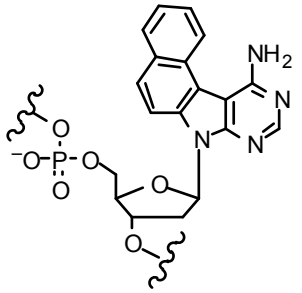

NDA

Table 1. ODNs used in this study.

	Sequences
ODN(NDA)	5'-d(CGCAATND**A**TAACGC)-3'
ODN(N)[a]	5'-d(GCGTTA**N**ATTGCG)-3'
ODN(F-3-NDA)[b]	5'-d(**F**AATND**A**TAACGCACACG)-3'
ODN(N-3)[a]	5'-d(CGTGTGCGTTA**N**ATT)-3'
ODN(F-3-A)[b]	5'-d(**F**AATATAACGCACACG)-3'
ODN(3-NDA)	5'-d(AATND**A**TAACGCACACG)-3'
ODN(F-4-NDA)[b]	5'-d(**F**AAATND**A**TAACGCACACG)-3'
ODN(N-4)[a]	5'-d(CGTGTGCGTTA**N**ATTT)-3'
ODN(F-5-NDA)[b]	5'-d(**F**AAAATND**A**TAACGCACACG)-3'
ODN(N-5)[a]	5'-d(CGTGTGCGTTA**N**ATTTT)-3'

[a]"N" denotes C, T, G and A. [b]"F" denotes 6-(fluorescein-6-carboxamido)hexanol.

Scheme 1[a]

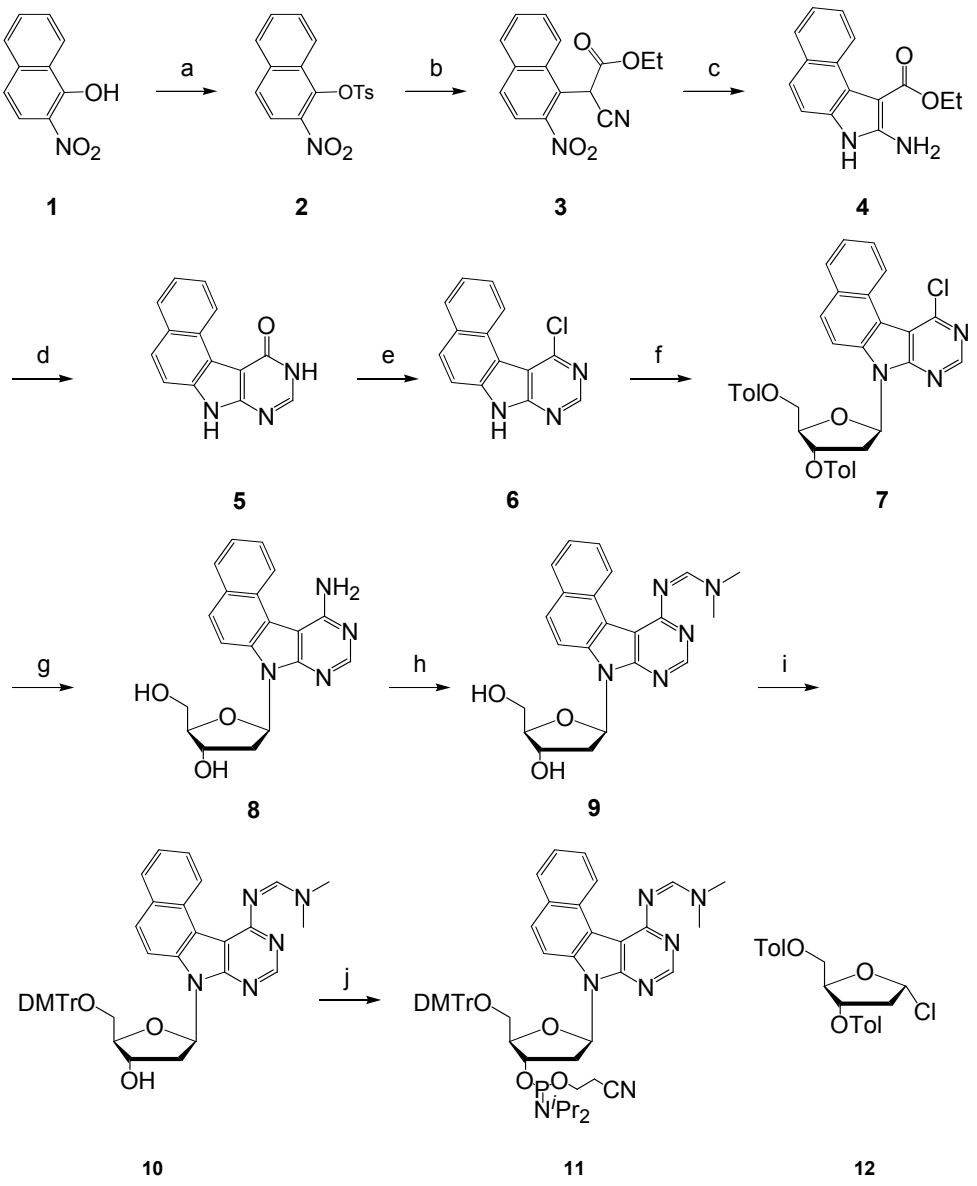

[a]Reagents and condition: (a) 2-nitro-1-phenol (**1**), pyridine, *p*-toluenesulfonyl chloride, r.t., 6 h, 55%; (b) ethyl cyanoacetate, THF, *tert*-butoxide, reflux, 7 h, 65%; (c) Zn powder, acetic acid, 44 °C, 7 h, 67%; (d) sodium methoxide, formamide, 220 °C, 6 h, 37%; (e) $POCl_3$, *p*-dioxane, reflux, 3 h, 67%; (f) **12**, sodium hydride, acetonitrile, 55 °C, 1 h, 86%; (g) methanolic ammonia, 150 °C, 8 h, 86%; (h) dimethylformamide demethylacetal, DMF, r.t., 3 h, 66%; (i) 4,4'-demethoxytrityl chloride, pyridine, 4-demethylaminopyridine, r.t., 4 h, 30%; (j) $(^{i}Pr_2N)_2PO(CN_2)_2CN$, tetrazole, acetonitrile, r.t., 1.5 h, *quant.*

The fluorescence spectrum of the duplex possessing a C base as a complementary base of NDA, **ODN(NDA)/ODN(C)**, showed a fluorescence peak at 383 nm using an excitation wavelength of 350 nm (Φ = 0.027). In contrast, when the complementary base of NDA was other bases than C, the fluorescence intensity was very low (Φ < 0.005). The fluorescence of **ODN(NDA)/ODN(C)** was approximately 9 times stronger than that observed for **ODN(NDA)/ODN(T)**. For single-stranded **ODN(NDA)**, an appreciably strong fluorescence was observed at 378 nm (Φ = 0.010), which was comparable to the peak intensity observed for **ODN(NDA)/ODN(C)**.

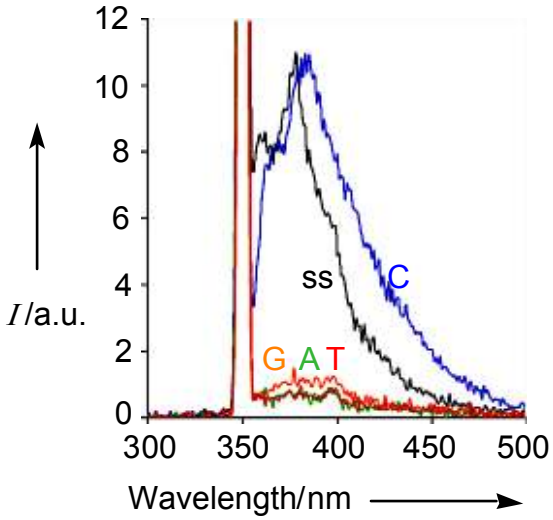

Figure 1. Fluorescence spectra of 2.5 μM **ODN(NDA)** hybridized with 2.5 μM **ODN(T)**, **ODN(C)**, **ODN(G)** or **ODN(A)** (50 mM sodium phosphate, 0.1 M sodium chloride, pH 7.0, room temperature). Excitation wavelength was 350 nm. "ss" denotes single-stranded **ODN(NDA)**.

The fluorescence emission spectrum of NDA (λ_{em}^{max} = 375 nm) overlapped with the fluorescence excitation spectrum of fluorescein (λ_{exc}^{max} = 494 nm) in the wavelength range of 400–500 nm (Figure 2). Thus, the interaction of these two fluorophores that are separated by defined base pairs may allow an efficient energy transfer to result in a dominant fluorescence emission of fluorescein at 520 nm using a 350 nm excitation wavelength. As shown in Table 1, we designed a series of FRET-BDF probes containing NDA as the FRET donor and fluorescein as the acceptor that were separated by three (**ODN(F-3-NDA)**), four (**ODN(F-4-NDA)**), and five (**ODN(F-5-NDA)**) A/T base pairs to systematically analyze the fluorescence properties.

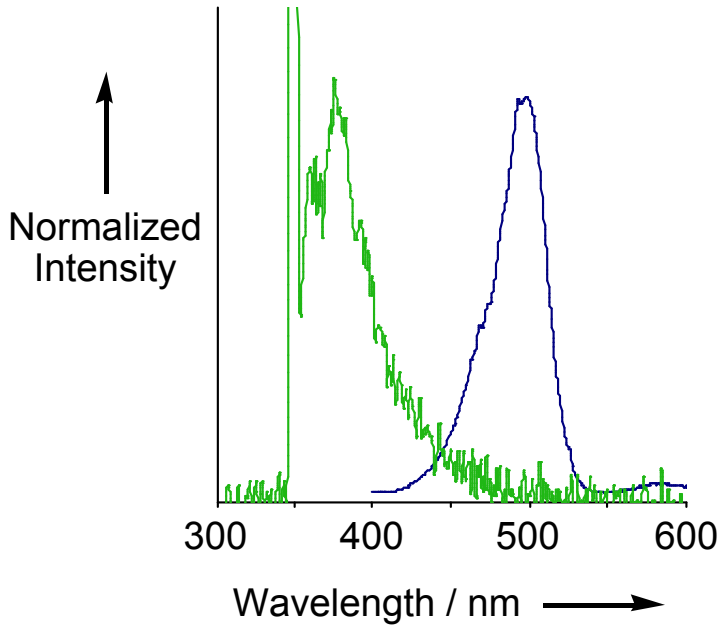

Figure 2. A fluorescence emission spectrum of **ODN(3-NDA)** (green) and a excitation spectrum of **ODN(F-3-A)** (blue).

Initially we investigated the fluorescence properties of the **ODN(F-3-NDA)** FRET-BDF probe. The fluorescence spectra of the **ODN(F-3-NDA)/ODN(N-3)** duplex, measured using various complementary bases of NDA (N), are shown in Figure 3a. The fluorescence emission from **ODN(F-3-NDA)/ODN(N-3)** was observed selectively when "N" was C. The quenching efficiency (Q_F) of NDA in **ODN(F-3-NDA)/ODN(C-3)** was 83% (Table 2). The fluorescence lifetime of **ODN(F-3-NDA)/ODN(C-3)** obtained after excitation at 337 nm was 0.59 ns, which was much shorter than that of **ODN(3-NDA)/ODN(C-3)**, Which does not possess a FRET acceptor fluorescein (1.10 ns). These observations suggest that effective FRET from NDA to fluorescein occurs in **ODN(F-3-NDA)/ODN(C-3)**. In contrast, the hybridization of **ODN(F-3-NDA)** with **ODN(N-3)** where "N" is T, G, or A results in a weaker emission, as shown in Figure 3a. These weak fluorescence peaks become negligible after subtraction of the fluorescence spectra of the NDA-free duplex **ODN(F-3-A)/ODN(N-3)** occurring as the background spectrum, suggesting that these weak fluorescence peaks arise from the NDA-independent excitation of fluorescein (Figure 3b). The fluorescence behavior showed that the fluorescence emission of **ODN(F-3-NDA)** via FRET occurs selectively when the complementary base of NDA is C. In addition, it is noteworthy that the fluorescence in the single-stranded state is effectively suppressed by the use of a FRET system, unlike the strong fluorescence in single-stranded **ODN(NDA)**. Therefore, the present FRET-BDF probe method using the interaction between NDA and fluorescein constitutes a powerful tool for typing single nucleotide alterations where C base is concerned.

To further analyze the character of the FRET interaction via NDA in detail, we examined the fluorescence properties of **ODN(F-4-NDA)/ODN(C-4)**, in which two fluorophores were separated by four A/T base pairs, and compared the fluorescence to that from **ODN(F-3-NDA)/ODN(C-3)**. The fluorescence quenching efficiency of NDA in **ODN(F-4-NDA)/ODN(C-4)** was 66%, which is much lower than that observed for

ODN(F-3-NDA)/ODN(C-3). The decrease in FRET efficiency also appeared in the

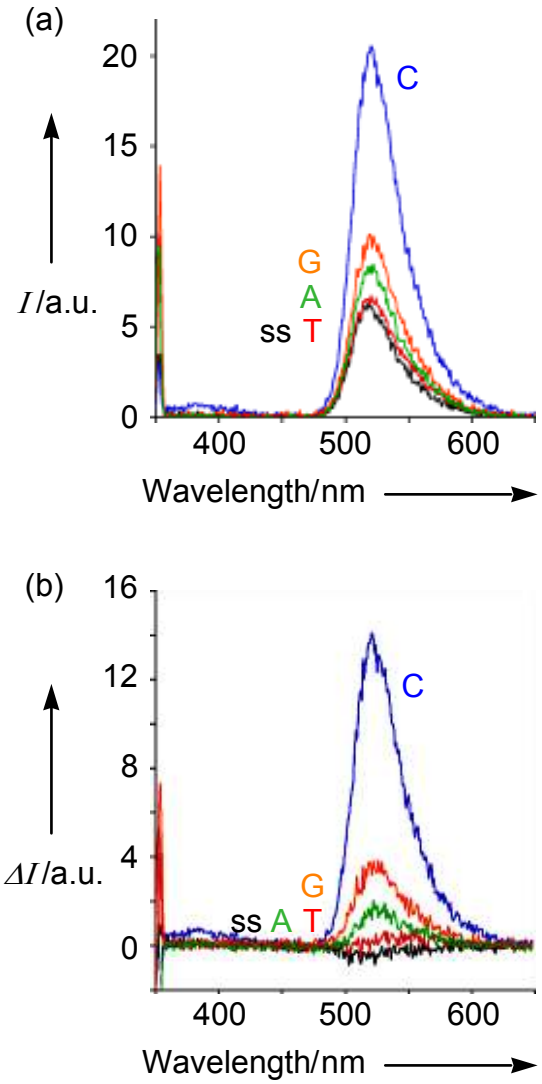

Figure 3. (a) Fluorescence spectra of 2.5 μM **ODN(F-3-NDA)** hybridized with 2.5 μM **ODN(T-3)**, **ODN(C-3)**, **ODN(G-3)** or **ODN(A-3)** (50 mM sodium phosphate, 0.1 M sodium chloride, pH 7.0, room temperature). Excitation wavelength was 350 nm. "ss" denotes single-stranded **ODN(F-3-NDA)**. (b) The spectra given by subtracting fluorescence spectra of 2.5 μM **ODN(F-3-A)** hybridized with 2.5 μM **ODN(T-3)**, **ODN(C-3)**, **ODN(G-3)** or **ODN(A-3)** from spectra (a).

fluorescence decay profile of **ODN(F-4-NDA)/ODN(C-4)**. The fluorescent decay profile of **ODN(F-4-NDA)/ODN(C-4)** was fitted to a biexponential function. The major short-lived component, corresponding to the FRET quenching of NDA, had an extended lifetime, and a longer lifetime component, corresponding to the quenching of NDA itself, newly appeared. This observation clearly shows the decrease in efficiency of the FRET from NDA to fluorescein. The lowering of this FRET efficiency gave the serious effect for the complementary base selectivity in the fluorescence emission of fluorescein. As can be clearly seen in Table 2, a remarkable decrease in C selectivity in the fluorescence emission was observed in **ODN(F-4-NDA)/ODN(C-4)**. In the duplex where the two fluorophores were more separated (**ODN(F-5-NDA)/ODN(C-5)**), the decrease in FRET efficiency was more marked. The Q_F of **ODN(F-5-NDA)/ODN(C-5)** decreased to 48%, and the C selectivity in the fluorescence emission was approximately half of that of **ODN(F-3-NDA)/ODN(C-3)**. The results of these fluorescence measurements for a series of fluorescence-labeled ODNs imply that the FRET efficiency between NDA as a FRET donor and fluorescein as an acceptor is strongly correlated with the complementary base selectivity in the fluorescence emission of fluorescein.

Conclusion

In conclusion, a clear distinction of C base on the complementary DNA strand using FRET-BDF probes has been achieved. By using FRET-BDF probes containing both NDA and fluorescein, the complementary base selective fluorescence of NDA was transferred to fluorescein. This system facilitates the detection of a single nucleotide alteration in a target sequence at the wavelength of fluorescein emission.

Table 2. Fluorescence data of FRET-BDF probes.

	τ_1/ns (%)	τ_2/ns (%)	τ_M/ns	Q_F[a]	C/T/ss ratio[b]
ODN(F-3-NDA)/ODN(C-3)	0.589		0.589	0.829	3.1/1.0/0.9
ODN(F-4-NDA)/ODN(C-4)	0.625 (98)	3.033 (2)	0.673	0.663	2.1/1.0/1.1
ODN(F-5-NDA)/ODN(C-5)	0.630 (97)	2.209 (3)	0.677	0.482	1.8/1.0/1.2
ODN(3-NDA)/ODN(C-3)		1.103	1.103	---	9.5/1.0/8.6[c]

[a]Q_F is the quenching efficiency for NDA. [b]The C/T/ss ratio shows the ratio of the fluorescence intensities of fluorescein (521 nm) from NDA/C duplexes, NDA/T duplexes, and single-stranded ODNs. [c]The ratio of the fluorescence intensities of NDA (376 nm) from NDA/C duplexes, NDA/T duplexes, and single-stranded ODNs.

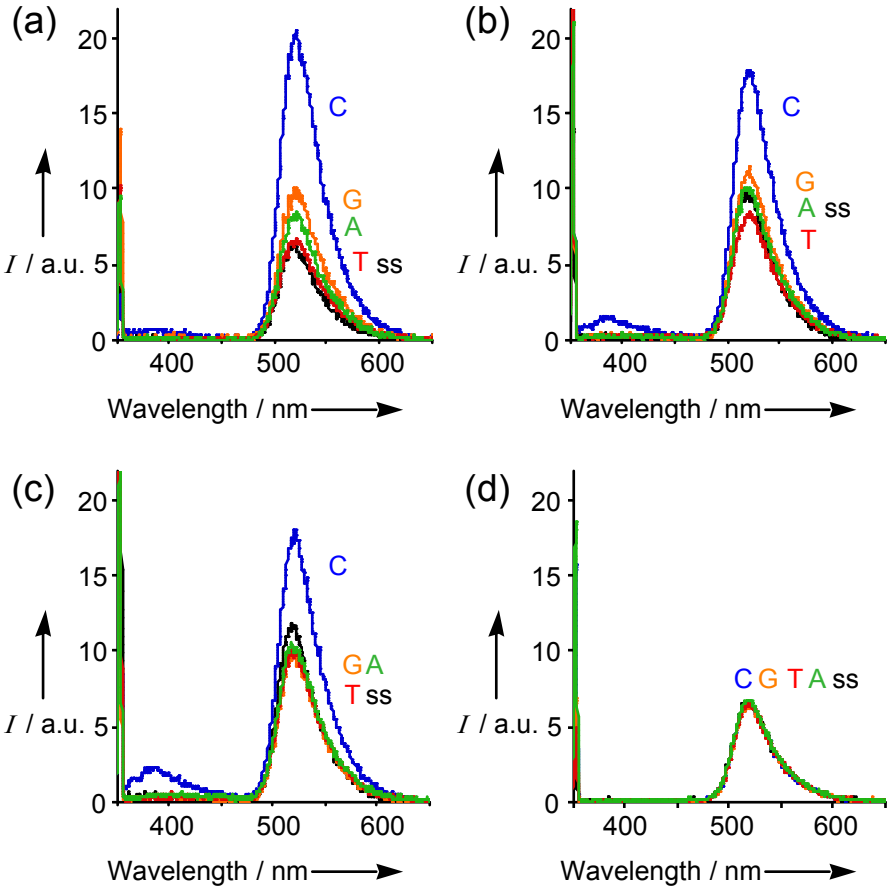

Figure 4. Fluorescence spectra of FRET-BDF probes. (a) **ODN(F-3-NDA)/ODN(N-3)**, (b) **ODN(F-4-NDA)/ODN(N-4)**, (c) **ODN(F-5-NDA)/ODN(N-5)**, (d) **ODN(F-3-A)/ODN(N-3)** as back ground spectra.

Experimental Section

General. ^{1}H NMR spectra were measured with Varian Mercury 400 (400 MHz) spectrometer. Coupling constant (*J* value) are reported in hertz. The chemical shifts are expressed in ppm downfield from tetramethylsilane, using residual chloroform (δ= 7.24 in ^{1}H NMR, δ= 77.0 in ^{13}C NMR) and dimethylsulfoxide (δ= 2.48 in ^{1}H NMR, δ= 39.5 in ^{13}C NMR) as an internal standard. FAB Mass spectra were recorded on JEOL JMS DX-300 spectrometer or JEOL JMS SX-102A spectrometer.

2-Nitronaphthyl *p*-toluenesulfonate (2). 2-Nitro-1-naphthol (**1**) (95%, 10.0 g, 50.1 mmol) was dissolved in pyridine (150 mL) and *p*-toluenesulfonyl chloride (12.0 g, 62.9 mmol) was added at 0 °C. The mixture was stirred at ambient temperature for 6 h. The resulting mixture was concentrated *in vacuo*. The crude product was purified by silica gel chromatography using chloroform to give **2** (9.4 g, 27.4 mmol, 55%) as an orange solid: ^{1}H NMR ($CDCl_3$) δ 8.18 (d, 1H, *J* = 8.8 Hz), 7.84–7.94 (m, 5H), 7.67 (ddd, 1H, *J* = 8.8, 7.2, 1.2 Hz), 7.59 (ddd, 1H, *J* = 8.8, 7.2, 1.2 Hz), 7.37 (d, 2H, *J* = 8.8 Hz), 2.49 (s, 3H) ; MS (FAB) (NBA/$CDCl_3$) *m*/*z* (%) 343 [M^+]; HRMS (FAB) calcd for $C_{17}H_{13}O_5NS$ [M^+] 343.0514, found 343.0514.

Cyano(2-nitronaphthalene-1-yl)acetic acid ethyl ester (3). To an ice-cold solution of ethyl cyanoacetate (4.62 mL, 42.6 mmol) in anhydrous THF (170 mL) was added potassium *tert*-butoxide (4.78 g, 42.6 mmol). The formed suspension was stirred for 15 min then treated with **2** (7.3 g, 21.3 mmol). The suspension was heated at reflux for 7 h. The solution was poured into water, and the aqueous mixture was acidified to pH 2 with concentrated HCl. The mixture was extracted with ether three times and then the combined organic phases were dried and concentrated *in vacuo*. The crude product was purified by silica gel chromatography (chloroform : methanol = 10 : 1) to give **3** (3.7 g, 13.8 mmol, 65%) as a yellow solid: ^{1}H

NMR (DMSO-d_6) δ8.43 (d, 1H, J = 8.4 Hz), 8.34 (d, 1H, J = 9.2 Hz), 8.23 (m, 1H), 8.14 (d, 1H, J = 9.2 Hz), 7.87 (m, 2H), 6.87 (s, 1H), 4.22 (dq, 2H, J = 7.2, 1.2 Hz), 1.18 (t, 3H, J = 7.2 Hz)

2-Amino-3*H*-benzo[*e*]indole-1-carboxylic acid ethyl ester (4). A solution of **3** (3.7 g, 13.8 mmol) in acetic acid (150 mL) was treated with a single charge of Zn dust (3.9 g, 60 mmol). The mixture was heated at 44 °C and sonicated 3.3 h, then treated with more Zn (2.4 g, 36.7 mmol). After heating and sonicating another 3.3 h the mixture was filtered. The filtrate was concentrated *in vacuo*. The crude product was purified by silica gel chromatography (chloroform : methanol = 20 : 1) to give **4** (2.34 g, 9.2 mmol, 67%) as a black solid: MS (FAB) (NBA) *m*/*z* (%) 254 [M^+]; HRMS (FAB) calcd for $C_{15}H_{14}O_2N_2$ [M^+] 254.1055, found 254.1056.

3,11-Dihydro-benzo[*e*]pyrimido[4,5-*b*]indol-4-one (5). A solution of **4** (1.1 g, 4,33 mmol), sodium methoxide (1.0 g, 18.5 mmol), and formamide (40 mL) was heated at 220 °C for 6 h and distilled at 220 °C to a solid. The solid was triturated in methanol and then filtered. The filtrate was concentrated to a solid. The crude product was purified by silica gel chromatography (chloroform : methanol = 10 : 1) to give **5** (379 mg, 1.61 mmol, 37%) as a yellow solid: ^{1}H NMR (DMSO-d_6) δ12.63 (s.,1H), 12.29 (s, 1H), 9.93 (d, 1H, J = 8.0Hz), 8.13 (s, 1H), 7.96 (d, 1H, J = 8.0 Hz) 7.83 (d, 1H, J = 8.8 Hz), 7.65 (d, 1H, J = 8.8 Hz) 7.57 (t, 1H, J = 8.8 Hz) 7.44 (t, 1H, J = 8.8 Hz); MS (FAB) (NBA) *m*/*z* (%) 235 [M^+]; HRMS (FAB) calcd for $C_{14}H_9ON_3$ [M^+] 235.0746, found 235.0746.

4-Chloro-11*H*-benzo[*e*]pyrimido[4,5-*b*]indole (6). A mixture of **5** (200 mg, 0.85 mmol), $POCl_3$ (20 mL), and *p*-dioxane (20 mL) was heated at reflux for 3 h. The mixture was concentrated to solid then washed with water. The crude product was purified by silica gel chromatography (chloroform : methanol = 40 : 1) to give **6** (145 mg, 0.57 mmol, 67%) as a yellow solid: ^{1}H NMR (DMSO-d_6) δ13.31 (s, 1H), 9.55 (d, 1H, J = 8.4 Hz),

8.78 (s, 1H), 8.15 (d, 1H, J = 8.8 Hz), 8.11 (d, 1H, 8.4 Hz), 7.79 (d, 1H, J = 8.8 Hz), 7.23 (t, 1H, J = 8.4 Hz); MS (FAB) (NBA/DMSO) m/z (%) 254 [$(M+H)^+$]; HRMS (FAB) calcd for $C_{14}H_8ClN_3$ [$(M+H)^+$] 254.0485, found 254.0487.

4-Chloro-11-(2'-deoxy-3',5'-di-*O*-*p*-toluoyl-β-$_D$-*erythro*-pentofuranosyl)-11*H*-benzo[*e*]pyrimido[4,5-*b*]indole (7). Compound **6** (112 mg, 0.44 mmol) was suspended in dry acetonitrile (10 mL) at room temperature. To this suspension was added sodium hydride (60% in oil; 19.2 mg, 0.48 mmol) and the mixture was stirred at 55 °C for 1 h. Then sodium hydride (12 mg, 0.3 mmol) was added and stirred for 30 min and sodium hydride (25 mg, 0.6 mmol). The compound **12** (184 mg, 0.47 mmol) was added and the mixture was stirred for 15 min, then evaporated to dryness, and the residue on purification by silica gel chromatography (chloroform : methanol = 10 : 1) to give **7** (234 mg, 0.38 mmol, 86%) as a yellow solid: ^{1}H NMR ($CDCl_3$) δ9.62 (d, 1H, J = 9.2 Hz), 8.76 (s, 1H), 7.99–8.03 (m, 6H), 7.89 (d, 1H, J = 8.0 Hz), 7.70 (t, 1H, J = 8.0 Hz) 7.64 (d, 1H, J = 8.8 Hz), 7.54 (t, 1H, J = 7.2 Hz), 7.31 (d, 2H, J = 8.0 Hz), 7.24–7.27 (m, 2H), 6.00 (m, 1H), 4.93 (dd, 1H, J = 12.0, 3.2 Hz), 4.77 (dd, 1H, J = 12.0, 4.0 Hz), 4.64 (dd, 1H, J = 7.2, 4.0 Hz), 3.56 (m, 1H), 2.65 (ddd, 1H, J = 8.0, 6.4, 2.8 Hz) 2.46 (s, 6H); MS (FAB) (NBA/$CHCl_3$) m/z (%) 606 [$(M+H)^+$]; HRMS (FAB) calcd for $C_{35}H_{28}ClN_3O_8$ [$(M+H)^+$] 606.1796, found 606.1795.

4-Amino-11-(2'-deoxy-β-$_D$-*erythro*-pentofuranosyl)-11*H*-benzo[*e*]pyrimido[4,5-*b*]indole (8, NDA). A suspension of **7** (101 mg, 0.167 mmol) in 40 mL methanolic ammonia (saturated at –76 °C) was stirred at 150 °C in a sealed bottle for 7 h. The mixture was evaporated to dryness, and the residue was purified by silica gel chromatography (chloroform : methanol = 10 : 1) to give **8** (55.6 mg, 0.158 mmol, 95%) as a white solid: ^{1}H NMR (DMSO-d_6) δ8.77 (d, 1H, J = 8.8Hz), 8.33 (s, 1H), 8.16 (d, 1H, J = 8.8 Hz), 8.05 (d, 1H, J = 8.8 Hz), 7.93 (d, 1H, J = 8.8 Hz), 7.65 (t, 1H, J = 8.8 Hz),

7.45 (t, 1H, J = 8.8 Hz), 7.07 (s, 2H), 6.99 (t, 1H), 5.35 (d, 1H, J = 4.0 Hz), 5.23 (t, 1H, J = 5.2 Hz), 4.52 (m, 1H), 3.91 (d, 1H, J = 3.2 Hz), 3.74 (m, 1H), 3.70 (m, 1H), 2.90 (m, 1H), 2.11 (ddd, 2H, J = 8.8, 6.4, 2.0 Hz) ; MS (FAB) (NBA) *m*/*z* (%) 351 [$(M+H)^+$]; HRMS (FAB) calcd for $C_{19}H_{19}O_3N_4$ [$(M+H)^+$] 351.1457, found 351.1449.

4-(*N,N′*-Dimethylaminomethylidenyl)amino-11-(2'-deoxy-β-D-*erythro*-pentofuranosyl)-11*H*-benzo[*e*]pyrimido[4,5-*b*]indole (9). A solution of **8** (55.6 mg, 0.158 mmol) in dimethylformamide (5 mL) containing *N,N*-dimethylformamide dimethylacetal (5 mL, 28 mmol) was stirred for 3 h at room temperature. The solvent was concentrated *in vacuo*. The silica gel chromatography (chloroform : methanol = 10 : 1) yielded **9** (42.5 mg, 0.105 mmol, 66%) as a yellow solid: ^{1}H NMR (DMSO-d_6) δ10.90 (d, 1H, J = 8.4 Hz) 9.03 (s, 1H), 8.53 (s, 1H), 8.18 (d, 1H, J = 8.4 Hz), 7.99 (d, 1H, J = 8.0 Hz), 7.93 (d, 1H, J = 8.0 Hz), 7.58 (t, 1H, J = 8.0 Hz), 7.46 (t, 1H, J = 8.0 Hz), 7.05 (t, 1H, J = 7.2Hz), 5.37 (d, 1H, J = 5.2 Hz), 5.25 (t, 1H, J = 5.6 Hz), 4.53 (m, 1H), 3.91 (m, 1H, J = 3.6), 3.72 (m, 2H), 2.92 (m, 1H), 2.11 (m, 1H) ; MS (FAB) (NBA/$CDCl_3$) *m*/*z* (%) 406 [$(M+H)^+$]; HRMS (FAB) calcd for $C_{22}H_{24}O_3N_5$ [$(M+H)^+$] 406.1879, found 406.1882.

4-(*N,N′*-Dimethylaminomethylidenyl)amino-11-(2'-deoxy-5'-*O*-dimethoxytrityl-β-D-*erythro*-pentofuranosyl)-11*H*-benzo[*e*]pyrimido[4,5-*b*]indole (10). A solution of **9** (42.5 mg, 0.104 mmol), 4,4'-dimethoxytrityl chloride (46.0 mg, 0.135 mmol) and 4-dimethylaminopyridine (3.1 mg, 0.026 mmol) was stirred in 15 mL anhydrous pyridine for 4 h at ambient temperature. The solvent was concentrated *in vacuo* to the brown oil. The crude product was purified by silica gel chromatography (chloroform : methanol = 10 : 1) to give **10** (22 mg, 0.031 mmol, 30%) as a white solid: ^{1}H NMR ($CDCl_3$) δ8.82 (d, 1H, J = 8.4 Hz), 8.87 (s, 1H), 8.57 (s, 1H), 8.07 (d, 1H, J = 8.8 Hz), 7.83 (d, 1H, J = 7.2 Hz), 7.55–7.15 (m,12H), 6.77 (d, 4H, J = 8.4 Hz), 4.95–4.91 (m, 1H), 4.10 (ddd, 1H, J = 4.0 Hz), 3.54 (dq, 2H, J = 25.6, 4.0 Hz), 3.73 (s, 6H), 3.44 (s, 6H), 3.26 (s,1H), 2.36 (s, 1H).

4-(*N*,*N'*-Dimethylaminomethylidenyl)amino-11-(2'-deoxy-5'-*O*-dimethoxytrityl-β-D-*erythro*-pentofuranosyl-3'-*O*-cyanoethyl-*N*,*N*'-diisopropylphosphoramidite)-11*H*-benzo[*e*]pyrimido[4,5-*b*]indole (11). A solution of **10** (22 mg, 0.031 mmol), 2-cyanoethyl tetraisopropylphosphorodiamidite (10.75 mL, 0.034 mmol) and tetrazole (2.38 mg, 0.034 mmol) in 0.40 mL acetonitrile was stirred at ambient temperature for 1.5h. The mixture was filtered and used for ODN synthesis with no further purification.

Modified ODN Synthesis. The modified ODNs were synthesized by a conventional phosphoramidite method using an Applied Biosystems 392 DNA/RNA synthesizer. The NDA phosphoramidite was prepared according to a protocol described in Supporting Information.[9] Synthesized ODNs were purified by reversed phase HPLC on a 5-ODS-H column (10 × 150 mm, elution with a solvent mixture of 0.1 M triethylammonium acetate (TEAA), pH 7.0, linear gradient over 30 min from 5% to 20% acetonitrile at a flow rate 3.0 mL/min). Mass spectra of ODNs purified by HPLC were determined with a MALDI-TOF mass spectroscopy (acceleration voltage 21 kV, negative mode) with 2',3',4'-trihydroxyacetophenone (THAP) as matrix, using T_8 ($[M–H]^-$ 2370.61) and T_{17} ($[M–H]^-$ 5108.37) as an internal standard.

ODN(NDA): MALDI-TOF [$(M–H)^-$] calcd 4025.72, found 4026.37.
ODN(F-3-NDA): MALDI-TOF [$(M–H)^-$] calcd 5189.59, found 5190.14.
ODN(3-NDA): MALDI-TOF [$(M–H)^-$] calcd 4652.14, found 4651.62.
ODN(F-4-NDA): MALDI-TOF [$(M–H)^-$] calcd 5502.80, found 5503.86.
ODN(F-5-NDA): MALDI-TOF [$(M–H)^-$] calcd 5816.01, found 5817.27.

Fluorescence Measurements. All the fluorescence spectra of the DNA duplexes were taken in a buffer solution containing 50 mM sodium phosphate buffer (pH 7.0) and 100 mM sodium chloride at room temperature. The fluorescence spectra were obtained using a SHIMADZU RF-5300PC spectrofluorophotometer.

Fluorescence Decay Measurements. Fluorescence decay was measured by a two-dimensional photon counting method using the picosecond fluorescence lifetime measurement system (C4780, Hamamatsu). An N_2 laser (337 nm) was used as the excitation light source. The fluorescence emission was collected at 380 nm.

References

1. Millar, D. P. *Curr. Opin. Struct. Biol.* **1996**, *6*, 322–326.
2. Glazer, A. N.; Mathies, R. A. *Curr. Opin. Biotech.* **1997**, *8*, 94–102.
3. Nazarenko, I.; Pires, R.; Lowe, B.; Obaidy, M.; Rashtchian, A. *Nucleic Acids Res.* **2002**, *30*, 2089–2095.
4. Marras, S. A. E.; Kramer, F. R.; Tyagi, S. *Nucleic Acids Res.* **2002**, *30*, e122.
5. Okamoto, A.; Tainaka, K.; Saito, I. *J. Am. Chem. Soc.* **2003**, *125*, 4972–4973.
6. Okamoto, A.; Tainaka, K.; Saito, I. *Chem. Lett.* **2003**, *32*, 684–685.
7. Okamoto, A.; Tanaka, K.; Fukuta, T.; Saito, I. *J. Am. Chem. Soc.* **2003**, *125*, 9296–9297.
8. Okamoto, A.; Tainaka, K.; Saito, I. *Tetrahedron Lett.* **2003**, *44*, 6871–6874.
9. Okamoto, A.; Tanaka, K.; Saito, I. *J. Am. Chem. Soc.* **2003**, *125*, 5066–5072.

CHAPTER 8

A New SNPs Typing Method Using Base-Discriminating Fluorescent Nucleosides

Abstract: For the development of a novel method SNP typing method using BDF, (base discriminating fluorescent), in a real biological sample, we examined the detection of single base alteration in BRCA1 gene with PCR products. The result of the BDF detection system was in a good agreement with sequencing data. A combination of these ^{MD}A- and ^{MD}I-containing BDF probes clearly facilitates the discrimination of the heterozygous sample. The sensitivity of BDF probes was examined by changing the concentration or the volume of BDF nucleoside-containing oligodeoxynucleotides (ODNs). The detection limits of ^{MD}A and ^{MD}I probe were 500 fmol and 1.25 pmol, respectively. The present SNP typing method using ^{MD}A- and ^{MD}I-containing BDF probes is a very powerful homogeneous assay that does not require a special device or time-consuming steps.

Introduction

The Human Genome Project is expected to yield thousands of single nucleotide polymorphisms (SNPs), which can be used to identify polygenic contributors to disease and ultimately to design individualized prognostic strategies and therapies. Exploiting these, however, will be required the automated scanning methods. Current techniques have their roots in allele-specific oligonucleotide hybridization (ASOH).[1] In its basic form (*i.e.,* hybridization, stringent washing, and signal detection), ASOH is limited by the difficult challenge of defining discriminatory assay conditions. Therefore, newer methods including additional steps furnishing more robust allele scanning are required. Such procedures include the ligation chain reaction (ASOH plus selective ligation and amplification),[2] mini-sequencing (ASOH plus a single base extension),[3] the DNA-attached electrode (ASOH was executed on the electrode),[4] and DNA "chips" (miniaturized ASOH with multiple oligonucleotide probe arrays).[5] Alternatively, ASOH with single- or dual-labeled probes has been merged with PCR, as in the 5' exonuclease assay,[6] and with molecular beacons.[7] While effective, these methods also entail considerable optimization efforts and/or costly enzymatic or oligonucleotide labeling steps.

We already reported on the clear distinction of pyrimidine bases on the complementary strand using the fluorescence from modified nucleosides, methoxy benzodeazainosine (^{MD}I) and methoxy benzodeazaadenine (^{MD}A).[8] Herein, we show a novel method for the discrimination of genotype with ^{MD}I- and ^{MD}A-containing ODN probe. Result of BDF analysis obtained form fluorescence emission of the mixtures containing probe ODN and PCR products of the human breast cancer 1 gene (BRCA1)[9] showed a good correlation with that of sequence analysis. This method does not require any time-consuming steps and expensive reagents.

Results and Discussion

The synthesis and the incorporation of ^{MD}A or ^{MD}I into ODNs were previously reported.[8,10] The principle of BDF-based detection system is that BDF nucleosides, methoxybenzodeazaadenine ^{MD}A and methoxybenzodeazainosine ^{MD}I, can emit strong fluorescence only when the base on the complementary strand is C and T, respectively.[10] Thus, the ^{MD}A- and ^{MD}I-containing ODNs can be used as a very effective BDF probe for the detection of single base alterations, such as SNPs and point mutations.

In order to verify the detection of SNP in a real biological sample, we examined the detection of a SNP sequence at a nucleotide position of 2311 in BRCA1 gene. Detection method for the determination of SNP type was illustrated in Scheme 1. First, PCR amplification was carried out between nucleotide positions of 1821 and 2829 with a biotinylated primer. (Table 1) After PCR amplification, PCR products were purified with magnetic beads on which surface streptavidin was covalently bound, and the single stranded DNAs containing C/T-allele were obtained.

According to the established method for the homogeneous assay with BDF probes, PCR products were mixed with ^{MD}A- or ^{MD}I-containing ODN, and fluorescence emission of BDF bases were measured by a fluorescence imager Versa Doc Imaging System (BioRad) equipped with a 365 nm transilluminator. (Figure 1a) Quantification of fluorescence emission of ^{MD}A- or ^{MD}I-containing sample was shown in Figure 1b, and the values that were calculated by the fluorescence intensity of ^{MD}A-containing sample minus ^{MD}I-containing sample were plotted in Figure 2. It was suggested that when the ^{MD}A-containing sample had much stronger fluorescence than the ^{MD}I-containing sample, the sample was C-allele. When the sample which showed small difference of fluorescence intensity between ^{MD}A-containing sample and ^{MD}I-containing sample, the sample was heterozygote.

Table 1. The primer sequences used in this study

	Sequence
S1 primer	5'-AAAGAATAGGCTGAGGAGGAAGTC-3'
A1 primer[a]	5'-Bio-TTTGGCATTATCAACTGGCTTA-3'

[a]Bio: 3-*O*-(*N*-biotinyl-3-aminopropyl)-triethyleneglycolyl-glyceryl-

Scheme 1. Preparation of the sample containing the BDF probe.

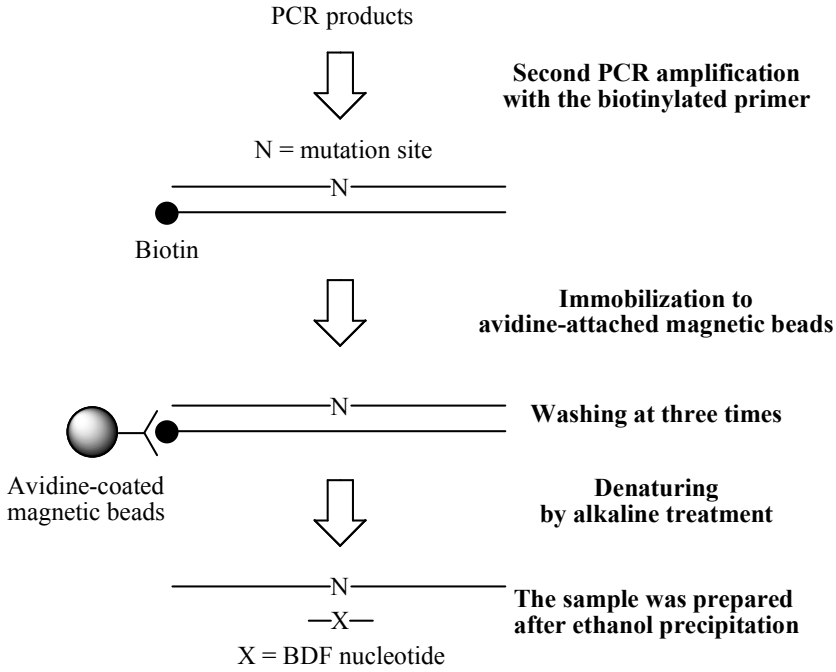

Scheme 2. Model of the instrument for fluorescence measurements.

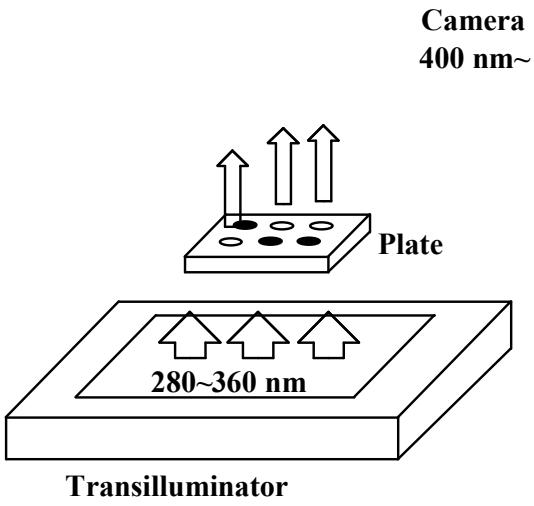

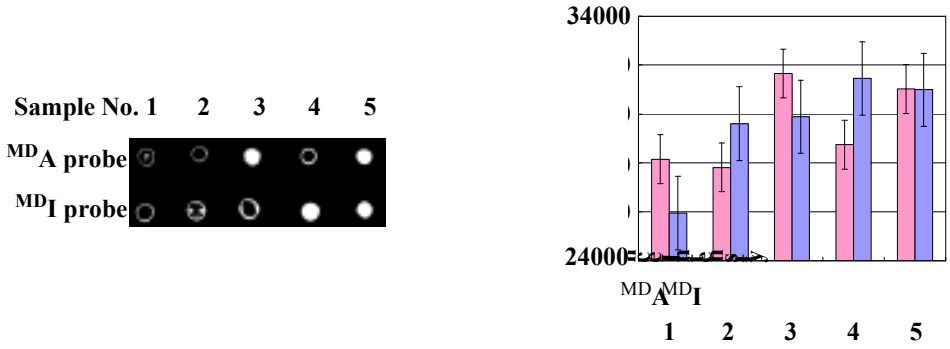

Figure 1. Determination of genotype in BRCA1 gene using the fluorescence change of BDF probes. (a) Fluorescence emission was detected with VarsaDoc 3000, and (b) quantitated. The left bar means the fluorescent intensity of ^{MD}A probe-containing sample and the right bar means that of ^{MD}I probe-containing sample. All measurements were examined in 5 μL of a solution containing 10 μM probe ODN, 50 mM sodium phosphate buffer (pH 7.0), and 100 mM sodium chloride at ambient temperature at 365 nm excitation with transilluminator.

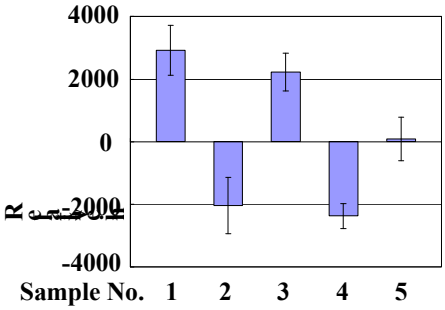

Figure 2. Difference of fluorescence intensity between ^{MD}A-containing samples and ^{MD}I-containing samples. Relative intensity was calculated by subtracting the fluorescence intensity of ^{MD}I probe from the fluorescence intensity of ^{MD}A probe. The bar height stands for allele type; the bar height is over and below zero means that this sample was classified in C and T allele, respectively. No difference of the intensity between ^{MD}A- and ^{MD}I-containing samples indicates that the sample was heterozygote.

For verifying the accuracy of the detection system based on BDF probes, SNP sequence of PCR products was confirmed with sequencing analysis. Single-base mutation site was indicated by arrow. As clearly seen in Figures 2 and 3, the result of BDF detection was in a good agreement with the sequencing analysis.

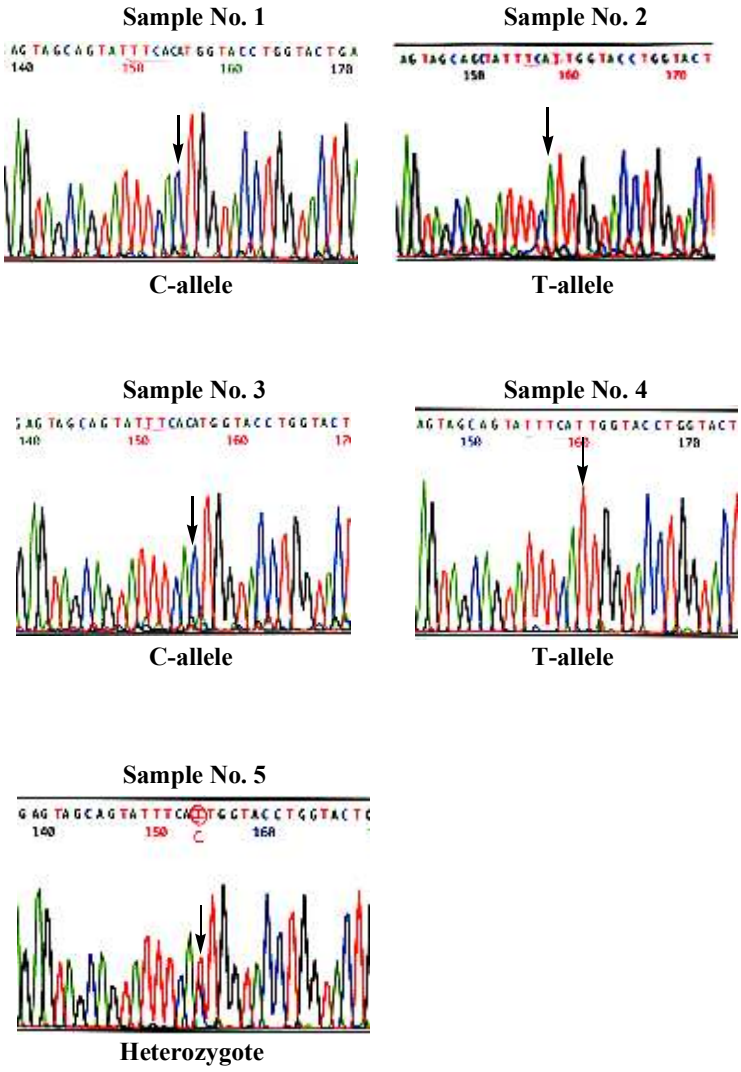

Figure 3. Sequencing analysis of PCR products at a nucleotide position of 2311 in BRCA1 gene. Single-base alteration site was indicated with an arrow, and discriminated genotype was shown at the below of each panel. These sequencing data were obtained in Ohtsuka Pharmaceutical co. ltd.

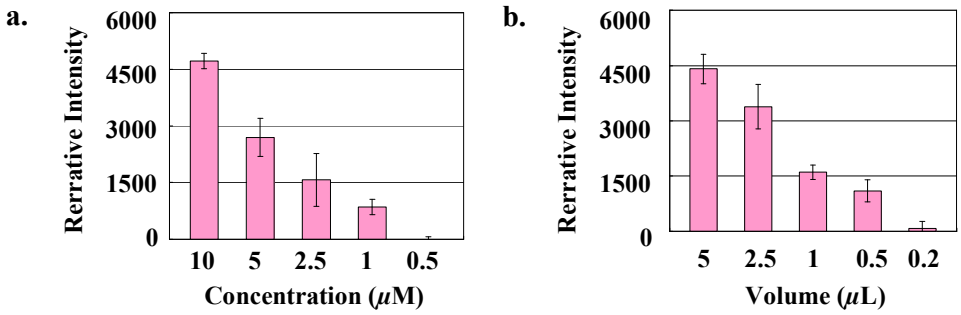

Figure 4. Detection limits of ^{MD}A prove. All measurements were accomplished in a solution containing 50 mM sodium phosphate buffer (pH 7.0) and 100 mM sodium chloride at room temperature. ^{MD}A-containing ODNs were illuminated at 365 nm with transilluminator. (a)Fluorescence intensity of the samples was measured in 5 μL of total volume. (b) Concentration of the duplex containing probe ODN was 25 μM. Relative intensity was calculated by subtracting the fluorescence intensity of ^{MD}A opposite to T from the fluorescence intensity of ^{MD}A opposite to C.

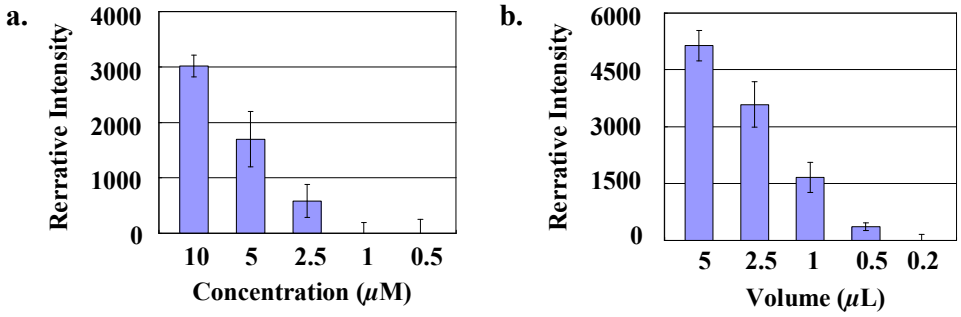

Figure 5. Detection limits of ^{MD}I prove. All measurements were accomplished in a solution containing 50 mM sodium phosphate buffer (pH 7.0) and 100 mM sodium chloride at room temperature. ^{MD}I-containing ODNs were illuminated at 365 nm with transilluminator. (a)Fluorescence intensity of the samples was measured in 5 μL of total volume. (b) Concentration of the duplex containing probe ODN was 25 μM. Relative intensity was calculated by subtracting the fluorescence intensity of ^{MD}I opposite to C from the fluorescence intensity of ^{MD}I opposite to T.

Next, detection limits of ^{MD}A and ^{MD}I probes were investigated by changing the concentration of BDF probe ODNs (Figure 4a, 5a) or the volume on the plate for fluorescence measurement (Figure 4b, 5b). In the case of ^{MD}A probe, minimum concentration was 1 μM, and minimum volume was 0.5 μL, respectively. Therefore, at 500 fmol per strand, ^{MD}A probe allowed the determination of the genotype for BRCA1 gene. ^{MD}I probe can detect the SNP at 2.5 μM minimum concentration and 0.5 μL minimum volume, and it was shown that the detection limit of ^{MD}I probe was 1.25 pmol. In recent studies, SNPs detection in fmol scale was achieved.[11,12] Comparing with these reported assays, our detection system based on BDF probes seemed to be low sensitivity. However, the sensitivity can be improved by using laser for excitation or fluorescence microscopy, which were commonly used in many laboratories. It is noted that BDF assay does not need a special instruments, time-consuming steps, and expensive reagents.

Conclusion

To apply BDF-based detection system to discriminate genotype in real biological samples, we have examined the detection of genotype in BRCA1 gene with PCR products. The result of BDF detection showed a good agreement with sequencing data. A combination of these ^{MD}A- and ^{MD}I-containing BDF probes clearly facilitates the T/C SNP typing of a heterozygous sample. Next, the sensitivity of each BDF probes was evaluated by changing the concentration of BDF probe ODNs or the volume on the plate for fluorescence measurement. The detection limits of ^{MD}A and ^{MD}I probe were 500 fmol and 1.25 pmol, respectively. The present SNP typing method using ^{MD}A- and ^{MD}I-containing BDF probes is a very powerful homogeneous assay that does not require a special device or time-consuming steps.

Experimental Section.

General. The reagents for the DNA synthesizer such as A, G, C, T-β-cyanoethyl phosphoramidite, biotin-TEG phosphoramidite and CPG support were purchased from Applied Biosystem, or GLEN RESEARCH. Masses of oligonucleotides were determined with a MALDI-TOF MS (acceleration voltage 21 kV, negative mode) with 2', 3', 4'-trihydroxyacetophenone as matrix, using T8 mer ($[M - H]^-$ 2370.61) and T17 mer ($[M - H]^-$ 5108.37) as an internal standard. HPLC was performed on a cosmosil 5C-18AR or CHEMCOBOND 5-ODS-H column (4.6 × 150 mm) with a Gilson Chromatography Model 305 using a UV detector Model 118 at 254 nm. MicroAmp Optical, GeneAmp 5700 Sequence Deection System was used in PCR amplification. *Taq* DNA polymerase (*TaKaRa ExTaq*), dNTP blend, and magnetic beads (MAGNOTEX-SA) were purchased from *TaKaRa* (Japan). ODNs were purchased from QIAGEN. Fluorescence measurements were using with BIO-RAD VersaDoc 3000. PCR products extracted from human blood were obtained from Ohtsuka Pharmaceutical co. ltd. Sequencing of PCR products were also accomplished in Ohtsuka Pharmaceutical co. ltd.

Oligonucleotide Synthesis and Characterization. Oligodeoxynucleotide sequences were synthesized by conventional phosphoramidite method by using an Applied Biosystems 392 DNA/RNA synthesizer. Oligonucleotides were purified by reverse phase HPLC on a 5-ODS-H column (10 × 150 mm, elution with a solvent mixture of 0.1 M triethylamine acetate (TEAA), pH 7.0, linear gradient over 30 min from 5 % to 35 % acetonitrile at a flow rate 3.0 mL/min). Oligonucleotides containing modified nucleobases were fully digested with calf intestine alkaline phosphatase (50 U/mL), snake venom phosphodiesterase (0.15 U/mL) and P1 nuclease (50 U/mL) at 37 °C for 3 h. Digested solutions were analyzed by HPLC on a cosmosil 5C-18AR or CHEMCOBOND 5-ODS-H column (4.6 × 150 mm), elution with a solvent mixture of 0.1 M

triethylamine acetate (TEAA), pH 7.0, linear gradient over 20 min from 0 % to 10 % acetonitrile at a flow rate 1.0 mL/min). Concentration of each oligonucleotides were determined by comparing peak areas with standard solution containing dA, dC, dG and dT at a concentration of 0.1 mM.

Second PCR Amplification. The amplicon which was extracted from human blood, and amplified with PCR (initial 2 min, 96 °C; 30 s, 96 °C; 30 sec, 55 °C; 90 sec, 72 °C, 30 times), biotinylated A1 primer and S1 primer (2.5 μM each), the appropriate dNTPs (200 μM each final concentration) were mixed with reaction buffer and *TaKaRa Ex Taq*^{TM} DNA polymerase (12.5 U) and adjusted to a final volume of 500 μL with water. The experiments were cycled (initial 2 min, 96 °C; 30 s, 96 °C; 30 sec, 55 °C; 90 sec, 72 °C) 30 times.

Purification of PCR Products. Target DNA solutions after PCR amplification, same volume of the binding buffer (20 mM Tris-HCl, 2 mM EDTA, 2 M NaCl, 0.2% TritonX-100, pH 8.0) and 20 mg of MAGNOTEX-SA particles which were kept on magnetic stand for 1 min and removed the supernatant previously were mixed in a test tube. After mixing, the mixture was left at room temperature for 10 min, followed by kept on a magnet for 1 min, and the supernatant was removed. The particles were washed with 1 mL of the diluted binding buffer (10 mM Tris-HCl, 1 mM EDTA, 1 M NaCl, 0.1% TritonX-100, pH 8.0) for three times, and 500 μL of denaturing buffer (0.1 M NaOH, 0.1 M NaCl) was added. The supernatant was precipitated with 800 μL of ethanol. The precipitated DNA was washed with 100 μL of 80 % cold ethanol and dried *in vacuo*.

Fluorescence Measurement and Quantification. All fluorescence emissions from PCR products were taken in 5 μL of a solution containing the precipitated DNA purified with above method, 10 μM probe ODN, 50 mM sodium phosphate buffer (pH 7.0) and 100 mM NaCl at room temperature, irradiated 365 nm wavelength with a transilluminator.

Detection limits of concentration were taken in 5 μL, and detection limits of volume were determined in a solution containing 25 μM probe ODN.

References

1. Stoneking, M.; Hedgecock, D.; Higuchi, R. G.; Vigilant, L.; Erlich, H. A. *Am. J. Hum. Genet.* **1991**, *48*, 370-382.
2. Wu, D. Y.; Wallace, R. B. *Genomics* **1989**, *4*, 560-569.
3. Syvanen, A. C. *Methods Mol. Biol.* **1998**, *98*, 291-298.
4. Boon, E. M.; Ceres, D. M.; Drummond, T. G.; Hill, M. G.; Barton, J. K. *Nat. Biotechnol.* **2000**, *18*, 1096-1100.
5. Lipshutz, R. J.; Morris, D.; Chee, M.; Hubbell, E.; Kozal, M. J.; Shah, N.; Shen, N.; Yang, R.; Fodor, S. P. A. *Bio Techniques* **1995**, *19*, 442-447.
6. Heid, C. A.; Stevens, J.; Livak, K. J.; Williams, P. M. *Genome Res.* **1996**, *6*, 986-994.
7. Tyagi, S.; Kramer, F. R. *Nat. Biotechnol.* **1996**, *14*, 303-308.
8. Okamoto, A.; Tanaka, K.; Saito, I. *J. Am. Chem. Soc.* **2003**, *125*, 5066-5071.
9. (a) Haga, H.; Yamada, Y.; Ohnishi, Y.; Nakamura, Y.; Tanaka, T. *J. Hum. Genet.* **2002**, *47*, 605-610. (b) http://snp.ims.u-tokyo.ac.jp/cgi-bin/SnpInfo.cgi?SNP_ID=IMS-JST005851.
10. Okamoto, A.; Tanaka, K.; Fukuta, T.; Saito, I. *J. Am. Chem. Soc.* **2003**, *125*, 9296-9297.
11. Patolsky, F.; Lichtenstein, A.; Willner, I. *Nat. Biotechnol.* **2001**, *19*, 253-257.
12. Yamashita, K.; Takagi, M.; Kondo, H.; Takenaka, S. *Chem. Lett.* **2000**, *9*, 1038-1039.

CHAPTER 9

2-Amino-7-Deazaadenine Forms Stable Base Pairs with Cytosine and Thymine

Abstract: 2-Amino-7-deazaadenine (^{AD}**A**) was incorporated into oligodeoxynucleotides (ODN) and their base-pairing properties with natural nucleobases were investigated. In melting temperature (T_m) experiments, the duplex containing a ^{AD}**A**/T base pair, which is expected to have extra hydrogen-bonding with thymine, showed a higher T_m than that of a 7-deazaadenine/T base pair, as 2-aminoadenine/T duplex was more stable than A/T duplex. When guanine or adenine was incorporated opposite ^{AD}**A**, the duplex was remarkably destabilized. In contrast, the duplex containing a ^{AD}**A**/C base pair showed a high duplex stability as comparable to G/C pair. In order to know the efficiency of the base-pairing of 7-deazapurines with four natural nucleobases, we examined a single-nucleotide insertion reaction mediated by the Klenow fragment of DNA polymerase I (*exo*-) using a template containing ^{AD}**A**. The incorporation efficiency of dCTP was only 1.8% for TTP in single-nucleotide insertion reactions using the Klenow fragment of DNA polymerase I (*exo*-). While ^{AD}**A** was an effective degenerate base, only TTP was incorporated opposite ^{AD}**A** in a single-nucleotide insertion reaction, and the incorporation of dCTP was inefficient. Owing to its unique base-pairing property, 7-deazaadenine ^{AD}**A** is useful not only as a superior degenerate base that can be used for sequence-alternative hybridization, but also as a potent mutagen for site-directed mutagenesis which can induce the G/C to A/T transition during the DNA replication step.

Introduction

Synthetic 7-deazapurine, a purine analogue in which the N7 is replaced by a carbon atom, is a promising nucleobase for studying the structure and function of nucleic acids.[1-8] Several groups have incorporated these deazapurine analogues into oligodeoxynucleotides (ODNs), and their binding affinity toward DNA has been studied.[9,10] In recent years, deazapurine has also been used as a tool for probing nucleic acid structures.[11-13] While the thermodynamic parameters for the duplex formation of ODNs containing 7-deazapurine have been thoroughly studied, little is known about the base selectivity and fidelity of the base-pairing of 7-deazapurine. An investigation of the base-pairing properties of 7-deazapurine is important not only for structural studies of nucleic acids, but also for antisense and mutagenesis studies. We now wish to report that 2-amino-7-deazaadenine ($^{\mathbf{AD}}\mathbf{A}$), a family of 2-aminoadenine (**3**) which is known to form a tight base pair with thymine by extra hydrogen bonding,[14-16] acts as a superior degenerate base to form a stable base pair with both cytosine and thymine.

Results and Discussion

Nucleoside $^{\mathbf{AD}}\mathbf{A}$[17] was incorporated into ODNs using the conventional phosphoramidite method. The protected phosphoramidite of $^{\mathbf{AD}}\mathbf{A}$ was prepared as shown in Scheme 1. The thermal stabilities of the duplexes containing $^{\mathbf{AD}}\mathbf{A}$ and **3** were evaluated by determining the melting temperature (T_m) of the duplexes, 5'-d(TTTGGTT**X**TTT)-3'/5'-d(AAA**Y**AACCAAA)-3' (X=$^{\mathbf{AD}}\mathbf{A}$ or **3**, Y=T or C), and from the change of A_{260} on heating. The normalized melting profile of the duplexes is shown in Figure 1. The duplex containing a $^{\mathbf{AD}}\mathbf{A}$/T base pair showed a T_m value (13.8 ˚C) close to that of a **3**/T base pair (14.0 ˚C). The stability observed in the duplex containing a 'mismatched' **3**/C base pair (11.5 ˚C) remarkably

decreased as compared with that for a **3**/T base pair, whereas the T_m of the duplex containing a ^{AD}**A**/C base pair (19.0 ˚C) was 5.2 ˚C higher than that containing a ^{AD}**A**/T base pair. The stable base pair with cytosine observed for ^{AD}**A** was striking, and in contrast to the destabilization of the **3**/C base pair.

Scheme 1[a]

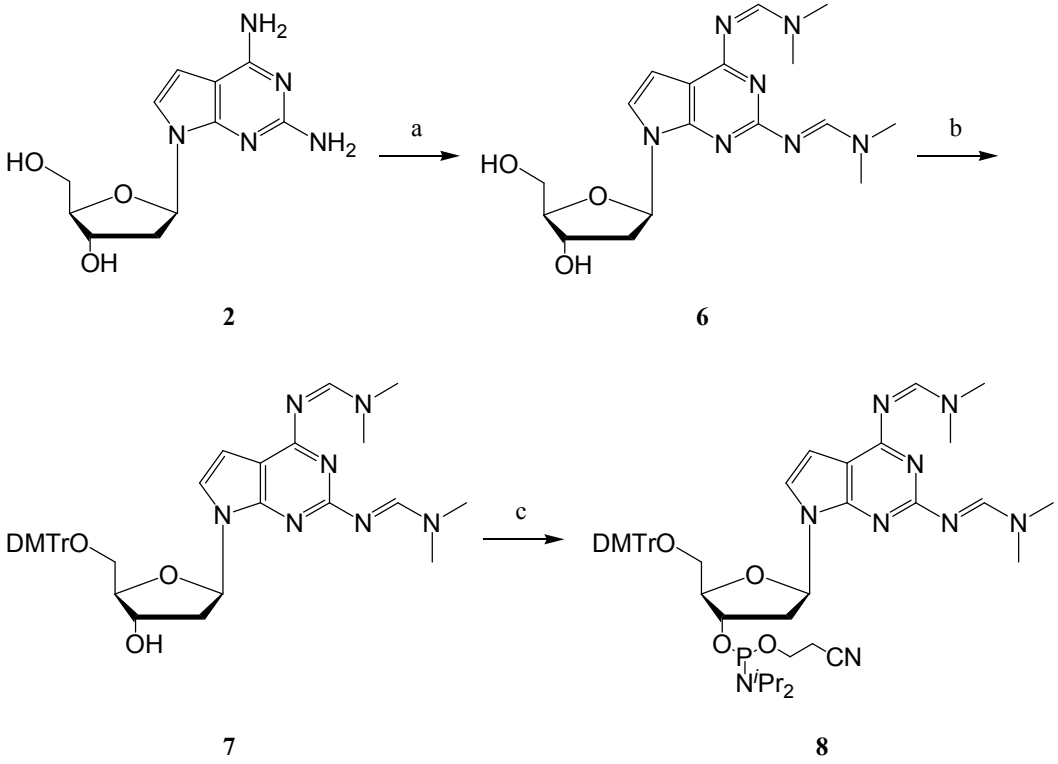

2 **6** **7** **8**

[a]*Reagents*: (a) *N*,*N*-dimethylformamide dimethylacetal, DMF, 55˚C, 8 h, 81%; (b) 4,4'-dimethoxytrityl chloride (DMTCl), DMAP, pyridine, rt, 3 h, 86%; (c) $(i\mathrm{Pr_2N})_2\mathrm{PO(CH_2)_2CN}$, tetrazole, acetonitrile, rt, 4 h, quant.

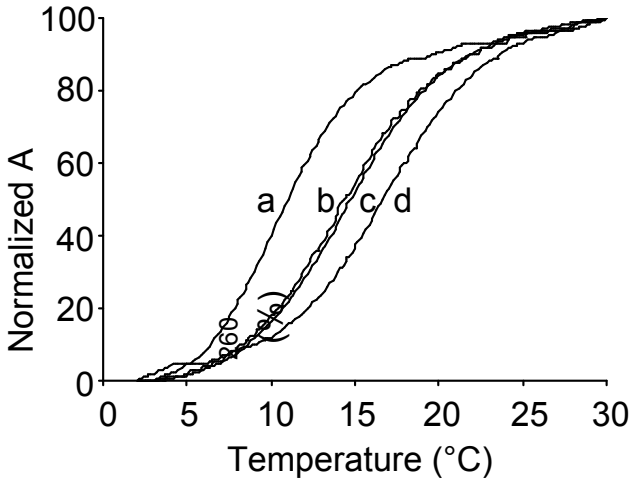

Figure 1. Normalized melting profile of the duplex 5'-d(TTTGGTT**X**TTT)-3'/5'-d(AAA**Y**AACCAAA)-3' (**X**=^{AD}**A** or **3**, **Y**=T or C). (a) **3**/C, (b) ^{AD}**A**/T, (c) **3**/T, (d) ^{AD}**A**/C.

The thermal stabilities of the duplexes containing ^{AD}**A**/C or ^{AD}**A**/T base pair were compared with those of the duplexes replaced by other base pairs. The T_m values of the duplexes are summarized in Table 1. The duplex containing a ^{AD}**A**/T base pair, which is expected to have extra hydrogen-bonding to thymine, showed a higher T_m than that of a 7-deazaadenine (**1**)/T base pair, as **3**/T duplex was more stable than A/T duplex. When guanine or adenine was incorporated opposite ^{AD}**A**, the duplex was remarkably destabilized. In contrast, the duplex containing a ^{AD}**A**/C base pair showed high duplex stability comparable to the G/C pair. It is worth noting that deazaadenine ^{AD}**A** can form a stable base pair not only with thymine, but also with cytosine.

Table 1. The melting temperatures (T_m) of duplexes containing various base pairs[a]

5'-TTTGGTT**X**TTT-3'
3'-AAACCAA**Y**AAA-5'

Entry	**X**/**Y**	T_m (°C)	Entry	**X**/**Y**	T_m (°C)
1	**1**/T	12.2	8	A/T	12.8
2	**2**/T	13.8	9	G/C	19.8
3	**3**/T	14.0	10	A/C	6.8
4	**2**/C	19.0	11	**4**/T	9.3
5	**3**/C	11.5	12	**4**/C	8.5
6	**2**/G	7.0	13	**5**/T	6.7
7	**2**/A	-[b]	14	**5**/C	7.8

[a]Conditions: 2.5 μM duplex, 10 mM sodium cacodylate, pH 7.0.

[b]No sigmoidal melting curve was observed.

Base pairs with both thymine and cytosine can be formed by the well-known degenerate bases *O*6-methylguanine (**4**)[18,19] and 2-amino-6-methoxyaminopurine (**5**)[20,21] (Figure 2). We measured the T_m of the ODNs containing these degenerate bases under the same conditions. Indeed, the degenerate bases **4** and **5** formed base pairs with both thymine and cytosine with similar stabilities (Table 1, entries 11–14). However, these base pairs remarkably destabilized the duplexes when compared to the duplexes containing normal A/T and G/C base pairs. Thus, the T_m experiments demonstrated that ^{AD}**A** is a superior degenerate base which can form a stable base pair with both cytosine and thymine without the duplex destabilization commonly observed for known degenerate bases like **4** and **5**.

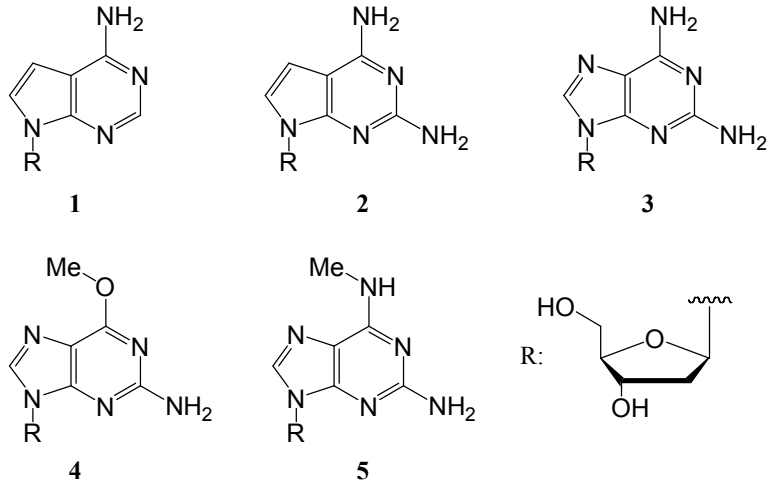

Figure 2. Structures of synthetic 2'-deoxynucleosides used in this study.

High stability of the ^{AD}**A**/C duplex comparable to that of the ^{AD}**A**/T duplex was observed also in the T_m experiments using GC-rich sequences. We measured the T_m of 5'-d(GCGATG^{AD}**A**GTAGCG)-3'/5'-d(CGCTAC**N**CATCGC)-3' (**N**=C and T) in 10 mM PIPES (pH 7.0). The T_m of the duplex containing a ^{AD}**A**/C base pair was 44.4˚C, showing that the ^{AD}**A**/C duplex stability was nearly equal to the ^{AD}**A**/T duplex stability (T_m=44.7 ˚C for ^{AD}**A**/T). In contrast, when T_m was measured in high salt concentration, the ^{AD}**A**/C duplex was less stable than that observed for the ^{AD}**A**/T duplex. In 10 mM PIPES in the presence of 100 mM sodium chloride and 10 mM magnesium chloride,[22] the T_ms of the duplexes containing the ^{AD}**A**/C and ^{AD}**A**/T base pairs were 56.1 and 62.0˚C, respectively. Although the T_m of the ^{AD}**A**/C duplex was risen under high salt condition, the stabilization of the ^{AD}**A**/C duplex by high salt was not so great as that observed for the ^{AD}**A**/T duplex.

In order to find out the efficiency of the base-pairing of 7-deazapurines with four natural nucleobases, we examined a single-nucleotide insertion

reaction mediated by polymerase using a template containing ^{AD}**A**. The primer–template duplex was incubated with one of four natural deoxynucleotide triphosphates in the presence of a Klenow fragment (*exo*-) at 37˚C, and the incorporation efficiency of these four bases opposite ^{AD}**A** was determined by gel electrophoresis (Table 2).[22] The steady-state kinetic parameters, V_{max} and K_m of the single-nucleotide insertion reaction were derived from a Lineweaver–Burk plot calculated from the intensities of the gel bands.[23] As shown in Table 2, the efficiency of dCTP insertion was considerably low: only 1.8% of that for TTP insertion, although the formation of a stable ^{AD}**A**/C base pair was observed in the T_m experiments. Table 2 shows that the low dCTP insertion efficiency was due to its large K_m value. The K_m of dCTP insertion was 25 times larger than that observed in TTP insertion, indicating that ^{AD}**A**/C base-pairing was inefficient in the interior of the enzyme pocket.

Table 2. The steady-state kinetic parameters for the insertion of a single nucleotide into a template-primer duplex mediated by a Klenow fragment (*exo*$^-$)[a]

5'-TAATACGACTCACTATAGGGAGA(**N**) -3'
3'-ATTATGCTGAGTGATATCCC TCT **2** GTCA-5'

dNTP	V_{max} (pmol U^{-1} min^{-1})	K_m (μM)	Efficiency (V_{max}/K_m)	Relative frequency
TTP	45.3	1.14	39.7	100
dCTP	18.7	25.6	0.730	1.84
dATP	13.1	62.0	0.211	0.531
dGTP	0.994	22.0	0.0452	0.114

[a]Primer-template duplex was incubated with dNTP in the presence of a Klenow fragment (*exo*$^-$) as a polymerase at 37 °C. V_{max} and K_m were calculated from a Lineweaver-Burk plot after three trials.

In order to confirm the T_m of the duplex elongated by single-nucleotide insertion, the T_m of the duplex consisting of the template and a 12-mer, 5'-d(CTATAGGGAGA)-3', possessing thymine or cytosine at the 3' end of the truncated primer (opposite ^{AD}**A** on a template strand) was measured. The ^{AD}**A**/C duplex showed a slightly higher T_m (28.0˚C) than the ^{AD}**A**/T duplex (26.2˚C), which was consistent with the T_m results shown in Table 1. Although the ^{AD}**A**/C base pair was as stable as the ^{AD}**A**/T base pair, the insertion of the dCTP opposite ^{AD}**A** was much slower than the TTP insertion. These results suggest that the ^{AD}**A**/C base pair formation in the polymerase reaction is more complicated as compared with the ^{AD}**A**/T base pair formation.

Conclusion

In summary, 7-deazaadenine ^{AD}**A** formed a stable base pair not only with thymine but also with cytosine without any duplex destabilization. While ^{AD}**A** was an effective degenerate base, only TTP was incorporated opposite ^{AD}**A** in a single-nucleotide insertion reaction, and the incorporation of dCTP was inefficient. Owing to its unique base-pairing property, 7-deazaadenine ^{AD}**A** is useful not only as a superior degenerate base that can be used for sequence-alternative hybridization, but also as a potent mutagen for site-directed mutagenesis which can induce the G/C to A/T transition during the DNA replication step.

Experimental Section

General. ^{1}H NMR spectra were measured with Varian Mercury 400 (400 MHz) spectrometer. ^{13}C NMR spectra were measured with JEOL JNM a-500 (500 MHz) spectrometer. Coupling constants (*J* value) are reported in hertz. The chemical shifts are expressed in ppm downfield from tetramethylsilane, using residual chloroform (δ = 7.24 in ^{1}H NMR, δ = 77.0 in ^{13}C NMR) and dimethyl sulfoxide (δ = 2.48 in ^{1}H NMR, δ = 39.5 in ^{13}C NMR) as an internal standard. FAB mass spectra were recorded on a JEOL JMS DX-300 spectrometer or JEOL JMS SX-102A spectrometer. HPLC was performed on a CHEMCOBOND 5-ODS-H column (4.6 × 150 mm) with a Gilson chromatography model 305 using a UV detector model 118 at 254 nm.

4-(*N,N'*-Dimethylaminomethylidene)amino-6-methoxy-9-(2'-deoxy-β-$_{D}$-*erythro*-pentofuranosyl)-9*H*-pyrimido[4,5-*b*]indole (6). A solution of **2** (200 mg, 0.75 mmol) and *N,N*-dimethylformamide dimethylacetal (2 mL) in *N,N*-dimethylformamide (2 mL) was stirred for 8 h at 55 ˚C. The reaction mixture was concentrated to a brown oil and purified by column chromatography on silica gel, eluting with 10% methanol in chloroform to give compound **6** (221 mg, 81%). ^{1}H NMR ($CDCl_3$): δ 8.80 (br, 1H), 8.71 (br, 1H), 6.88 (d, 1H, *J* = 3.7 Hz), 6.50 (d, 1H, *J* = 3.7 Hz), 6.30 (dd, 1H, *J* = 5.7, 9.0 Hz), 4.72 (d, 1H, *J* = 5.6 Hz), 4.11 (d, 1H, *J* = 1.8 Hz), 3.72–3.92 (m, 2H), 3.14 (d, 6H, *J* = 10.5 Hz), 3.09 (d, 6H, *J* = 9.3 Hz), 2.23–3.05 (m, 2H). ^{13}C NMR ($CDCl_3$): δ 161.4, 157.5, 157.0, 152.7, 123.7, 109.4, 100.5, 88.0, 87.8, 77.2, 73.3, 63.4, 41.2, 41.0, 40.9, 40.1, 35.1, 34.9. MS (FAB, NBA/CH_2Cl_2) m/z (%) 376 $[M + H]^+$, HRMS (FAB) calc. for $C_{17}H_{26}O_3N_7$ $[M + H]^+$ 376.2095, found 376.2113.

4-(*N,N'*-Dimethylaminomethylidene)amino-6-methoxy-9-(2'-deoxy-5'-*O*-dimethoxytrityl-β-$_{D}$-*erythro*-pentofuranosyl)-9*H*-pyrimido[4,5-*b*]indole (7). A solution of **6** (450 mg, 1.13 mmol), 4-dimethylaminopyridene (41

mg, 0.33 mmol) and 4,4'-dimethoxytrityl chloride (494 mg, 1.50 mmol) was stirred in anhydrous pyridine (15 mL) for 3 h at ambient temperature. The reaction mixture was concentrated to a brown oil and purified by column chromatography on silica gel, eluting with a mixed solution of 10:10:1 (v/v/v) hexane, ethyl acetate, and methanol containing 1% triethylamine to give compound **7** (656 mg, 86%). ^{1}H NMR ($CDCl_3$): δ 8.91 (br, 1H), 8.67 (br, 1H), 6.96 (d, 1H, J = 3.7), 6.78–7.42 (m, 14H), 6.51 (d, 1H, J = 3.8), 4.55 (m, 1H), 3.76 (s, 6H), 3.26 (m, 2H), 3.14 (d, 6H, J = 10.5 Hz), 3.09 (d, 6H, J =9.3 Hz), 3.05 (m, 1H), 2.41 (m, 2H). ^{13}C NMR ($CDCl_3$): δ 158.54, 158.49, 157.5, 157.1, 153.8, 144.5, 135.83, 135.81, 135.71, 135.69, 130.0, 128.2, 127.9, 126.8, 120.6, 113.1, 107.8, 101.5, 86.4, 84.8, 77.2, 72.8, 64.2, 64.1, 55.23, 55.22, 45.8, 41.0, 40.9, 40.6, 35.2, 34.8. MS (FAB, NBA/CH_2Cl_2) m/z (%) 678 $[M + H]^+$, HRMS (FAB) calc. for $C_{38}H_{43}O_5N_7$ $[M + H]^+$ 678.3401, found 678.3390.

2,4-Bis(*N,N'*-dimetylaminomethylidene-7-(2-deoxy-5-*O*-dimethoxytrityl-β-$_D$-*erythro*-pentofuranosyl-3-*O*-cyanoetyl-*N,N'*-diisopropylphosphoramidite)-7*H*-pyrrolo[2,3-*d*]pyrimidine (8). A solution of **7** (100 mg, 150 μmol), 2-cyanoethyl tetraisopropylphosphorodiamidite (52 μL, 160 μmol), and tetrazole (12 mg, 160 μmol) in acetonitrile (1.5 mL) were stirred at ambient temperature for 4 h. The mixture was filtered and used without further purification.

Modified ODN Synthesis. Modified ODNs were synthesized by the conventional phosphoramidite method using an Applied Biosystems 392 DNA/RNA synthesizer. Synthesized ODNs were purified by reversed phase HPLC on a 5-ODS-H column (10 × 150 mm, elution with a solvent mixture of 0.1 M triethylammonium acetate (TEAA), pH 7.0, linear gradient over 30 min from 5 to 20% acetonitrile at a flow rate 3.0 mL/min) or 15% denaturing polyacrylamide gel electrophoresis (PAGE). Mass spectra of ODNs purified by HPLC were determined with ESI-TOF mass spectroscopy or MALDI-TOF mass spectroscopy (acceleration voltage 21

kV, negative mode) with 2',3',4'-trihydroxyacetophenone as matrix, using T8 ([M - H]$^-$ 2370.61) and T17 ([M - H]$^-$ 5108.37) as an internal standard. The ODNs purified by PAGE were characterized by Maxam-Gilbert sequencing reactions.

***T*$_m$ Measurement.** All T_ms of the oligonucleotides (2.5 μM, final base concentration) were taken in various buffers showing at each table. Absorbance vs temperature profiles were measured at 260 nm using a JASCO TPU-550 UV/VIS spectrometer connected with a JASCO TPU-436 temperature controller. The absorbance of the samples was monitored at 260 nm from 2 °C to 80 °C with a heating rate of 1 °C/min. From these profiles, first derivatives were calculated to determine T_m values.

Preparation of ^{32}P-5'-End-Labeled Oligomers. The ODNs (400 pmol-strand) were 5'-end-labeled by phosphorylation with 4 μL of [γ-^{32}P]ATP (Amersham) and T4 polynucleotide kinase using a standard procedure. The 5'-end-labeled ODN was recovered by ethanol precipitation and further purified by 15% denaturing polyacrylamide gel electrophoresis (PAGE) and isolated by the crush and soak method.

Single–Nucleotide Insertion Reaction. Primer–template duplex was annealed by mixing in the buffer (10 mM Tris–HCl, pH 7.3, 10 mM $MgCl_2$, 1 mM DTT, and 0.1 mg/mL BSA), heating to 90 ˚C, and slow cooling to ambient temperature. Primer–template duplex (5 μM) was incubated with dNTP in the presence of Klenow fragment (*exo*$^-$, Ambion) as polymerase at 37 ˚C. The reaction was stopped at each time by 80% formamide loading buffer (a solution of 80% v/v formamide, 1 mM EDTA, 0.1% xylene cyanol, and 0.1% bromophenol blue) and analyzed with PAGE (20% polyacrylamide, 7 M urea). V_{max} and K_m was calculated from Lineweaver–Burk plotting after three trials.

References

1. Davoll, J. *J. Chem. Soc.* **1960**, 131-138.
2. Noell, C. W.; Robins, R. K. *J. Heterocycl. Chem.* **1964**, *1*, 34-41.
3. Kazimierczuk, Z.; Cottam, H. B.; Revankar, G. R.; Robins, R. K. *J. Am. Chem. Soc.* **1984**, *106*, 5379-5381.
4. Seela, F.; Ramzaeva, N.; Chen, Y. *Bioorg. Med. Chem. Lett.* **1995**, *5*, 3049-3052.
5. Buhr, C. A.; Wagner, R. W.; Grant, D.; Froehler, B. C. *Nucleic Acids Res.* **1996**, *24*, 2974-2980.
6. Ramzaeva, N.; Mittelbach, C.; Seela, F. *Helv. Chim. Acta* **1997**, 80, 1809-1822.
7. Balow, G.; Mohan, V.; Lesnik, E. A.; Johnston, J. F.; Monia, B.P.; Acevedo; O. L. *Nucleic Acids Res.* **1998**, *26*, 3350-3357.
8. Okamoto, A.; Taiji, T., Tanaka, K.; Saito, I. *Tetrahedron Lett.* **2000**, *41*, 10035-10039.
9. Seela, F.; Driller, H. *Biochemistry* **1987**, *26*, 2232-2238
10. Grein, T.; Lampe, S.; Mersmann, K.; Rosemeyer, H.; Thomas, H.; Seela, F. *Bioorg. Med. Chem. Lett.* **1994**, *4*, 971-976.
11. Milligan, J. F.; Krawczyk, S. H.; Wadwani, S.; Matteucci, M. D. *Nucleic Acids Res.* **1993**, *21*, 327-333.
12. Dierick, H.; Stul, M.; DeKelver, W.; Marynen, P.; Cassiman, J. *J. Nucleic Acids Res.* **1993**, *21*, 4427-4428.
13. Seela, F. ; Wei, C.; Becher, G.; Zulauf, M.; Leonard, P. *Bioorg. Med. Chem. Lett.* **2000**, *10*, 289-292.
14. Chollet, A.; Kawashima. E. *Nucleic Acids Res.* **1988**, *16*, 305-317.
15. Lamm, G. M.; Blencowe, B. J.; Sproat, B. S.; Iribarren, A. M.; Ryder, U.; Lamond, A. I. *Nucleic Acids Res.* **1991**, *19*, 3193-3198.
16. Bailly, C.; Waring, M. *J. Nucleic Acids Res.* **1998**, *26*, 4309-4314.
17. Seela, F.; Steker, H.; Driller, H.; Bindig, U. *Liebigs Ann. Chem.* **1987**, 15-19.
18. Leonard, G. A.; Thomson, J.; Watson, W. P.; Brown, T. *Proc. Natl.*

Acad. Sci. U.S.A. **1990**, *87*, 9573-9576.
19. Vojtechovsky, J.; Eaton, M. D.; Gaffney, B.; Jones, R.; Berman, H. M. *Biochemistry* **1995**, *34*, 32-39.
20. Lin, P. K. T.; Brown, D. M. *Nucleosides Nucleotides* **1991**, *10*, 675-677.
21. Hill, F.; Loakes, D.; Brown, D. M. *Proc. Natl. Acad. Sci. U.S.A.* **1998**, *95*, 4258-4263.
22. McMinn, D. L.; Ogawa, A. K.; Wu, Y.; Liu, J.; Schultz, P. G.; Romesberg, F. E. *J. Am. Chem. Soc.* **1999**, *121*, 11585-11586.
23. Boosalis, M. S.; Petruska, J.; Goodman, M. F. *J. Biol. Chem.* **1987**, *262*, 14689-14696.

CHAPTER 10

Public-Key Cryptography with DNA for Key Delivery

Abstract:

Novel public-key system using DNA has been developed. To solve key distribution problem, the public-key cryptography system based on the one-way function has developed. The message-encoded DNA hidden in dummies can be restored by PCR amplification, followed by sequencing. We used these operations as a one-way function, and constituted a novel method for the key distribution based on the public-key system using DNA. We will show the way of holding a key in common just between specific two persons.

Introduction:

In encryption technology, we must overcome a major issue, key distribution problem. To solve this problem, Rivest et al. (1978) have reported the first public-key cryptography system based on the one-way function which is easy to evaluate in the forward direction but impracticable to reckon in the reverse direction without additional information, and recent studies show physical one-way functions for the constitution of higher security key-distribution systems (Diffie et al., 1976; Pappu et al., 2002). Recently, applications of DNA to informational media were reported (Arita and Ohashi, 2004; Cox, 2001; Wong et al., 2003). Furthermore, since it is easy to extract the specific sequence from a DNA pool, the steganography using DNA has recently been developed (Clellaud et al., 1999). The message-encoded DNA hidden in dummies can be restored by PCR amplification, followed by sequencing (Clellaud et al., 1999). We used these operations as a one-way function: it is easy to hide the message, but not possible to extract the message-encoded sequence without knowing the correct primer pair. Herein we report a novel method for the key distribution based on the public-key system using DNA. In our system, everyone can make a pool in which a message-encoded DNA were hidden in dummies, whereas only the possessor of the public key can extract a message from this pool.

Materials and Methods:

Preparation of the Public Key A and Encoding of the Secret Key. Followed by mixing in these solid supports (**ODN A**, 1 mg; **ODN A_n**, 20 mg each), the secret message was synthesized with a mixed solid support, the public key A. After synthesis of the message-encoded sequence, ODNs were deprotected in concentrated aqueous ammonia at 55 °C for 3 h. After dried up, solid support was used for next step.

Enzymatic Ligation of the Public Key B. Ligation was accomplished in 500 μL of the reaction buffer, which contained 66 mM Tris-HCl (pH 7.6), 6.6 mM $MgCl_2$, 10 mM DTT, 0.1 mM ATP, the ODNs mixture of the public key B (**ODN B** and **ODN cB** were about 6 μM final concentration), and 350 units of T4 DNA ligase (from *TaKaRa*, Japan). The mixture was incubated for 16 h at 14 °C. After deprotection and cleavage from solid support in concentrated aqueous ammonia at 80 °C for 8 h, ODNs were captured by magnetic beads, and directly used in PCR reaction.

PCR Amplification. For the PCR amplification experiments, primers (2.5 μM each) and 2 μg of the particles, as well as the appropriate dNTPs (200 μM each final concentration), were mixed with ×10 reaction buffer containing SYBR Green and *TaKaRa Ex Taq*™ DNA polymerase (2.5 U) and adjusted to a final volume of 100 μL with water. The experiments were cycled (initial 2min, 96 °C; 15 s, 96 °C; 15 sec, 55 °C; 30 sec, 72 °C) 20 times. The amount of DNA from PCR amplification was detected by GeneAmp 5700 Sequence Detection System.

Results:

The outline of the protocol is shown in Figure 1. The message-receiver designs a primer sequence as a public key, and fixes it on solid supports (Step 1). Next, the DNA sequence that has the secret message encoded is connected to the public key by the message-sender (Step 2). After the treatment with the public key B (Step 3), DNAs immobilized to magnetic beads are sent back to the message-receiver (Step 4). Since the receiver can amplify the message-encoded sequence, only the receiver can decode it (Step 5). Consequently, a secret message is sharable only between the receiver and the sender.

Oligodeoxynucleotides (ODNs) used in this study are shown in Table 1. First, we prepared two public key sets. We synthesized **ODN A** as a forward primer attached to solid supports which consists of universal supports and hexaethyleneglycol linker. Solid supports with dummy DNAs, for example **ODN A_1**, **A_2** and **A_3**, were mixed for hiding solid supports containing **ODN A** without deprotection. This mixture was named as "public key A". On the other hand, the duplex of 5′-biotinylated **ODN B** as a reverse primer and **ODN cB** had a sticky end at 3′ end was also prepared. The mixture containing **ODN B** and **ODN cB** concealed with **ODN B_1**, **ODN cB_1**, and **ODN B_2** was named as "public key B".

In this study, we used a 21-mer secret-key-sequence, which means the word, "MESSAGE", encoded according to Table 2 (Clellaud et al., 1999). The secret-key sequence was added to the public key A using a DNA synthesizer. The resulting support mixture was treated with 25% ammonia for deprotection without cleavage from supports. Subsequently, ligation reaction with public key B was executed with T4 DNA ligase. Biotinylated ODNs were cleaved from solid supports by heating at 80 ˚C, and then captured by avidin-coated magnetic beads (Step 4). The pool of magnetic beads is sent to the receiver.

PCR amplification was accomplished with **Primer A** and **Primer B**. The amount of PCR products is evaluated by the change of fluorescence of SYBR Green (Figure 2). The reaction mixture containing the correct primer pair showed the increase of fluorescence intensity during thermal cycles. The polyacrylamide gel electrophoresis (PAGE) analysis of a PCR mixture showed that only when the correct primer pair was used in PCR, a product band was observed (Figure 3, lane 3). As is clear from lane 3

and 4, the addition of dummy DNAs did not influence in the amplification step. Lastly, sequencing analysis for the PCR product revealed only one sequence containing a secret key to be translated to the original word, 'message' (Figure 4).

Discussion:

The possibility of tapping in this system was investigated. There are two possible approaches for tapping. Firstly, the interceptor gets the sending sample and undergoes sequencing reaction using various primer pairs. However, even if an adversary somehow caught such a sending sample, it would still be extremely difficult to pick out the message-encoded sequence without knowing the correct primer pairs, because the interceptor must choose two primer sequences from about 10^{23} kinds of sequences (the number of combination taking 2 sequences from 4^{20} candidates). For verifying this expectation, PCR with or without a correct forward primer was executed. Only when both of the primer sequences were correct, the amplification curve was shown (Figure 4(i)). On the other hand, when one of a primer pair is incorrect, the amplification was not efficient (Figure 4(ii)). This result supports that the message-encoded sequence would be restored only by the message-receiver. That is, only the receiver can easily find a target sequence in a haystack of dummy DNAs. Thus, even if an enemy is trying to detect the primer sequences, they would face an extremely difficult experimental barrier. Second possibility is that the interceptor finds out the correct primer sequences from both public keys. For this possibility, not only primer sequences were hidden in dummies, but also ODNs were immobilized to magnetic beads because amplicon-attached magnetic beads can inhibit an enemy from connecting known sequences at both ends for PCR or cloning analysis. In the case of both public key A and B, the coating with hexaethyleneglycol linker and biotin at the end are expected to be obstacles, respectively.

The key transportation using DNA has two strong points. Firstly, owing to previous automation machines, a series of operations could be simple (Suyama, 2003). By the progress of molecular biology-techniques in recent years, anyone could quickly perform sequencing with high accuracy. Moreover, various methods of transporting DNA were developed, for example a DNA ink and a DNA book (Kamei et al., 2002;

Kawai and Hayashizaki, 2003). Improvement of transporting methods would decrease the cost for transportation and increase security. Secondarily, this system is protected with experimental barrier. The discovery of new algorithm and development of computational ability always threaten previous encryption system with decryption. In contrast, since, even if the operation were simple, the difference between the amount of time spent by a regular recipient as opposed to a tapping person would be still significant, the public key system generated from a physical one-way function would be free of potential risks of algorithmic decryption. On the other hand, it could prove difficult to create a practical method for the physical distribution of keys. The first public key system using a physical one-way function was realized with DNA.

In summary, we described the first example for key distribution using DNA based on public-key system. The message-sender prepares the DNA pool containing the message-encoded sequence between primer sequences as the public key of the message-receiver. The message-receiver can pick up the significant sequence from the pool, and restore the message. In addition, for demonstration of infeasibility of wiretapping, PCR with the incorrect primer pair was performed. It was clearly shown that any amplified product was not acquired. It can be concluded that security on this system is insured by mathematical and experimental barriers.

References:

Adleman, L. M. 1994, Molecular Computation of Solution to Combinatorial Problems. Science 266, 1021-1025.

Arita, M., Ohashi, Y. 2004, Secret Signatures Inside Genomic DNA. Biotechnol. Prog. 20, 1605-1607.

Clelland, C. T., Risca, V., Bancroft, C. 1999, Hiding messages in DNA microdots. Nature 399, 533–534.

Cox, J. P. L. 2001, Long-term data storage in DNA. Trends Biotechnol. 19, 247-250.

Diffie, W., Hellman, M. 1976, New directions in cryptography. IEEE Trans. Inf. Theory IT-21, 644–654.

Kamei, T., Kishii, N., Kurihara, K., Kobayashi, T., Iwamoto, H., Tsuboi, H., 2002, DNA-containing inks and personal identification system using them without forgery. Jpn. Kokai Tokkyo Koho, pp. 8.

Kawai, J., Hayashizaki, Y. 2003, DNA Book. Genome Res. 13, 1488–1495.

Pappu, R., Recht, B., Taylor, J., Gershenfeld, N. 2002, Physical One-Way Functions. Science 297, 2026–2030.

Rivest, R. L., Shamir, A., Adleman, L. 1978, A Method for Obtaining Digital Signatures and Public-Key Cryptosystems. Commun. ACM 21, 120–126.

Suyama, A. 2003, Super parallel DNA computer: Adleman's experiment. Saibo Kogaku 22, 75-79.

Wong, P. C., Wong, K., Foote, H. 2003, Organic Data Memory Using the DNA Approach. Comm. ACM 46, 95-98.

Tables and Figures:

Table 1. Oligodeoxynucleotides (ODNs) used in this study

	Sequence
ODN A[a]	5′-CCCTATAGTGAGTCGTATTA-TEG-uni-3′
ODN A_1[a]	5′-ATGGTCGCCCTTATTGTCGG-TEG-uni-3′
ODN A_2[a,b,c]	5′-Ac-GATCGGCAATXXXXXXXXXX-TEG-uni-3′
ODN A_3[a,d]	5′-pGATCGGCAATXXXXXXXXXX-TEG-uni-3′
ODN B[e]	5′-bio-TTTGGCATTATCAACTGGCTTA-3′
ODN cB[c]	3′- AAACCGTAATAGTTGACCGAATXXXXX-5′
ODN B_1[e]	5′-bio-CGCACGCCGTAAGTTGCATAC-3′
ODN cB_1[c]	3′- GCGTGCGGCATTCAACGTATGXXXXX-5′
ODN B_2[e]	5′-bio-AAGTTAGACGGGCCAATCAGACG-3′
m[c,f]	5′-pTCCGGTACGACGCGATTTGGT-3′
Primer A	5′-TAATACGACTCACTATAGGG-3′
Primer B	5′-TTTGCATATCAACTGGCTTA-3′
Primer C	5′-AAAGAATAGGCTGAGGAGGAAGTC-3′

[a]TEG-uni: Hexaethyleneglycol-attached universal support. [b]Ac: Acetyl group. [c]X: A, G, T or C. [d]P: 5′-Phosphorylated end. [e]bio: 1-*O*-(*N*-biotinyl-1-aminopropyl)-triethyleneglycolyl-glycerol group. [f]The encoded message can be translated to the plain text, “message”, according to Table 2.

Table 2. Translation table from alphabets to DNA nucleotides[a]

A=CGA	H=CGC	O=GGC	V=CCT	2=TAG	9=GCG
B=CCA	I=ATG	P=GGA	W=CCG	3=GCA	=ATA
C=GTT	J=AGT	Q=AAC	X=CTA	4=GAG	, =TCG
D=TTG	K=AAG	R=TCA	Y=AAA	5=AGA	. =GAT
E=GGT	L=TGC	S=ACG	Z=AAT	6=GGG	: =GCT
F=ACT	M=TCC	T=TTC	0=TTA	7=ACA	; =ATT
G=TTT	N=TCT	U=CTG	1=ACC	8=AGG	-=ATC

[a]This table was based on Clellaud et al. (1999).

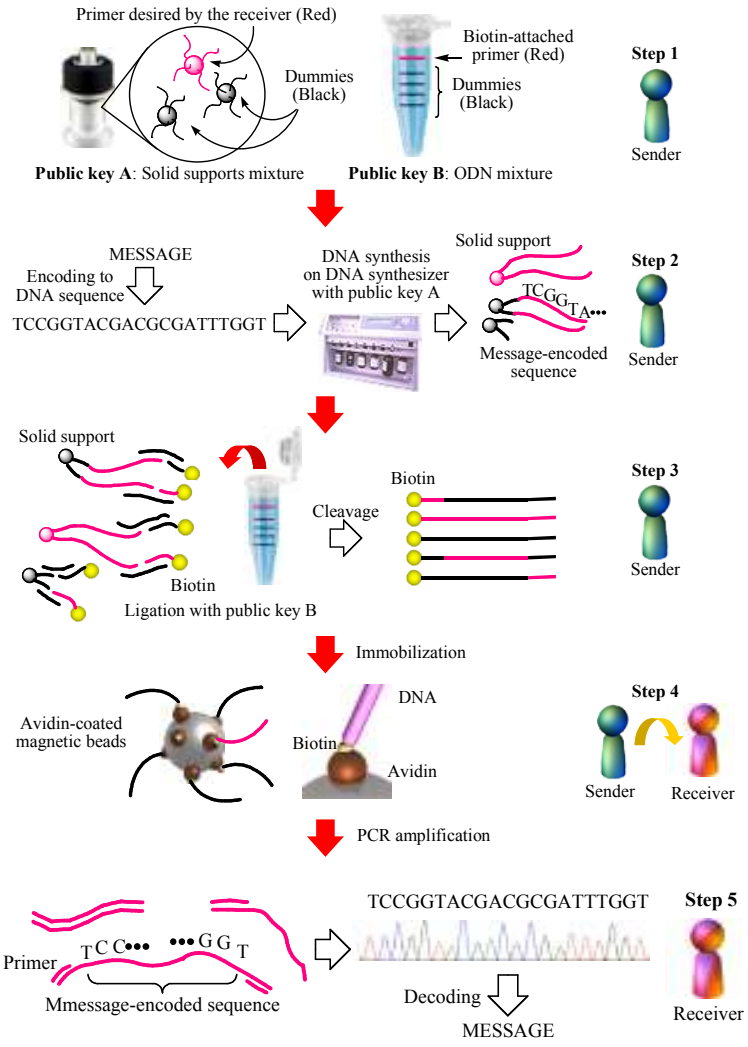

Figure 1. The schematic procedure for exchanging the secret key. Step 1: encoding step. The message-sender chooses the public key which belongs to the message-receiver. Step 2: DNA synthesis step. The sender synthesizes the message-encoded sequence on DNA synthesizer with the public key A containing a forward primer. Step 3: ligation step. The public key B containing a reverse primer is ligated. Step 4: immobilization step. The message-encoded DNA concealed with dummies is attached to magnetic beads, and sent to the possessor of the public keys. Step 5: amplification step. Only the secret key-encoded sequence which is put between a correct primer sequences can be amplified by PCR method. They can exchange the secret key by sequencing analysis.

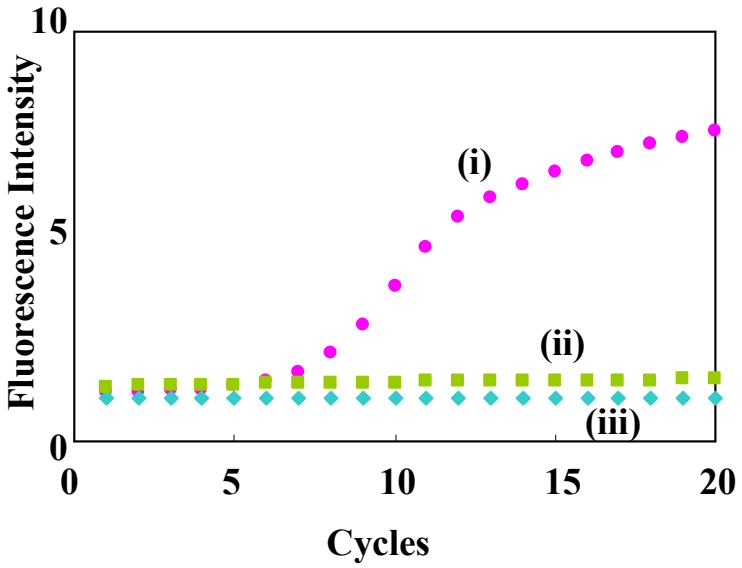

Figure 2. Fluorescent detection for the evaluation of PCR products. Increase of fluorescence intensity corresponds to amplification of products. (i) PCR amplification with the correct primer pair, Primer A and Primer B, (ii) with the incorrect primer pair, Primer A and Primer C, and (iii) without a primer as a negative control.

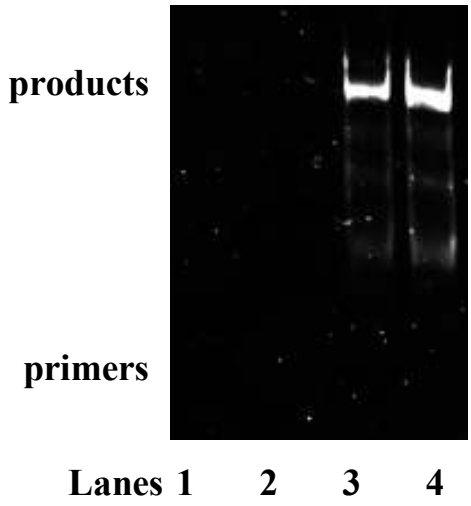

Figure 3. Gel analysis of the PCR products. The 10% native polyacrylamide gel stained by SYBR Green was illuminated with a 365 nm transilluminator. Lane 1, the reaction solution before PCR; lane 2, after PCR solution with an incorrect primer, Primer A and Primer C; lane 3, the PCR product with dummies; lane 4, the PCR product without dummies.

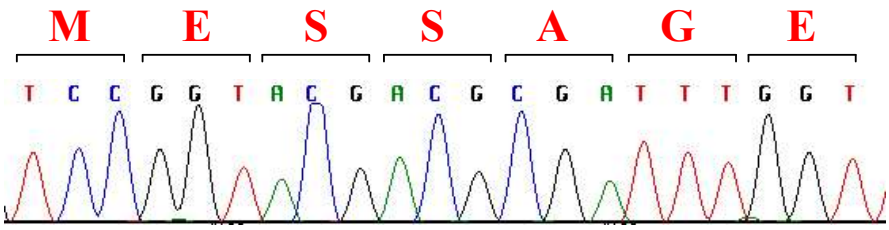

Figure 4. The message shared with two persons. After sequencing analysis of PCR product obtained from Figure 3, the message-encoded DNA sequence was translated to a plain text according to Table 2.

List of Publications

Chapter 1 **Rational Design of a DNA Wire Possessing an Extremely High Hole Transport Ability**
Okamoto, A.; Tanaka, K.; Saito, I.
J. Am. Chem. Soc. **2003**, *125*, 5066-5071.

Chapter 2 Protocol for the Construction of Logic Gates Using DNA
Tanaka, K.; Okamoto, A.; Saito, I.
J. Am. Chem. Soc. **2004**, *126*, 9458-63.

Chapter 3 Enzymatic Ligation and Extension of DNA Wire
Tanaka, K.; Nishiza, K.; Okamoto, A.; Saito, I.
Nucleic Acids Res. Suppl. **2003**, *3*, 39-40.

Enzymatic Synthesis of DNA Nanowire
Tanaka, K.; Nishiza, K.; Okamoto, A.; Saito, I.
Bioorg. Med. Chem. **2004**, *12*, 5875-80.

Chapter 4 Unique Hole-Trapping Property of the Degenerate Base, 2-Amino-7-deazaadenine
Okamoto, A.; Tanaka, K.; Saito, I.
Bioorg. Med. Chem. Lett. **2002**, *12*, 3641-3643.

Chapter 5 Development of the Drug Release System in Hole Transfer Reaction through DNA
Tanaka, K.; Okamoto, A.; Saito, I.
Nucleic Acids Res. Suppl. **2003**, *3*, 153-154.

A Novel Nucleobase That Releases Reporter Tags upon DNA Oxidation
Okamoto, A.; Tanaka, K.; Saito, I.

J. Am. Chem. Soc. **2004***, 126,* 416-417.

Chapter 6 Design of Base-Discriminating Fluorescent Nucleoside and Its Application to T/C SNP Typing
Okamoto, A.; Tanaka, K.; Fukuta, T.; Saito, I.
J. Am. Chem. Soc. **2003**, *125*, 9296-9297.

Chapter 7 Cytosine Detection by a Fluorescein-Labeled Probe Containing Base-Discriminating Fluorescent Nucleoside
Okamoto, A.; Tanaka, K.; Fukuta, T.; Saito, I.
Chembiochem **2004**, *5*, 958-63.

Chapter 8 Clear Distinction of Pyrimidine Bases on the Complementary Strand by Fluorescence Change of Novel Fluorescent Nucleosides
Tanaka, K.; Okamoto, A.; Saito, I.
Nucleic Acids Res. Suppl. **2003**, *3*, 171-172.

Chapter 9 2-Amino-7-deazaadenine Forms Stable Base Pairs with Cytosine and Thymine
Okamoto, A.; Tanaka, K.; Saito, I.
Bioorg. Med. Chem. Lett. **2002**, *12*, 97-99.

Chapter 10 Public-Key System Using DNA as a One-Way Function for Key Distribution
Tanaka, K.; Okamoto, A.; Saito, I.
Biosystems **2005**, *81*, 25-9.

Other Publication

Synthesis and Duplex Stability of Oligonucleotides Containing 7-Vinyl-7-Deazaguanine as a Strong Electron-Donating Nucleobase
Okamoto, A.; Taiji, T.; Tanaka, K.; Saito, I.
Tetrahedron Lett. **2000**, *41*, 10035-10039.

List of Oral and Poster Presentations

1. "Synthesis of 2-Amino-7-Deazaadenine and Its Incorporation into DNA."
   Okamoto, A.; Tanaka, K.; Saito, I.
   77th Annual Meeting of Chemical Society of Japan, Funabashi, March, 2000.

2. "Synthesis and Application of DNA Containing Super Electron-Rich Nucleobase, 2-Amino-7-deazaadenine."
   Okamoto, A.; Tanaka, K.; Saito, I.
   78th Annual Meeting of Chemical Society of Japan, Nara, September, 2000.

3. "Base-Pairing Ability of Adenine Derivative, 2-Amino-7-Deazaadenine with Cytosine."
   Okamoto, A.; Tanaka, K.; Saito, I.
   79th Annual Meeting of Chemical Society of Japan, Kobe, March, 2001.

4. "Synthesis of the Oligonucleotides containing Novel Nucleobases for Effective Hole Migration."
   Okamoto, A.; Tanaka, K.; Saito, I.
   79th Annual Meeting of Chemical Society of Japan, Kobe, March, 2001.

5. “Novel Degenerated Base Stable Base-Pairing with Thymine and Cytosine.”
   Okamoto, A.; Tanaka, K.; Saito, I.
   80th Annual Meeting of Chemical Society of Japan, Chiba, September, 2001.

6. “Novel Nucleobase toward Functional Molecular Wire.”
   Okamoto, A.; Tanaka, K.; Saito, I.
   80th Annual Meeting of Chemical Society of Japan, Chiba, September, 2001.

7. “Evaluation of Charge Transfer Efficiency of DNA Wire containing Artificial Nucleobase, Benzodeazaadenine.”
   Okamoto, A.; Tanaka, K.; Saito, I.
   81th Annual Meeting of Chemical Society of Japan, Tokyo, March, 2002.

8. “Fluorescent Property of DNA Oligomer containing Novel Modified Nucleobase, Benzodeazaadenine.”
   Okamoto, A.; Tanaka, K.; Saito, I.
   81th Annual Meeting of Chemical Society of Japan, Tokyo, March, 2002.

9. “Mechanistic Studies of Photo-Induced Charge Transport in DNA Containing a New Nucleobase, Benzodeazaadenine.”
   Tanaka, K.; Okamoto, A.; Saito, I.
   XIXth IUPAC Symposium on Photochemistry, Budapest, Hungary, July, 2002.

10. “Synthesis and Evaluation of a Novel Nucleobase for a DNA Wire.”
    Tanaka, K.; Okamoto, A.; Saito, I.
    82th Symposium on Organic Synthesis, Tokyo, November, 2002.

11. “Oligonucleotides containing Novel Nucleobases for Effective Hole Migration.”
    Tanaka, K.; Okamoto, A.; Saito, I.
    83th Annual Meeting of Chemical Society of Japan, Tokyo, March, 2003.

12. “Development of the Drug Release System in Hole Transfer Reaction through DNA.”
    Tanaka, K.; Okamoto, A.; Saito, I.
    The 39th IUPAC Congress and the 86th Conference of the Canadian Society for Chemistry, Ottawa, Canada, August, 2003.

13. “Mechanistic Studies of Photo-Induced Charge Transport in DNA containing a New Nucleobase, Benzodeazaadenine.”
    Tanaka, K.; Okamoto, A.; Saito, I.
    Japanese-German Biochemistry Meeting, Marburg, Germany, September, 2003.

14. “Development of the Drug Release System in Hole Transfer Reaction through DNA.”
    Tanaka, K.; Okamoto, A.; Saito, I.
    3rd International Symposium on Nucleic Acids Chemistry, Hokkaido, September, 2003.

15. “Clear Distinction of Pyrimidine Bases on the Complementary Strand by Fluorescence Change of Novel Fluorescent Nucleosides.”
    Tanaka, K.; Okamoto, A.; Saito, I.
    3rd International Symposium on Nucleic Acids Chemistry, Hokkaido, September, 2003.

16. “Modulation of hole transport efficiency by complementary bases in hole transport reaction through DNA.”

1st Joint Symposium on Biofunctional Chemistry and Biotechnology, Kumamoto, October, 2003.

17. “Development of a Novel Nucleobase That Releases Functional Molecules upon DNA Oxidation.”
Tanaka, K.; Okamoto, A.; Saito, I.
84th Annual Meeting of Chemical Society of Japan, Hyogo, March, 2004.